

Performance of Lime- and Cement- based Treatments of Sulfate-rich Soil via RC Testing

by

AZADEH ASGHARIASTANEH

Presented to the Faculty of the Graduate School of
The University of Texas at Arlington in Partial Fulfillment
of the Requirements
for the Degree of

MASTER OF SCIENCE IN CIVIL ENGINEERING

THE UNIVERSITY OF TEXAS AT ARLINGTON

August 2017

Abstract

Performance of Lime- and Cement- based Treatments of Sulfate-rich Soil via RC Testing

Azadeh Asghariastaneh, MS

The University of Texas at Arlington, 2017

Supervising Professor: Laureano R. Hoyos

Chemical treatment of expansive sulfate-rich soils, particularly lime- and cement-based methods, had been rather popular due to their relatively low cost and ready availability. However, over the last few decades, extensively documented pavement failures, mainly caused by excessive heaving and/or shrinkage of lime- and cement-treated subgrades with moderate-to-high sulfate content, have led to thorough investigations to assess the actual feasibility and effectiveness of calcium based stabilizers in sulfate-rich soils. Studies have concluded, with solid experimental evidence, that the calcium present in the chemical stabilizers react with the sulfate and alumina of the treated soil to form *Ettringite*, an expansive mineral that has detrimental effects on the overall performance of the treated soil. Most of these studies have mainly focused on detrimental effects of lime- and cement-based treatment methods in terms of Atterberg limits, swell-shrink potential, and unconfined compressive strength.

The present study is aimed at gaining valuable insight into the effects of lime- and cement-based treatment methods on stiffness of sulfate-rich soils, namely, shear modulus and damping, which are fundamental properties in the analysis and design of pavement infrastructure. To achieve this goal, a thorough series of resonant column (RC) tests was conducted on several chemically stabilized specimens of high-plasticity, sulfate-rich expansive clay from Sherman, Texas. Test results were analyzed to assess the influence of lime- and cement-based stabilizer dosage, curing time, and confining pressure on the shear modulus and damping of the treated soil, including 8%lime + 2% fly ash, 6% lime + 4% fly ash, and 3% cement + 2% fly ash. In general, results show a detrimental effect of all treatment methods on soil stiffness, only rendering 6% lime + 4% fly ash as a potentially viable treatment method with curing time longer than 14 days.

Acknowledgements

This is my honor to appreciate Dr. Laureano R. Hoyos's guidance and support for this accomplishment. Dr. Hoyos has been my advisor through this program at the University of Texas at Arlington and I should express my most sincere gratitude for his precious guidance and advice through my course works and research. I would also like to thank Dr. Aravind Pedarla for his valuable guidance through this research. I would also like to express my gratitude to Dr. Xinbao Yu and Dr. Sharareh Kermanshachi as my committee members. This is my honor to use their valuable advice and suggestions. I would also like to express my appreciation to Mrs. Roya Davoodi-Bilesavar for her help and guidance through all the experimental procedures. I would also like to appreciate Dr. Jairo Yepes for providing me with his valuable experience through my experiments.

I would also like to appreciate my husband, Maziar Mahdavi deeply for his great support and help through my Master's program and thesis. I am also thankful to my parents Abolghasem Asghariastaneh and Atefeh Sabouri and my family for all their support during my personal and academic life. And finally, I would like to appreciate all my friends for their help and supports through this program.

Table of Contents

■ Chapter1 - Introduction	1
1.1 Background and Importance	1
1.2 Objective	2
1.3 Organization	2
■ Chapter 2 - Literature Review	3
2.1 Introduction	3
2.2 Fundamentals of Soil Stabilization	3
2.3 Sulfate Heave Case Histories	4
2.3.1 Joe Pool Dam, Texas	4
2.3.2 Sulfate heave issues at DFW airport, Texas	5
2.3.3 Sulfate Attack on a Tunnel Shotcrete liner, Dallas, Texas (Talluri, N. (2013))	6
2.3.4 Stewart Avenue, Las Vegas, Nevada	7
2.4 Stabilization of High Sulfate Soil	7
2.4.1 Double application of lime	7
2.4.2 Combined Lime and Cement Treatment	8
2.4.3 Stabilization with Low Calcium Based Stabilizers	8
2.5 Sulfate Heave Mechanism	8
■ Chapter 3 - Fundamentals of Resonant column (RC) Testing Technique	10
3.1 Basic components of Proximitor-Based Resonant Column device	10

<u>3.1.1 Resonant column main cell</u>	10
<u>3.1.2 Electrical Servo motor driver</u>	12
<u>3.1.3 Digital Servo Controller and Acquisition System</u>	12
<u>3.1.4 Resonant Column Software</u>	14
<u>3.2 Pressure control monitoring system</u>	16
<u>3.3 Calculation of Shear Modulus</u>	17
<u>3.4 Calculation of Damping Ratio</u>	17
<u>3.5 Summery</u>	18
Chapter 4 - Test Soil and Experimental Variables	19
<u>4.1 Introduction</u>	19
<u>4.2 Test Soil</u>	19
<u>4.3 Chemical Stabilizers</u>	19
<u>4.4 Specimen Preparation</u>	20
Chapter 5 - Experimental Program and Analysis of test results	22
<u>5.1 Introduction</u>	22
<u>5.2 Specimen symbolization</u>	22
<u>5.3 Experimental Program and Procedure</u>	23
<u>5.4 Linear Soil Response at Low-Amplitude Shear Strain</u>	27
<u>5.4.1 Threshold strain limit, γ_{th}</u>	27
<u>5.4.2 Typical frequency response</u>	28
<u>5.4.3 Natural (control) sulfate rich soil- Untreated</u>	29
<u>5.4.4 8% lime, 2% fly ash treated soil,</u>	33
<u>5.4.5 6% lime+4% fly ash treated soil</u>	36
<u>5.4.6 3% cement+2% fly ash treated soil</u>	39

5.4.7 Curing duration	42
5.4.8 Confinement Pressure	46
5.4.9 Normalized shear modulus G/G_{max}	50
Chapter 6 - Summary, Conclusions, and Recommendations	60
6.1 Summary	60
6.2 Main Conclusions	60
6.3 Recommendations for Future work	61
■ References	62
■ APPENDIX I: “ETTRINGITE” Formation Figures	64
■ APPENDIX II: C.A.T.S Software Outputs	66
■	68
■ Appendix III- Typical Test Results	68
Appendix IV – Variation normalized shear modulus over shear strain for treated and untreated soils for different curing durations	79
■ Appendix V Test Repeatability	81
■ Appendix VI: Class F Fly ash	83

Table of Figures

Figure 2-1 heaving in lime treated subgrade (Reproduced from Talluri, 2013)	5
Figure 2-2 heave distress pattern on west shoulder of taxiway - (Reproduced from Talluri, 2013)	6
Figure 2-3 Distress region on tunnel lining (c-3), (Puppala et al.2010)	6
Figure 2-4: Stewart Avenue cracks (Hunter 1988)	7
Figure 2-5: SEM photograph of needle-like Ettringite (Mallat,2006)	9
Figure 2-6: schematic of the mineral structure of Ettringite (Intharasombat, 2003)	9
Figure 3-1: General layout of the proximator-based RC device (BRAVO,A.(2013)	10
Figure 3-2: Main cell's columns	11
Figure 3-3: Acrylic plastic reinforcement for the cell	11
Figure 3-4: Electrical servo motor driver	12
Figure 3-5: GCTS SCON-1500 Digital System Controller	13
Figure 3-6: C.A.T.S software environment	13
Figure 3-7:Test results obtained from the software	14
Figure 3-8: Frequency response curve obtained by the software	15
Figure 3-9: The specimen properties required for the software	15
Figure 3-10: PCP-15U pressure panel	16
Figure 3-11: The air flushing equipment	16
Figure 3-12: bandwidth method determination of damping ratio (D)	18
Figure 4-1: US-82	20
Figure 4-2: Soil mixture wrapped with plastic bag for mellowing	20
Figure 4-3: Triaxial loading frame	21
Figure 4-4: Extruder device	22
Figure 5-1: Applying pressure of 20 KPa	23
Figure 5-2: The specimen information input	24
Figure 5-3: G_{max} and f_r reported	24
Figure 5-4: Typical Frequency response curves under different confining pressure for control soil.	25

Figure 5-5: Typical Frequency response curves under different confining pressure for cement treated soil	26
Figure 5-6: Typical back-bone curve from control soil	27
Figure 5-7: Typical back-bone curve from 3C 5DM 3DC	27
Figure 5-8: Typical frequency response curve from control specimen	28
Figure 5-9: Typical frequency response curve from C3-F2-14D	29
Figure 5-10: Variation of G_{max} with confining pressure for control soil	30
Figure 5-11: Variation of D_{min} with confinement pressure for control soil	31
Figure 5-12: Variation of G_{max} with confining pressure for control soil	32
Figure 5-13: Variation of D_{min} with confining pressure for control soil	32
Figure 5-14: Variation of G_{max} with curing time for control and 8% lime+2% fly ash treated soil for different pressures	34
Figure 5-15: Variation of D_{min} with curing time for control and 8% lime+2% fly ash treated soil for different pressures	34
Figure 5-16: Variation of G_{max} with σ_0 for 8L-2F-5DM treated soil for different curing period	35
Figure 5-17: Variation of D_{min} with σ_0 for 8L-2F-5DM treated soil for different curing times	35
Figure 5-18: variation of G_{max} with curing time for control and 6% lime+4% fly ash treated soil for different pressures	37
Figure 5-19: Variation of D_{min} with curing time for control and 6% lime+4% fly ash treated soil for different pressures	37
Figure 5-20: Variation of G_{max} with σ_0 for 6L-4F-5DM treated soil for different curing period	38
Figure 5-21: Variation of D_{min} with σ_0 for 6L-4F-5DM treated soil for different curing times	38
Figure 5-22: Variation of G_{max} with curing time for control and 3% cement+2% fly ash treated soil for different pressures	40
Figure 5-23: Variation of D_{min} with curing time for control and 3% cement+2% fly ash treated soil for different pressures	40
Figure 5-24: Variation of G_{max} with σ_0 for 3C-2F-5DM treated soil for different curing period	41
Figure 5-25: Variation of D_{min} with σ_0 for 3C-2F-5DM treated soil for different curing times	41

Figure 5-26: Variation of G_{max} with pressure for 3day curing time for control and treated specimen	43
Figure 5-27: Variation of D_{min} with pressure for 3day curing time for control and treated specimen	43
Figure 5-28: Variation of G_{max} with pressure for 7day curing time for control and treated specimen	44
Figure 5-29: Variation of D_{min} with pressure for 7day curing time for control and treated specimen	45
Figure 5-30: Variation of G_{max} with pressure for 14day curing time for control and treated specimen	45
Figure 5-31: Variation of D_{min} with pressure for 14day curing time for control and treated specimen	46
Figure 5-32: Variation of G_{max} with curing time for 20 KPa for control and treated specimen	47
Figure 5-33: Variation of D_{min} with curing time for 20 KPa for control and treated specimen	48
Figure 5-34: Variation of G_{max} with curing time for 80 KPa for control and treated specimen	48
Figure 5-35: Variation of D_{min} with curing time for 80 KPa for control and treated specimen	49
Figure 5-36: Variation of G_{max} with curing time for 160 KPa for control and treated specimen	49
Figure 5-37: Variation of D_{min} with curing time for 160 KPa for control and treated specimen	50
Figure 5-38: variation normalized shear modulus over shear strain for untreated soil	51
Figure 5-39: Variation normalized shear modulus over shear strain for 8L-2FA-5DM-3DC treated soil	52
Figure 5-40: Variation normalized shear modulus over shear strain for 6L-4FA-5DM-3DC treated soil	53
Figure 5-41: Variation normalized shear modulus over shear strain for 8L-2FA-5DM-3DC treated soil	54
Figure 5-42: Variation normalized shear modulus over shear strain for 8L-2FA-5DM-7DC treated soil	55
Figure 5-43: Variation normalized shear modulus over shear strain for 6L-4FA-5DM-7DC treated soil	56
Figure 5-44: variation normalized shear modulus over shear strain for 3C-2FA-5DM-7DC treated soil	57
Figure 5-45: Variation normalized shear modulus over shear strain for 8L-2FA-5DM-14DC treated soil ..	58
Figure 5-46: Variation normalized shear modulus over shear strain for 6L-4FA-5DM-14DC treated soil ..	59
Figure 5-47: Variation normalized shear modulus over shear strain for 8L-2FA-5DM-3DC treated so	59

Chapter1 - Introduction

Background and Importance

In civil engineering, soil definition is a natural material, which is unconsolidated. The three-major kinds of soil can be named as sand, silt, and clay. It is important to take this fact into consideration that each kind of soil has its own specific problems since it has its own characteristics like texture, mineral content, and structure.

Both pre-construction and post-construction problems are observed in the soil. One of the problematic happenings may be that the soil doesn't reach the required bearing capacity to bear the structure above it. As a matter of fact, the soil underneath bridges, dams, highways or other supporting structures may not be appropriate enough. Indeed, it may become problematic after construction.

The other problem possible at the construction site is settlement, which happens by soil movement caused by the surcharge or water table change. Indeed, preventing the settlement is very important which cannot happen unless there is enough recognition of the soil type and the solution appropriate for each type of soil is prone to settlement.

The ground improvement technics have been developing during time. For instance, in the past if the soil was not strong enough from bearing capacity aspect, was susceptible to liquefaction, or covered with soft clay or organic soil, then it was abandoned due to not being practical for construction purposes. This crisis had led to natural resources scarcity. Nowadays, however, the problematic soils such as soft clay or organic clay are improved by stabilizers so that they meet the design specifications. As a matter of fact, there is no construction site ideal for engineering properties without modification.

The stabilization of the soil leads to either the water proofing the particles, bonding them together, or both functions together. These processes happen by increasing the soil strength and water softening resistance increasing. All the stabilization procedures are in two categories of mechanical and chemical stabilization. For instance, two simple ones are compaction and drainage and adding binders to the weak soil to achieve better particle size gradation.

During the past decades, many pavement failure cases were reported where heaving was the problem. The soil of these cases was sulfate rich soils stabilized by cement or lime. The main goal of this study is to assess the improvement in stiffness properties of chemically stabilized sulfate-rich soils

Objective

The primary aim of this study to investigate the stiffness response of chemically stabilized, sulfate rich expansive clay from Sherman, TX. For this purpose, three kinds of stabilizers, lime, fly ash and cement were used. A series of free -fixed type of resonant column tests were performed by the Proximitor Resonant Column Instrument at small shear strain amplitude levels ($< 0.0001\%$) for different stabilizer type, curing time and confining pressure. The stiffness properties obtained from the test results are linear shear modulus G_{\max} and material damping ratio D_{\min} , which were calculated by means of half-power bandwidth method (Richart et al. 1970). For studying the effects of torsional shearing on the rate of degradation of normalized modulus G/G_{\max} of treated soil, the tests were conducted at the range of 0.0001 to 0.01% or small strain amplitudes.

Organization

The thesis is organized into six chapters. Chapter 1 is an introduction that has given an overview of the thesis and states the main objectives of this work.

In Chapter 2, principal concepts of soil stabilization are illustrated by discussing former studies regarding the subject topic.

In Chapter 3, fundamentals of Proximitor Resonant Column (RC) testing techniques are demonstrated. This chapter also gives an overview of the RC test device used to accomplish the experimental program.

In Chapter 4, a brief description of the basic properties of the test soil and the test procedures used to accomplish this thesis are presented. This chapter also summarizes the experimental variables and specimen preparation methods.

In Chapter 5, the experimental program and analysis of test results are presented. The chapter includes all test results and data plots, providing a thorough analysis of all resonant column test results.

Chapter 6 summarizes the main conclusions from this thesis work and provides some recommendations for future studies.

Chapter 2 - Literature Review

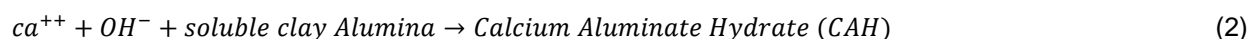
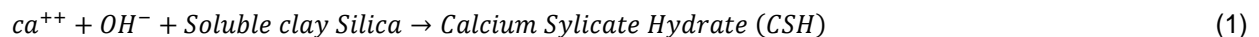
Introduction

The expansive soil issue has always been a concern for geotechnical engineers and has been a research topic of a lot of researchers which led to a variety of laboratory tests. The current literature survey is referring to the engineering behavior and properties of sulfate-rich expansive clays found on northeast Texas. In addition, some case studies regarding soil heaving phenomenon in this region is discussed. On the other hand, this review mostly focuses on different chemical stabilization methods.

Fundamentals of Soil Stabilization

The concept of stabilizing the soil can go back to 5000 years ago. For instance, the stabilized earth roads were used in ancient Mesopotamia and Egypt (McDowell 1959). The first test involving soil stabilization in the United States was performed in 1904 (Clare and Crunchily 1957). Lime was used first in 1924 for purpose of modern construction practice on short stretches of highway (McCausland 1925). Also, Cement was used as a stabilizer in 1915 on a street in Sarasota, FL (ACI 1997). As mentioned in the study cases above, lime or cement are used for stabilizing the expansive soil, so that the improved soil experiences an increase in soil strength, stiffness and durability and experiences a reduction in soil plasticity and swelling/shrinkage potential (Hausmann 1990; Sherwood 1995; Prusniski and Bhattacharya 1999).

Since Lime has low cost and is available everywhere, it is preferred often. The chemical reaction due to lime stabilization can be categorized in two kinds of processes: Modification Reactions and stabilization reactions. The modification reactions can be named as cation exchange and flocculation. These two reactions lead to improvement of plasticity, shear strength and workability. These reactions are short-term ones. The two other kinds of reaction which are long-term are agglomeration and pozzolan. The function of pozzolan reaction is that, as lime increases the PH to 12.4, the alumina and silica are released and pozzolanic compounds are formed when combining by water and calcium as shown below:



Also, the pozzolonic compound and increase in curing time improve the strength of the clay soil or sandy or silty soil containing at least seven percent clay because of the release of the existing silica and alumina in the clay (Talluri 2013).

However, in the recent decades, some pavement failure cases have been reported because of heave phenomenon that is a probable outcome of stabilizing with lime or cement (Mitchell 1986; Hunter 1988; Little et al. 1989, Perrin 1992; Kota et al. 1996; Ksaibati et al. 1999; Rollings et al. 1999). Also, the pozzolonic compound and increase in curing time improve the strength of the clay soil or sandy or silty soil containing at least seven percent clay because of the release of the existing silica and alumina in the clay (Talluri 2013). The sulfate attack in stabilized soil containing gypsum and sodium sulfate which are sulfate minerals produces a highly expansive crystalline mineral named Ettringite ($\text{Ca}_6[\text{Al}(\text{OH})_6]_2(\text{SO}_4)_3 \cdot 26\text{H}_2\text{O}$) and Thaumascite ($\text{Ca}_6[\text{Si}(\text{OH})_6](\text{SO}_4)(\text{CO}_3)_2 \cdot 24\text{H}_2\text{O}$). These chemicals are unstable sulfate minerals, that after being exposed to hydration, expand. Based on this fact, the researchers call the lime treated sulfate-rich soils as “manmade expansive soil” (Puppala et al., 2012). This Phenomenon results in differential heaving and distress-induced cracking of pavements and spread footings. While some protection methods against sulfate attack have been introduced, based on the sulfate exposure level (ACI 1982; DePuy 1994), the chemical reactions and products have not completely been investigated.

Although the number of researches on this subject is limited, a little guidance about dealing with this problem is available. There are some factors effective when stabilized soils are prone to sulfate attack the same as cement concrete. These factors are the pH value, moisture availability, temperature, sulfate levels, and clay mineralogy, which should be determined when the sulfate attack is impending in the soil.

In Texas also, there are a lot of cases in which damages have been observed in several roads, pavement and parking lots, which were the result of some calcium-based stabilizers (Perrin 1992). Summarizing the damaging outcome of three projects, it is concluded that the areas of poor drainage had more severe damages. Also, the bumps or ridges caused by heaves were 300 mm deep in both the transverse and longitudinal directions.

Sulfate Heave Case Histories

Joe Pool Dam, Texas

Many heaving problems were observed in several park roads in Joe Pool Lake during 1988 and 1989 (Perrin, 1992). The area's soil was clean clays and clayey sand belonging to Eagle Ford Shale formation with less than 3% swelling clay minerals. The subgrade layers of the pavement were stabilized with 5-6% lime. Although, the soil barely had sulfate content, the base material was lime-treated and

contained 2,000-9,000 ppm sulfate. The heaving phenomenon is obvious in Figure 2-1. It was investigated later that Ettringite and Thaumascite were the main cause of the heaving. They had recompact the road, but the issue kept happening. At last, they have replaced the entire lime treated layer with gravel base and non-expansive fill ending the problem of heaving.



Figure **Error! No text of specified style in document.**-1 heaving in lime treated subgrade (Reproduced from Talluri, 2013)

Sulfate heave issues at DFW airport, Texas

In Dallas/Fort Worth international airport (DFW), one of the taxiway sections depicted signs of heave. Areas of heave were considered along both shoulders of the taxiway section. The main taxiway section didn't show any signs of heave that is mainly because it was made of rigid reinforced concrete pavement overlaying a four to twelve-inch lime-treated base course. The natural subgrade was shale made of clay with sandy seams and occasional Gypsum deposits. The base course consists of the native subgrade soil stabilized with lime.

Several pavement cracking related to heave distress were observed and their range was 5cm to 30 cm. The heave pattern was that much irregular that sometimes it affected the diameter of one to two feet in some areas. There were some other cracks observed near the junction between rigid concrete and asphalt concrete sections. Although, in some locations, considerable lateral movement of edge has occurred, the rigid pavement was in a good condition with only few minor cracks.

The heave phenomenon in this area was investigated and the reasons were found to be the location of drainage ditches near the shoulders and the topography of the site. Due to the rain fall in the last six months of 1996 and early 1997, the increased water level under the pavement section can contribute to heaving by means of helping chemical reactions needed for formation of Ettringite and Thaumascite

compounds. Also, the west shoulder depicted more damage than the east shoulder. One reason for that can be the water pooling near the west shoulder. Also, the east shoulder was prone to better drainage because of the special topographical features.



Figure **Error! No text of specified style in document.**-2 heave distress pattern on west shoulder of taxiway - (Reproduced from Talluri, 2013)

Sulfate Attack on a Tunnel Shotcrete liner, Dallas, Texas (Talluri, N. (2013))

As cracking and water leakage was reported in a tunnel shotcrete in Dallas, Texas, a white powder material and gel-like substance were observed on the shotcrete liner. (Puppala et al.2010) (Fig 2-3).



Figure **Error! No text of specified style in document.**-3 Distress region on tunnel lining (C-3), (Puppala et al.2010)

The studies depicted the presence of Ettringite and Thaumassite. Since the safety of the tunnel was threatened due to sulfate presence and continuous moisture leakage, the continuous monitoring of the tunnel heave and using sulfate resistant cement Type V is suggested.

Stewart Avenue, Las Vegas, Nevada

Two years after construction of Stewart Avenue Street, Las Vegas, NV, severe heaving was observed, with maximum distress of 30 cm (Hunter 1998).

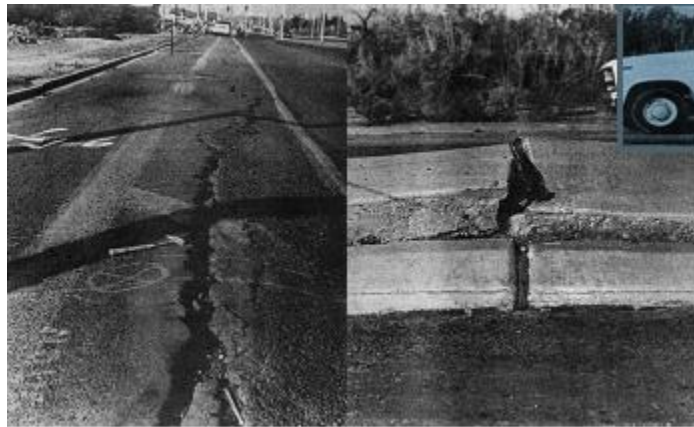


Figure **Error! No text of specified style in document.**-4: Stewart Avenue cracks (Hunter 1988)

Based on the forensic investigations, the cause of the heaving was found to be the reaction between lime and sulfates. Also, the presence of the Thaumassite was observed by means of (XRD) and (SEM) studies, since it can be formed below 15 degrees Celsius.

Stabilization of High Sulfate Soil

One of the techniques suggested for stabilization of the sulfate-rich soils is pre-compaction mellowing technique. Mellowing period is an important variable in the low-strain (linear) stiffness response of chemically stabilized soils (Semane 2014). The reason for success of this method was that, during the mellowing period all swelling happened. Also, there were no more sulfates after compaction, since all sulfates were consumed during the mellowing period.

Double application of lime

The double application of lime is effective in some soils since first the lime treatment leads to Ettringite formation, while the second application forms pozzolanic compounds which help the soil with

stabilization function. However, three days curing between the lime application should be considered. Since double application resulted in more heaving in some cases, it should be considered that this method is proved useful just for the soils with sulfate content up to 7000 ppm (Kota et al., 1996; Pas Harris et al.2004).

Combined Lime and Cement Treatment

Based on one study that was performed at the University of Texas at Arlington, the combination of lime and cement treatment on high plasticity clay soils at Arlington, resulted in increased strength and reduced shrinkage and swell in comparison with the lime treatment alone.

Stabilization with Low Calcium Based Stabilizers

The sulfate-induced heave is the result of calcium based treatment such as lime and cement. Fly ash is another calcium-based stabilizer. It is categorized in two classes of C and F, and their main difference is the availability of free calcium which is higher in class C. For that reason, class F fly ash is more appropriate for soil stabilization. Overall, the Fly ash usage decrease the plasticity index of the soil which leads to the swell and shrinkage decrease. Also, some research has been done on non-calcium based stabilizers, but most of them were found to be expensive, even some more costly than replacing the subgrade.

One of the stabilizers with no calcium can be named as ground granulated blast furnace, GGBFS. Replacement of cement or lime with GGBFS has been reported successful by many researchers. Appropriate added amount of GGBFS can help stabilize the soil by reducing the PH of the system and improving cementation properties.

Sulfate Heave Mechanism

As mentioned before, Ettringite is formed by reaction of sulfates in the soil and calcium and alumina existing in clay. This chemical has 26 molecules of water and can expand to 137% of its original volume. (Little et al.2010). Also, the formation and growth of Ettringite can lead to material softening. Depending on the time and PH during formation, Ettringite can have needle-like, lath-like, and rod-like shape. Figure 2-5 shows a needle-like structure of Ettringite with SEM. Also, mineral structure of Ettringite is depicted schematically in figure 2-6.

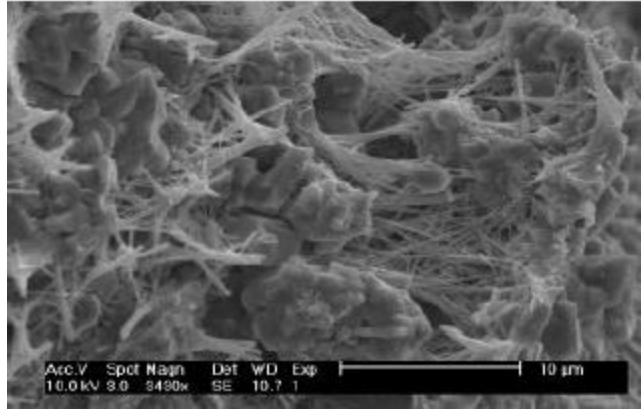


Figure Error! No text of specified style in document.-5: SEM photograph of needle-like Ettringite (Mallat, 2006)

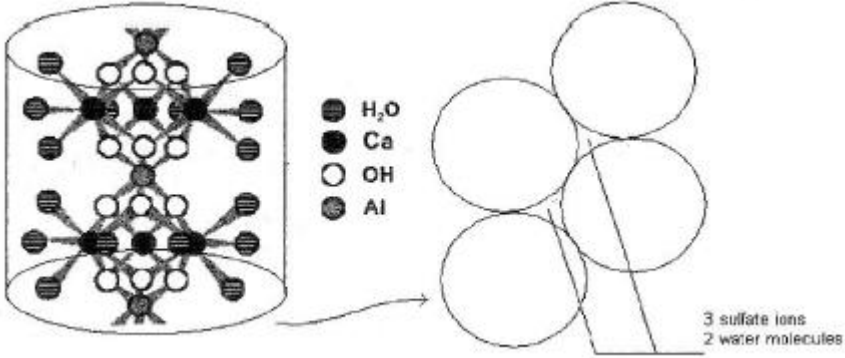


Figure Error! No text of specified style in document.-6: schematic of the mineral structure of Ettringite (Intharasombat, 2003)

Chapter 3 - Fundamentals of Resonant column (RC) Testing Technique

Basic components of Proximator-Based Resonant Column device

The way the proximator RC do the tests is that first a harmonic torsional excitation is applied to the top of the specimen by a motor, which works as an electromagnetic loading system. Also, the response curve is generated over a range of frequencies after a torsional harmonic load with constant amplitude is applied. On the other hand, measuring the first-mode resonant frequency, the shear wave velocity is measured, from which and the soil density the shear modulus can be calculated. The damping ratio can be calculated using half-power bandwidth.

The proximator system is capable of measuring shear modulus from low to high amplitude range strains. The system includes five major components: 1: the main cell, 2: servo controller and acquisition system, 3: deformation sensor, 4: resonant column software, and 5: computer unit.

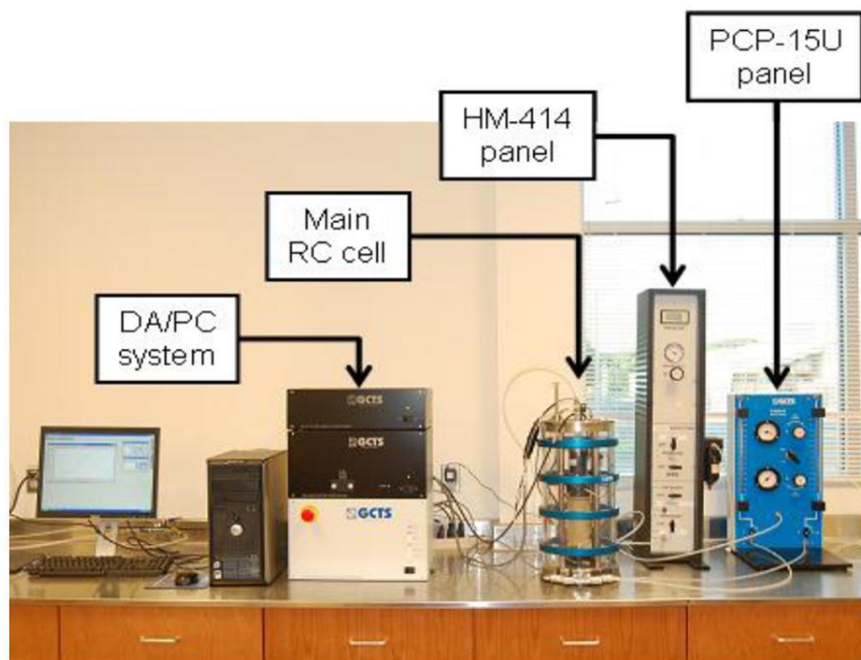


Figure **Error! No text of specified style in document.**-7: General layout of the proximator-based RC device (BRAVO, A. (2013))

Resonant column main cell

The resonant column main cell's four columns are designed for assembly as shown in Figure (3.2). Two of them has the function as displacement channels both for the driver system and displacement sensor. The external cell wall is made of transparent acrylic plastic reinforces the cell as shown in Figure (3.4). The

maximum allowed confining pressure is 1000 KPa. For making connections between the specimen and the electronic components, which are used for transferring internal angular displacement/velocity, axial deformation and torque, some feed connectors are utilized, which can be seen in Figure (3.2). Also for preventing the air entrance into the sample, a drainage system at the top and bottom of the sample was arranged.

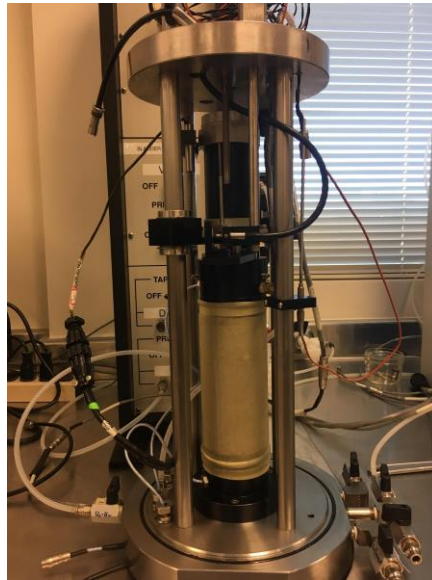


Figure Error! No text of specified style in document.-8: Main cell's columns



Figure Error! No text of specified style in document.-9: Acrylic plastic reinforcement for the cell

Electrical Servo motor driver

An electrical servo motor driver is utilized to apply torsional loads with a ± 2.33 KN-m (peak) capacity and 300 -Hz frequency. There is a servo amplifier for closed-loop control of torsional load or angular deformations, which is installed on an internal floating frame for large vertical deformations, as shown in Figure (3.4).

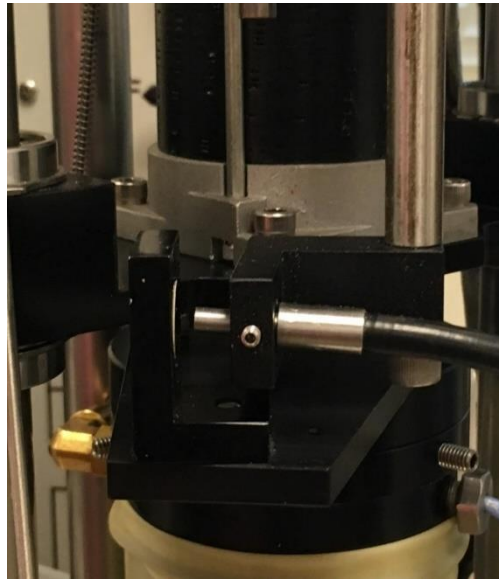


Figure **Error! No text of specified style in document.**-10: Electrical servo motor driver

Digital Servo Controller and Acquisition System

The Digital Servo Controller and Acquisition System, which is named GCTS SCON-1500 Digital System Controller, includes a lot of digital electronics. The software operates the settings and configurations. Angular and vertical displacement data are controlled, activated and stored by the system.

The SCON-1500 model DA/PC consists of a microprocessor based digital servo controller, data acquisition, function generator, and a digital I/O unit, as s shown in Figure (3-5).



Figure Error! No text of specified style in document.-11: GCTS SCON-1500 Digital System Controller

There is a C.A.T.S software, which monitors the performance of the resonant column. Also, the software registers and stores the data resulted from the tests as shown in Figure (3-6). Indeed, the soil properties including shear strain, shear modulus and damping ratio can be calculated for shear strain ranging from 10^{-4} % to 10%, as shown in Figure (3-7).

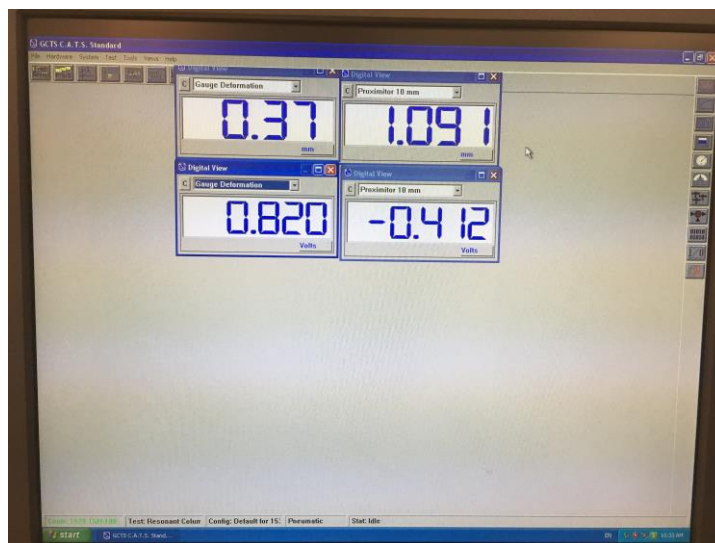


Figure Error! No text of specified style in document.-12: C.A.T.S software environment

Test Results: ,Completed
Axial Deformation: ,0.02,mm
Resonant Frequency: ,78.00,(Hz)
Max Shear Strain: ,0.00,(%)
Shear Velocity: ,86.85,(m/sec)
Shear Modulus: ,13.68,(MPa)
Damping Ratio: |
Free Vibration Decay: ,N/A
Half Power Bandwidth: ,5.45,(%)
Average Frequency from Free Vibration Data FFT Analysis: ,44.05,(Hz)
Natural Frequency:
from Resonant Frequency and Phase Shift: ,106.00,(Hz)
from Resonant Frequency and Free Vibration Decay,N/A
from FFT Frequency and Free Vibration Decay,N/A
Tested Frequencies: ,91

Figure **Error! No text of specified style in document.**-13: Test results obtained from the software

Resonant Column Software

The software is called CATS-RC and its function leads to obtaining dynamic response of soil specimens that are tested in RC in two ways. One is by assessing the resonant frequency and the other is by analyzing the data obtained from free vibration decay from which damping ratio can be determined.

The following variables were obtained by using CATS-RC.

- a) Resonant frequency (Hz)
- b) Shear wave velocity (m/s)
- c) Shear modulus (MPa)
- d) Maximum shear strain (fraction)
- e) Damping Ratio-Free vibration decay (%)
- f) Predominant frequency from free vibration data FFT Analysis
- g) Damping Ratio-Half power bandwidth (%)
- h) Natural frequency –from resonant frequency and free vibration decay (Hz)
- i) Natural frequency –from resonant frequency and phase shift (Hz)
- j) Natural frequency –from FFT frequency and free vibration decay (Hz)

Figure 3-8, demonstrates the Frequency response curve obtained by the software.

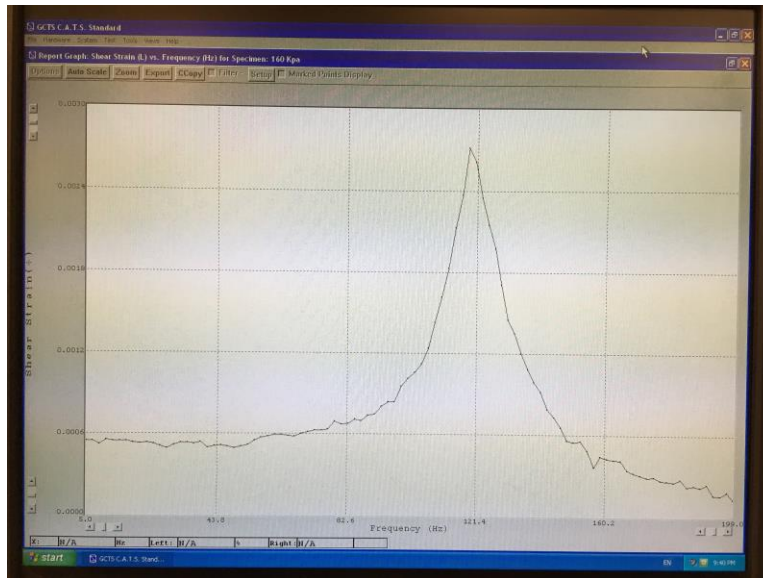


Figure Error! No text of specified style in document.-14: Frequency response curve obtained by the software

The software inputs which are required are some data regarding soil and specimen properties as shown in Figure (3.9). Also, some other inputs such as starting frequency, stop frequency, cycles until steady state and the Torque output amplitude. As soon as a test is performed and the graphs are resulted, one can import the calculated parameters.

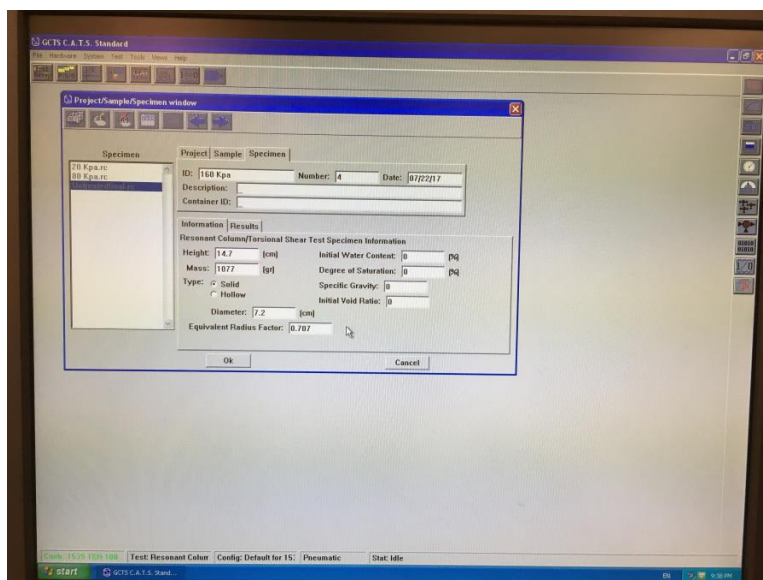


Figure Error! No text of specified style in document.-15: The specimen properties required for the software

Pressure control monitoring system

The HM-414 and the PCP-15U pressure panel's function is to regulate the external and pore-air pressure conditioning of the sample and as mentioned before the maximum tolerable pressure for the cell is 1 MPa. The PCP-15U pressure panel is shown in Figure (3-10). Also for removing the air, the panel has an equipment for flushing the air out of the cell as shown in Figure (3-11).



Figure Error! No text of specified style in document.-16: PCP-15U pressure panel



Figure Error! No text of specified style in document.-17: The air flushing equipment

Calculation of Shear Modulus

After the resonant column test the result converted to text file, and imported to excel data to plot the required graphs. The shear modulus of the soil was calculated by the software using the formula shown below:

$$G = \rho (2\pi L)^2 \left[\frac{f_r}{\beta} \right]^2$$

Where: G = shear modulus

L = length of specimen

f_r = maximum resonant frequency

$$\beta^2 = \frac{I}{I_0}$$

ρ = the total mass density of the soil

Calculation of Damping Ratio

The damping ratio of the specimen was calculated using Bandwidth Method (Richard et al., 1970). For that the half power point ($0.707 Y_{\max}$), (Fig 3-12). The software calculates the damping ratio, itself using the following formula:

$$D = \frac{1}{2} \left(\frac{f_2 - f_1}{f_r} \right)$$

Where:

f_r = the maximum resonant frequency (Hz)

f_1 and f_2 = Half-power frequencies (Hz)

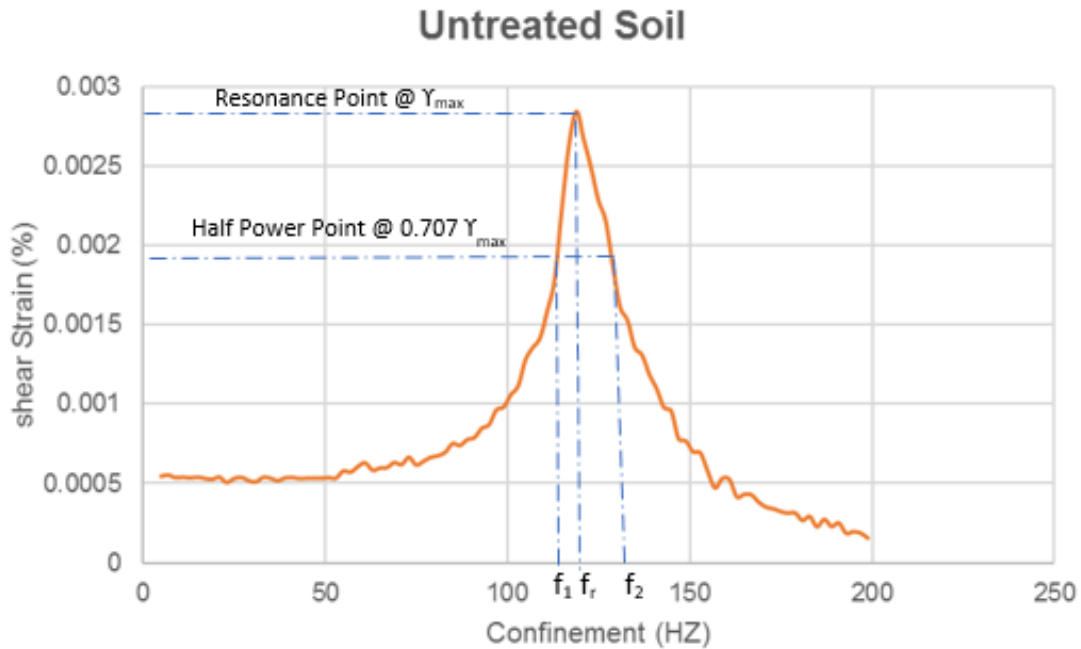


Figure Error! No text of specified style in document.-18: bandwidth method determination of damping ratio (D)

Summary

The basic components of the RC device are: Main Cell of the Resonant Column Apparatus, 2 Proximitors, 3 Digital Servo Controllers, and Acquisition System, Resonant Column Software, and Pressure control monitoring system. The frequency response curve can be obtained as soon as running a test, and the data can be converted to MS Excel text and the required stiffness parameters such as: Shear modulus (G), can then be obtained. Shear modulus (G), the resonant frequency (f_r), and Material damping ratio (D) can be obtained importing the data resulted from the test.

Chapter 4 - Test Soil and Experimental Variables

Introduction

The experimental program utilized in this study's purpose is to analyze the effect of curing time on the chemically stabilized sulfate-rich clays. Seven specimens and one control specimen, which were all identical made of highly expansive, sulfate-rich clay from Sherman, Texas were stabilized with three selected stabilizers discussed in chapter, and then using the Proximitor resonant column device described in chapter 3, the tests performed. The sections in the following describes the basic engineering properties of the soil and the physical and chemical properties of the chemical stabilizers, soil preparation method for RC testing and experimental variables.

Test Soil

The soil used in this investigation was sampled from US-82, Sherman, Texas Figure 4-1. This soil is a high-plasticity, sulfate-rich clay, with natural moisture content (w) of 24%, and dry density of 91 lb / ft³, liquid limit (LL) of 75 %, plasticity index (PI) of 50%, and soluble sulfate content of 52,000 ppm, which is CH in USCS classification. Table 4-1 summarizes the soil characteristics.

Table 4-1 test soil location and properties

Soil Location	Soluble Sulfates, ppm	Atterberg Limits			USCS Classification
		LL	PL	PI	
US-82 (Sherman, Texas)	52,000	75	25	50	CH

Chemical Stabilizers

Two kinds of stabilizers were utilized in this study including lime + fly ash and cement + fly ash. The fly ash used is class F fly ash, which has low amount of calcium. The soil and stabilizers mixtures were mellowed for five days following "Pre-compaction mellowing" technique Fig 4-2. The soils were kept in the moisture-controlled environment. After five days, the soil was compacted and the specimen was prepared. Then the specimens were cured for 7 days and 14 days curing. Also, one specimen was cured for 3 days. Overall 8 tests including the untreated (control) soil were conducted.



Figure Error! No text of specified style in document.-19: US-82



Figure Error! No text of specified style in document.-20: Soil mixture wrapped with plastic bag for mellowing

Specimen Preparation

The required amount of water and the dry soil were mixed together thoroughly. The soil is then covered with a plastic bag and kept in the moisture room for the desired the mellowing period. After the mellowing period, all specimens were compacted to 72 mm diameter and around 142 mm height by means of a conventional triaxial loading frame Fig 4-3. Then the sample was extruded using Sample Extruder Device Fig 4-4. After compacting the samples, they were cured for 7 and 14 and one of them for 3 days.

4.5 Summary

The soil selected for this study is US-82 which is a high-plastic, sulfate clay from Sherman, Texas. The reason for choosing Texas is its high plastic and containing high sulfate content soils. These factors are the most critical ones affecting the potential of sulfate-induced heaving. The stabilization methods used in this study is two different percentages of lime + fly ash and cement + fly ash. Also, the experimental variables considered in this work include different stabilizers and different curing time. Chapter 5 illustrates the experimental procedure utilized in this work and demonstrates an inclusive analysis of all test results.



Figure **Error! No text of specified style in document.**-21: Triaxial loading frame



Figure Error! No text of specified style in document.-22: Extruder device

Chapter 5 - Experimental Program and Analysis of test results

Introduction

Overall 120 resonant column tests were conducted on 10 specimens, which were made of sulfate rich clay. The experimental program followed in this work is illustrated in this chapter and the soil most important variable results which are obtained from analyzing the outputs from the test are presented including the soil's shear modulus (G_{max}), material damping ratio (D_{min}) and natural frequency (F_r).

Specimen symbolization

For simplifying reading different variables in the running of each RC test specimen, symbolizing the variables for each specimen was used. Those variables include: Stabilizer type and curing time. On the other hand, mellowing time was considered constant as 5 days for all the tests. Table (5-1) demonstrates all the notation symbols used for identifying RC test specimens. For example, the symbol of 6L_4F_5DM_7DC accounts for the fact that the specimen was treated with 6% lime+4% fly ash. Also, the soil and the water content mixture was kept in the moisture room for 5 days before the preparation of the sample. On the other hand, the sample was then cured for 7 days in the moisture room. It should be taken into the consideration that for example 6% lime means 6% lime from the overall dry soil weight. Also, the specimens were wrapped in the plastic bag and then put in the zip lock before being placed in the moisture room.

Table 5.1 testing variables and the notation used for specimens

Symbolization	Description
---------------	-------------

CONTROL	Control Untreated soil
8L-2F-5DM-3DC	8% Lime, 2% Fly ash, 5 Days Mellowing and 3 Days of curing
8L-2F-5DM-7DC	8% Lime, 2% Fly ash, 5 Days Mellowing and 7 Days of curing
8L-2F-5DM-14DC	8% Lime, 2% Fly ash, 5 Days Mellowing and 14 Days of curing
6L-4F-5DM-3DC	6% Lime, 4% Fly ash, 5 Days Mellowing and 3 Days of curing
6L-4F-5DM-7DC	6% Lime, 4% Fly ash, 5 Days Mellowing and 7 Days of curing
6L-4F-5DM-14DC	6% Lime, 4% Fly ash, 5 Days Mellowing and 14 Days of curing
3C-2F-5DM-3DC	3% cement, 2% Fly ash, 5 Days Mellowing and 3 Days of curing
3C-2F-5DM-7DC	3% cement, 2% Fly ash, 5 Days Mellowing and 7 Days of curing
3C-2F-5DM-14DC	3% cement, 2% Fly ash, 5 Days Mellowing and 14 Days of curing

Experimental Program and Procedure

All 10 RC test specimens of control and treated soil with stabilizers, which are listed above were tested in the proximator resonant column. Also, the procedure is summarized below:

Firstly, the specimen is fully compacted with the optimum moisture content and maximum dry density as it was described in chapter 4. Just after compaction, the sample was kept in a plastic wrap and a zip lock and placed in the moisture room for curing. After the curing duration, the weight and height of the sample were measured and the proximator resonant column instrument was assembled following the same step by step description in chapter 4. The initial pressure which was applied was 20 KPa for 7 hours, as shown in Figure 5-1. After this duration constant pressure application, first test was performed.



Figure Error! No text of specified style in document.-23: Applying pressure of 20 KPa

Torque value which was applied for all tests was equal to 1 pfs. The input data such as weight and height of the specimen and diameter of the specimen, a constant radius factor of 0.707 and some other parameters were defined for the program as shown in Figure (5.2), and then as the test was performed, a complete frequency response (fr) curve was generated. As a result, after exporting the data, the G_{max} and f_r were reported in a file which could be converted into excel sheet as shown in Figure (5.3). Also, the damping ratio (D_{min}) was calculated using the natural frequency and the frequency response curve.

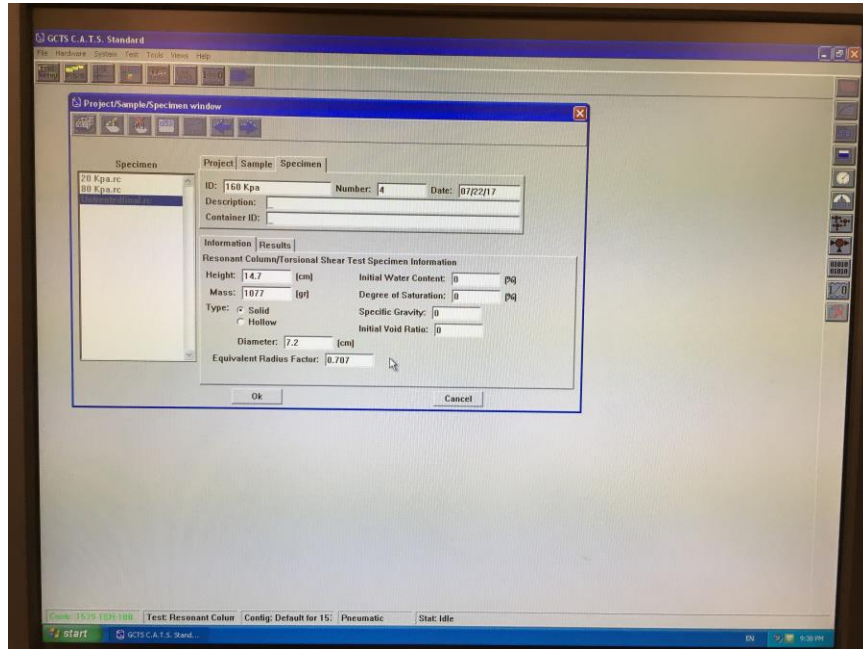


Figure Error! No text of specified style in document.-24: The specimen information input

Test Results: , Completed
 Axial Deformation: , 0.02, mm
 Resonant Frequency: , 78.00, (Hz)
 Max Shear Strain: , 0.00, (%)
 Shear Velocity: , 86.85, (m/sec)
 Shear Modulus: , 13.68, (MPa)

Figure Error! No text of specified style in

document.-25: G_{max} and f_r reported

Just after exporting the output of the test for 20 KPa pressure, a higher pressure with the magnitude of 80 KPa was applied through the pressure control panel and the same test was performed after 7 hours. The last pressure applied was equal to 160 KPa with the same duration of 7 hours.

The aim of applying 20 ,80 and 160 KPa pressure values is to specify the relation between different isotropic confining pressures and stiffens properties of the treated soil. Also, the values of 20, 80 and 160 KPa Were chosen, since the pavement and shallow foundation in various places are exposed to the same values of pressures approximately, illustrates typical frequency response curves established for specimen abbreviated as CONTROL and C3-F2-14D as shown in Figure 5-4 and 5-5. Comparing the results demonstrates that the resonant frequency (f_r) and indeed G_{max} increases with isotropic confinement.

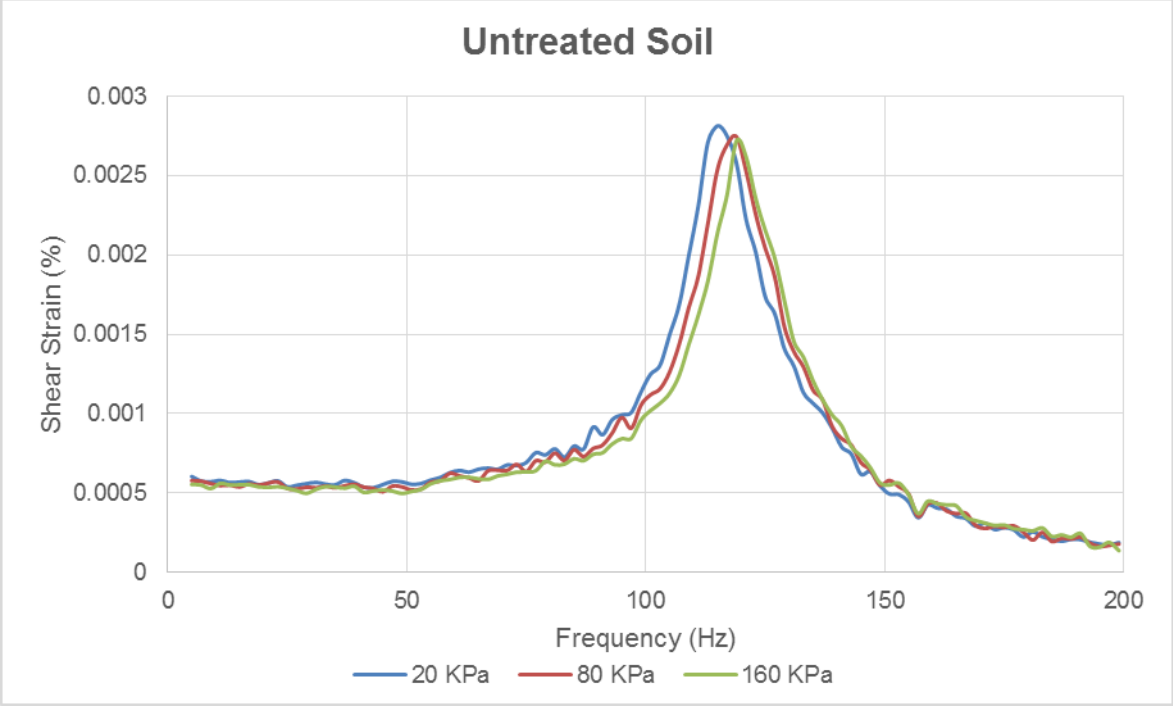


Figure Error! No text of specified style in document.-26: Typical Frequency response curves under different confining pressure for control soil.

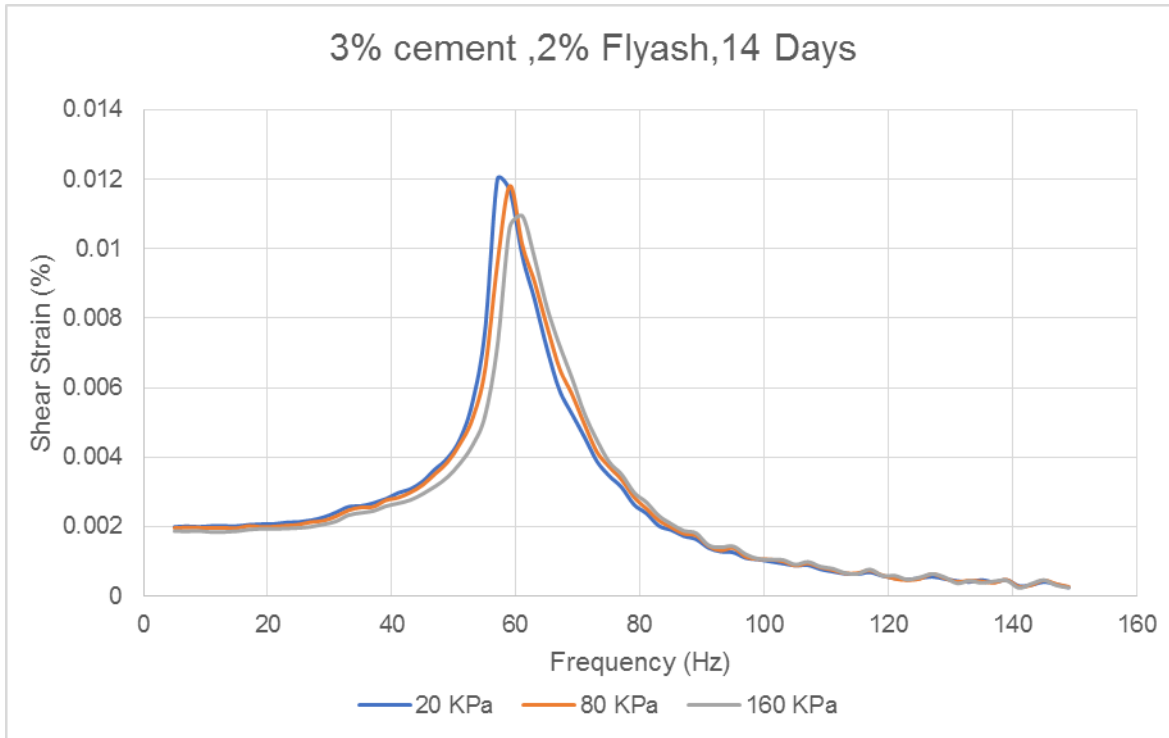


Figure **Error! No text of specified style in document.**-27: Typical Frequency response curves under different confining pressure for cement treated soil

As soon as the last RC test was performed by 160 KPa pressure, the pressure was kept constant and another 10 set of tests with constant 160 KPa pressure were performed by means of applying different Torques, the values of which were 1, 2, 3, 4, 5, 6, 7, 8, 9 and 10 pfs (Figures 5-6 and 5-7). The main goal of these tests was to approve the relation of increasing torques with depreciation of soil's stiffness properties of the control and treated specimen.

All 8 RC test specimen listed in Table (5-1), had been tested by the same steps and methods illustrated above. Also, the CONTROL soil mentioned above accounts for untreated soil which is the natural one, which was tested under same circumstance as other treated specimens including confining pressures and their duration.

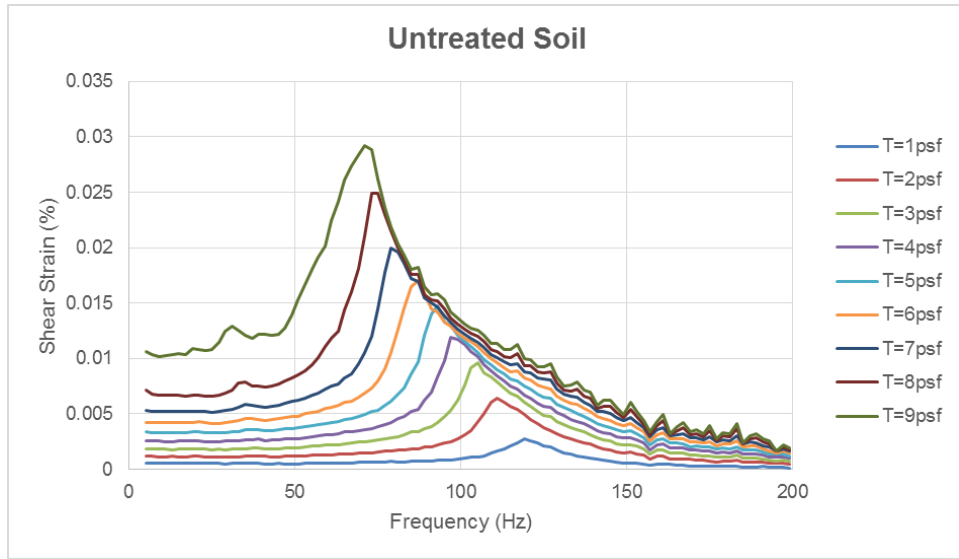


Figure Error! No text of specified style in document.-28: Typical back-bone curve from control soil

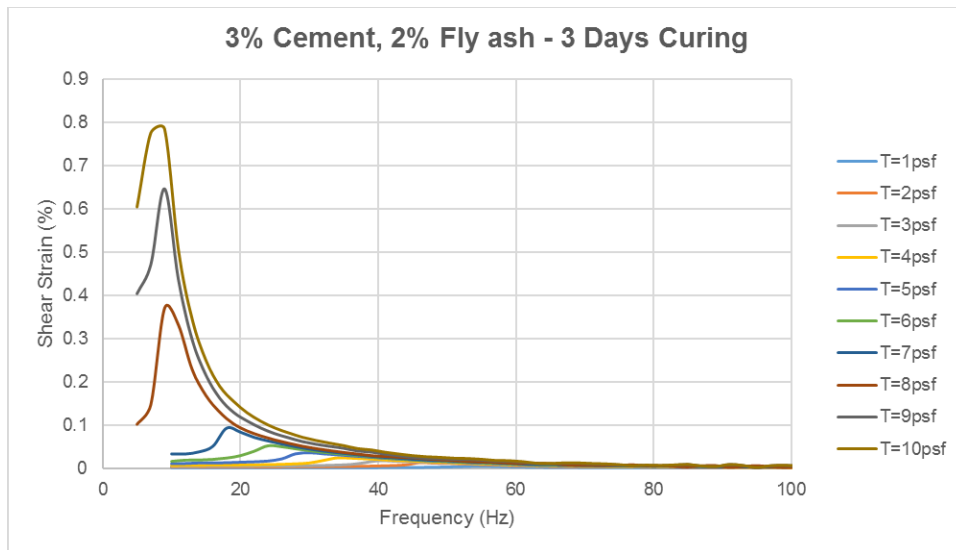


Figure Error! No text of specified style in document.-29: Typical back-bone curve from 3C_5DM_3DC

Linear Soil Response at Low-Amplitude Shear Strain

Threshold strain limit, γ_{th}

Low-amplitude shear strains account for the shear strains (γ) below one threshold limit. Since the soils stiffness properties above this threshold limit (γ_{th}) would show nonlinear behavior. On the other hand,

the stiffness behavior below this limit is linear elastic and independent of shearing strain. The most important fact about this threshold limit shear strain is that, the key soil stiffness properties such as low-amplitude shear modulus (G_{max}), and the low -amplitude (linear or minimum) damping ratio D_{min} are measured at these low amplitude shear levels.

Typical frequency response

Figure (5-8) and (5-9) demonstrates a typical frequency response curve resulted from RC test for the specimen of the control and C3-F2-14D under 80 KPa confinement pressure and the small Torque as 1 pfs. The linear dynamic properties including f_r , G_{max} and D_{min} are obtained a discussed in chapter 3. For instance, G_{max} is reported directly in test results. On the other hand, D_{min} is obtained using the half-power points (f_1 and f_2). The natural frequency (f_r) is also the point corresponding to the peak of the frequency response curve.

In this research work, each specimen listed in table 5.1, was tested under three different confinement and each pressure was held constant for around 7 hours. The reason behind this duration is that the sample needs to be approximately fully consolidated.

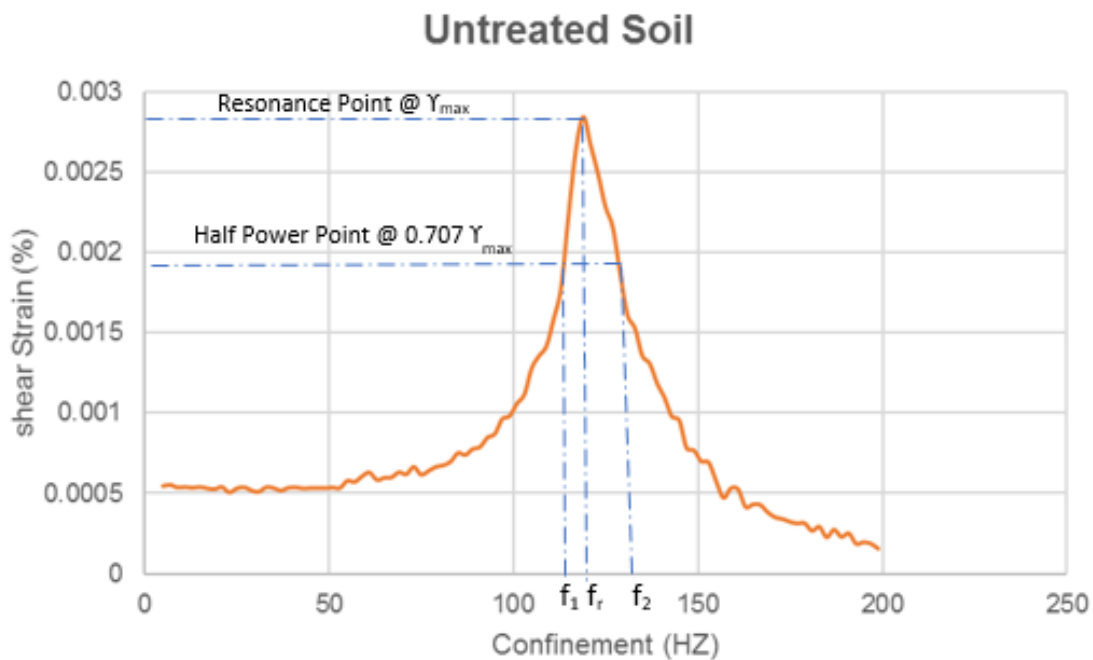


Figure Error! No text of specified style in document.-30: Typical frequency response curve from control specimen

3% cement ,2% Flyash,14 Days

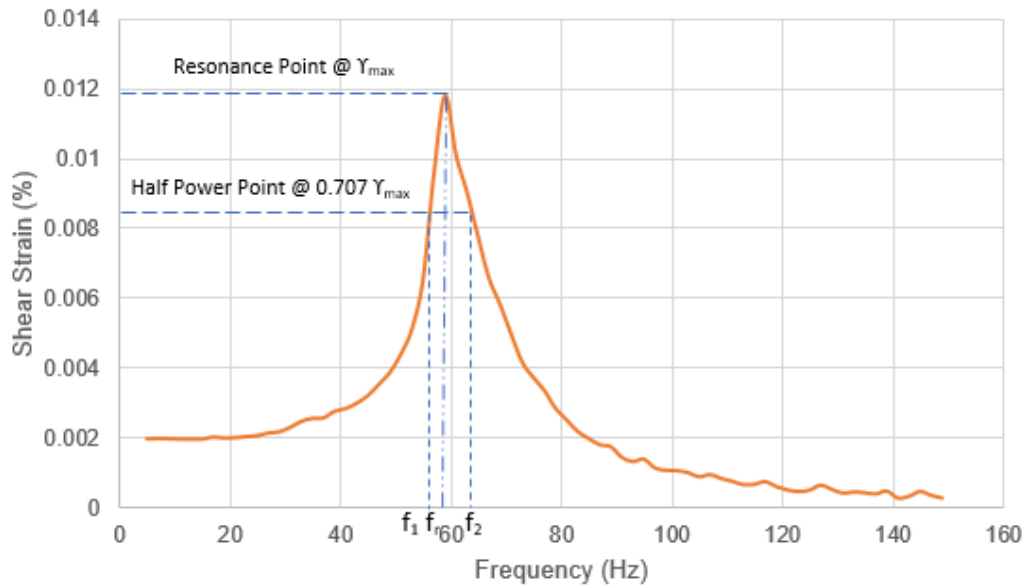


Figure **Error! No text of specified style in document.-31**: Typical frequency response curve from C3-F2-14D

Natural (control) sulfate rich soil- Untreated

The natural sulfate-rich soil which has been tested in this study is compacted at its optimum moisture content, so that the linear dynamic response of it be comparable with the stabilized soil. The soil specimen was tested for different confinement pressure and 7-hour constant duration for each confinement. Figure (5-10) and (5-11), show the relation between G_{max} and D_{min} with confinement pressure for the control soil, respectively.

It can be observed that low-amplitude shear modulus G_{max} increase with increasing confinement pressure. However, the G_{max} didn't show a substantial change from 80 to 160 KPa. Figure 5-12 and 5-13 demonstrate the variation of G_{max} and D_{min} with confining pressure for control soil.

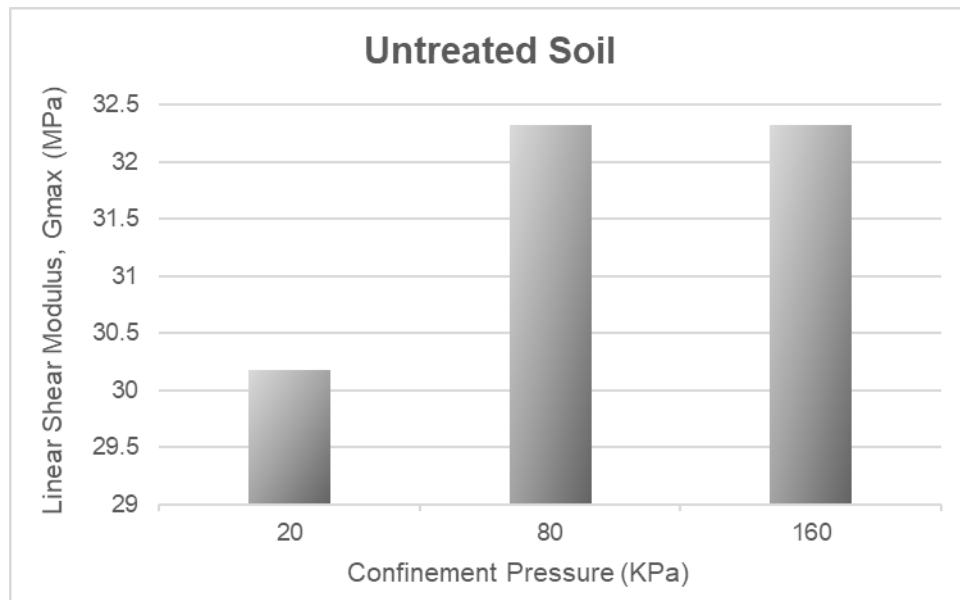


Figure **Error! No text of specified style in document.**-32: Variation of G_{max} with confining pressure for control soil

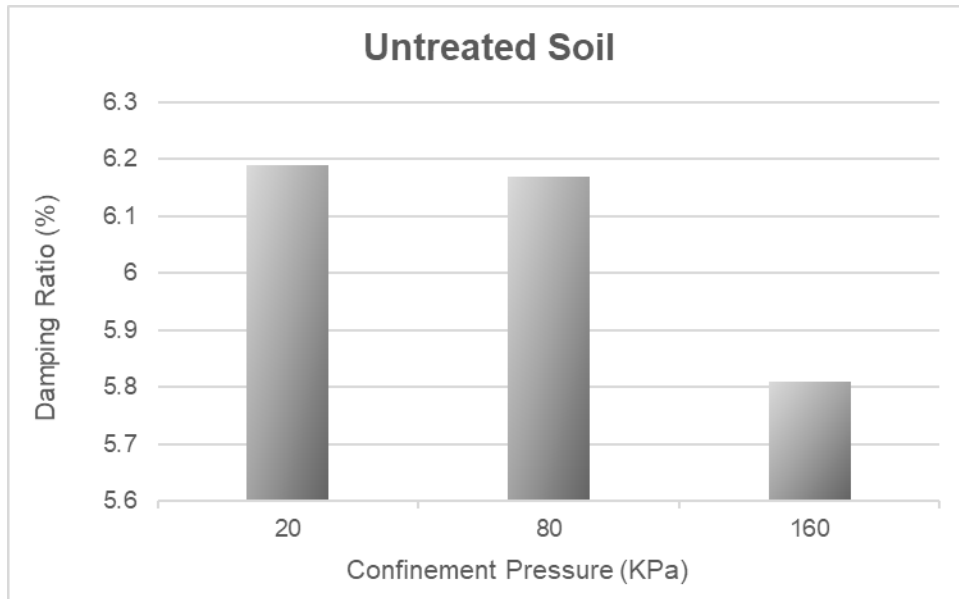


Figure Error! No text of specified style in document.-33: Variation of D_{min} with confinement pressure for control soil

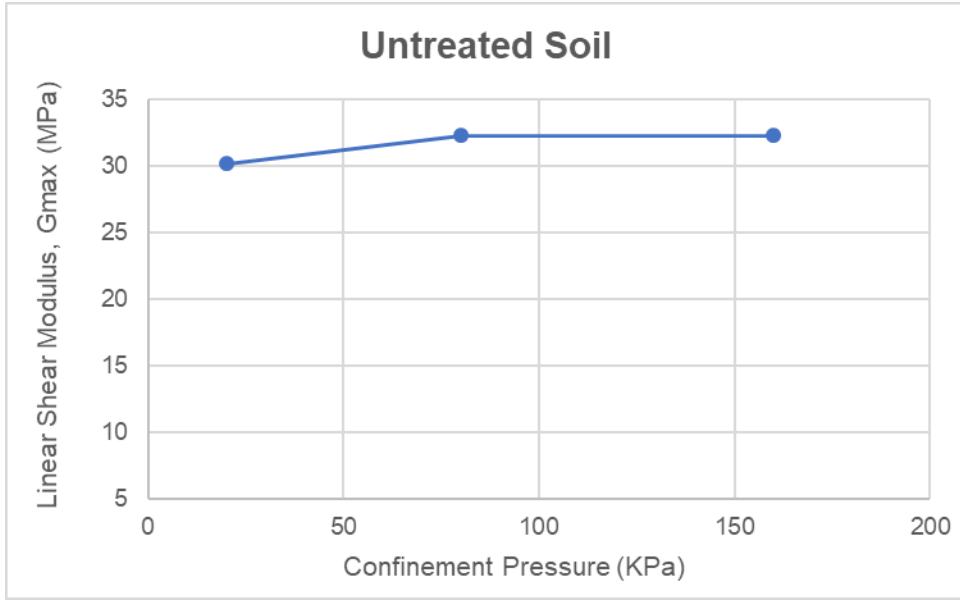


Figure Error! No text of specified style in document.-34: Variation of G_{max} with confining pressure for control soil

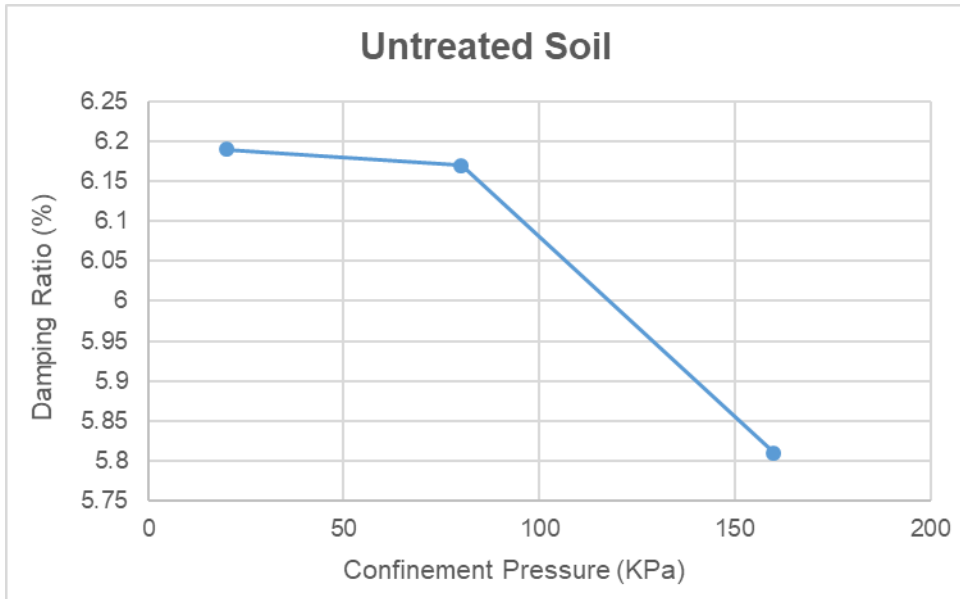


Figure Error! No text of specified style in document.-35: Variation of D_{min} with confining pressure for control soil

8% lime, 2% fly ash treated soil,

A series of tests on 8% lime, 2% fly ash treated soil has been performed with various confinement pressures of 20, 80 and 160 KPa and each test's duration was 7 hours to make the sample consolidated adequately. Also, the tests were performed for different samples of the same stabilizer with three different curing times, which were 3, 7 and 14 days.

Figure 5-14 shows the variation of G_{max} with confinement pressure and curing time. It can be inferred that the shear modulus G_{max} decreases with increasing confinement pressure for 8% lime, 2% fly ash.

On the other hand, comparing the untreated sample's G_{max} shows that, it is less than the G_{max} of 3-day curing, but more than G_{max} of 7 days and 14 days curing. Also, 7 and 14-day curing depict higher shear modulus than the control soil.

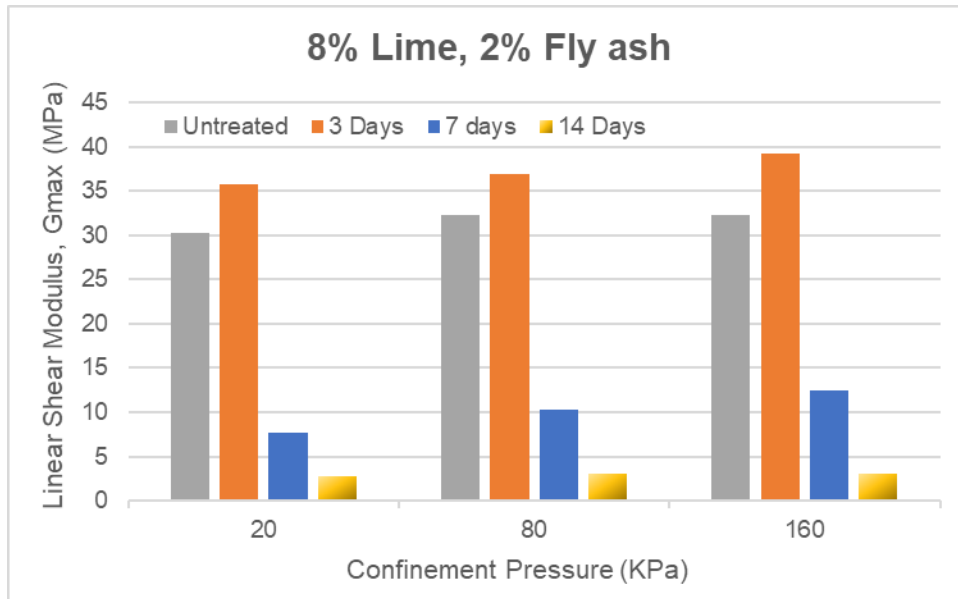


Figure Error! No text of specified style in document.-36: Variation of G_{max} with curing time for control and 8% lime+2% fly ash treated soil for different pressures

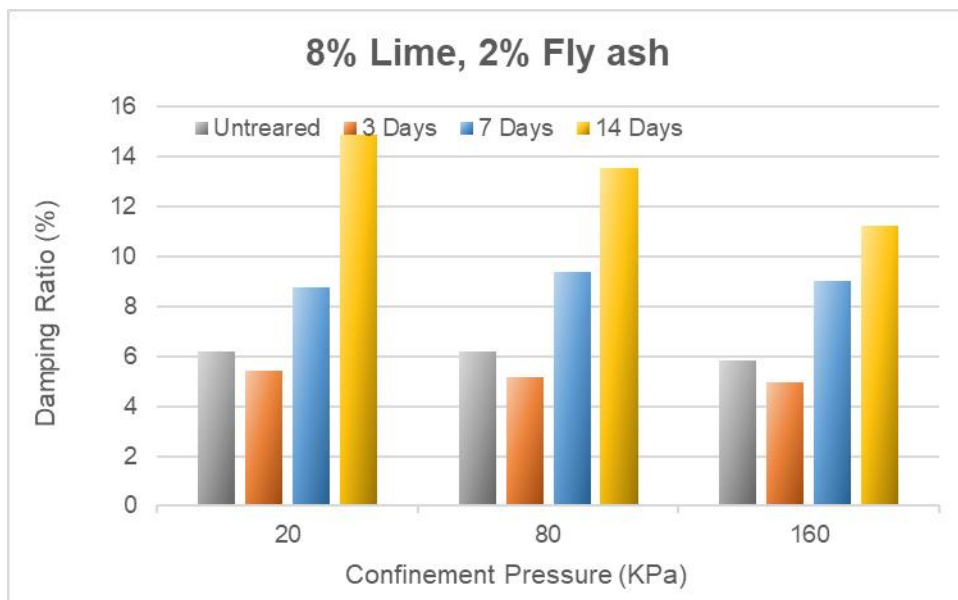


Figure Error! No text of specified style in document.-37: Variation of D_{min} with curing time for control and 8% lime+2% fly ash treated soil for different pressures

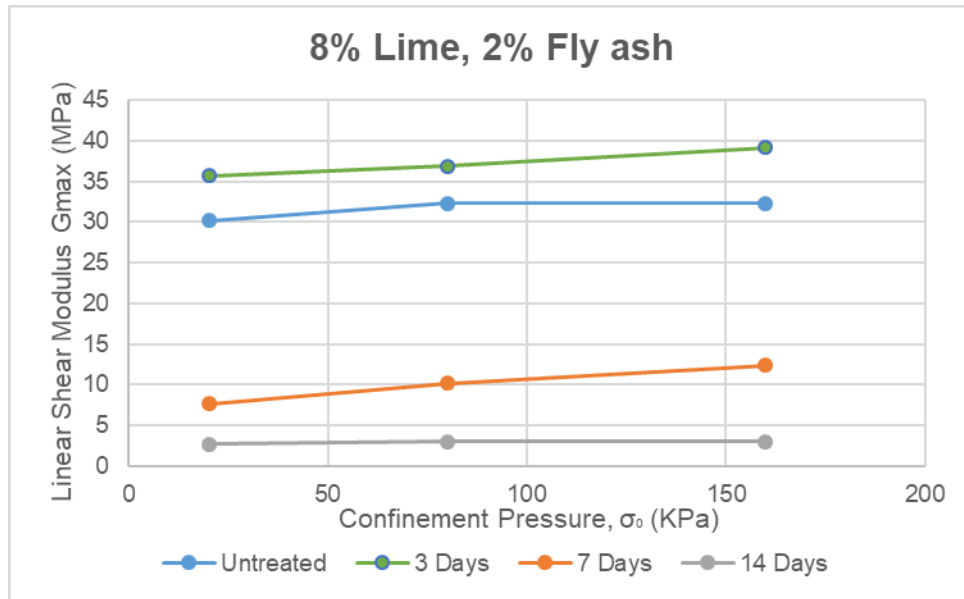


Figure Error! No text of specified style in document.-38: Variation of G_{max} with σ_0 for 8L-2F-5DM treated soil for different curing period

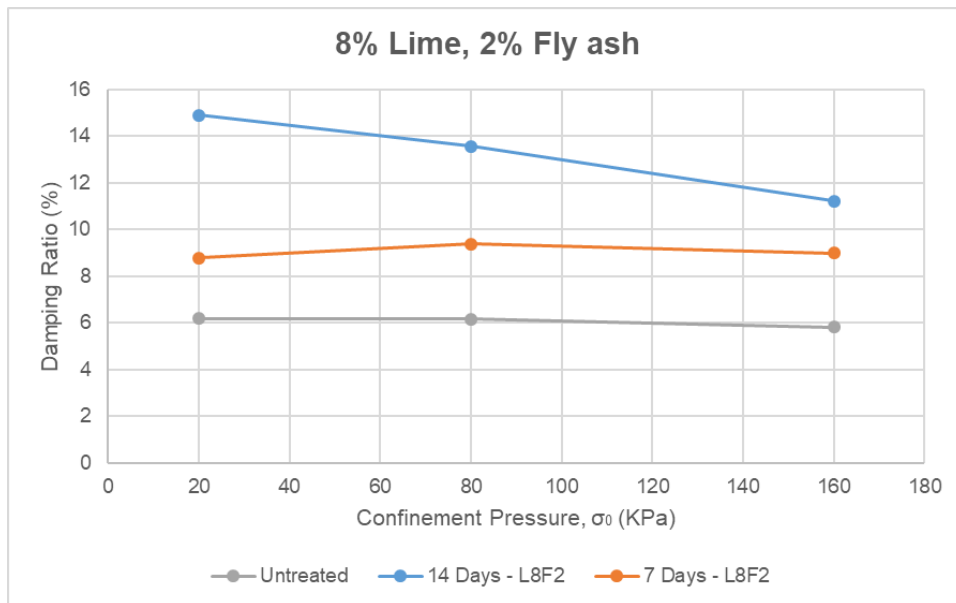


Figure Error! No text of specified style in document.-39: Variation of D_{min} with σ_0 for 8L-2F-5DM treated soil for different curing times

6% lime+4% fly ash treated soil

Figure 5-18 and 5-19 demonstrate the variation of low-amplitude shear modulus G_{\max} with low-amplitude damping ratio, D_{\min} with different confinement pressures and different curing durations. As it is obvious the shear modulus G_{\max} increases with increasing confinement pressure for 6% lime+4% fly ash specimen.

Comparing from the aspect of curing durations. It is obvious that, curing time has a direct relation with confining pressure for 6% lime +4% fly ash treated soil. That means the shear modulus increase as curing time increase for 6% lime+4% fly ash treated soil. On the other hand, the damping ratio, D_{\min} decreases as curing time increase.

The shear modulus of 6%lime+4% fly ash with 14 days curing demonstrate higher value for pressure of 160 KPa in comparison with the control soil.

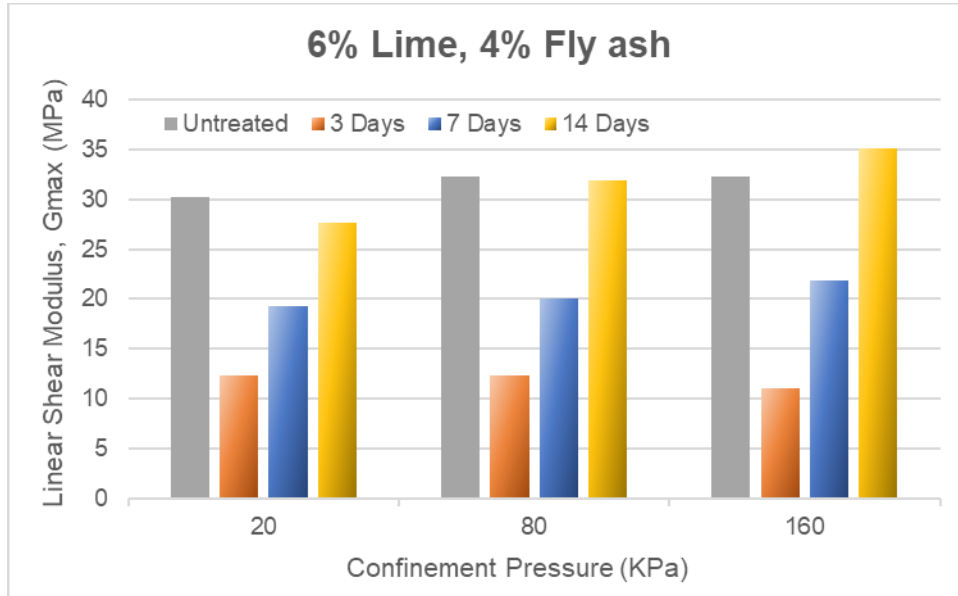


Figure Error! No text of specified style in document.-40: variation of G_{max} with curing time for control and 6% lime+4% fly ash treated soil for different pressures

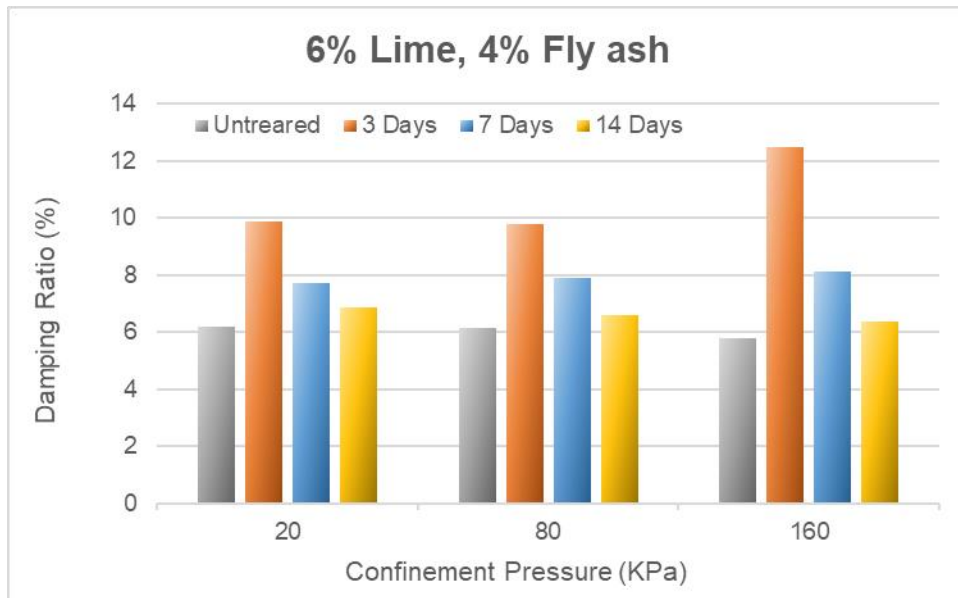


Figure Error! No text of specified style in document.-41: Variation of D_{min} with curing time for control and 6% lime+4% fly ash treated soil for different pressures

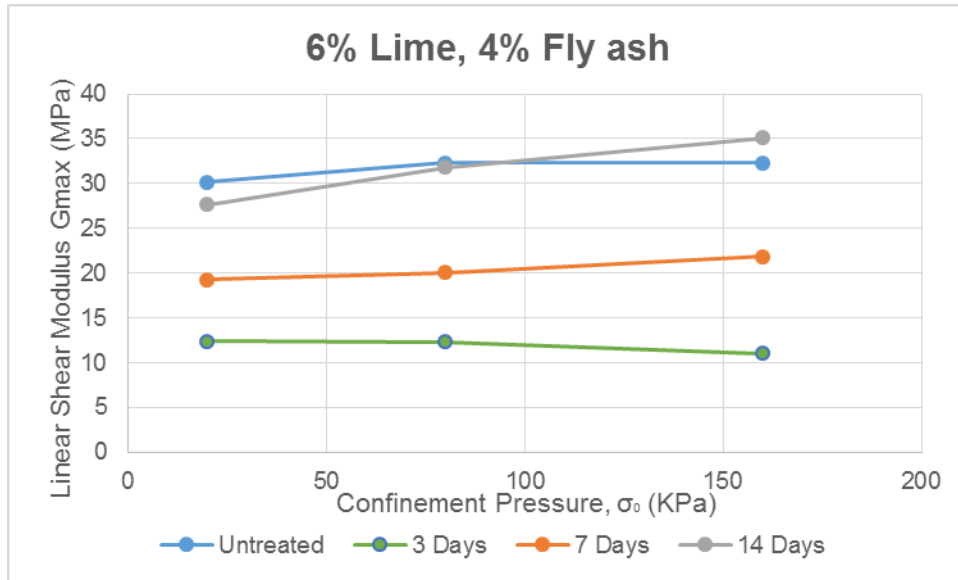


Figure Error! No text of specified style in document.-42: Variation of G_{max} with σ_0 for 6L-4F-5DM treated soil for different curing period

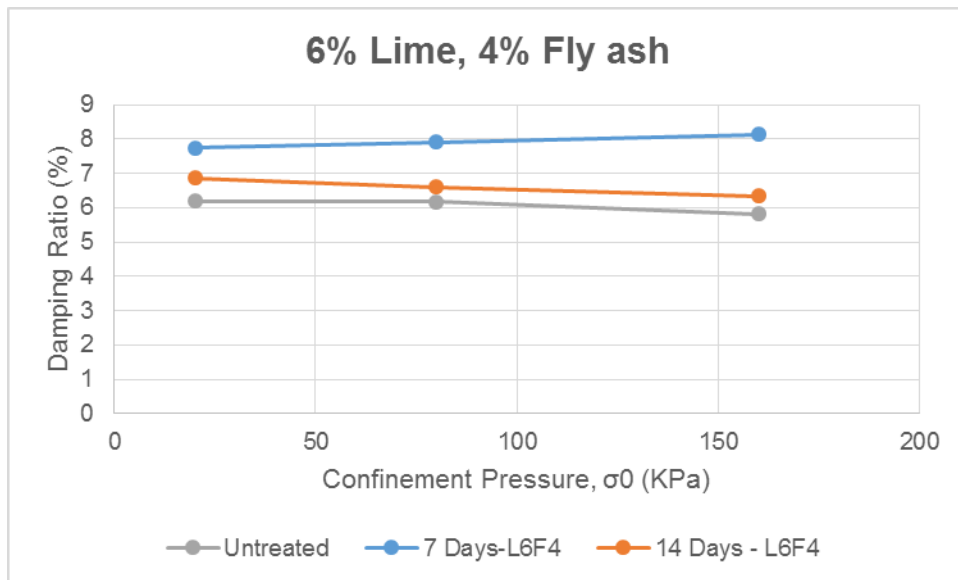


Figure Error! No text of specified style in document.-43: Variation of D_{min} with σ_0 for 6L-4F-5DM treated soil for different curing times

3% cement+2% fly ash treated soil

A set of tests has been performed on three samples with 3% cement +2% fly ash and three curing durations of 3,7 and 14 days. As shown in figure 5-22 and Figure 5-23, the results demonstrates that the G_{max} increase from 20 to 80 KPa and then decrease from 80 to 160 KPa.

Also, 7day curing shows the most G_{max} , while14 day's G_{max} is higher than 3-day curing's G_{max} . The untreated soil demonstrates a highest G_{max} among all soil treated with 3% cement+2% fly ash with different curing time.

Figures 5-24 and 5-25 show the variation of G_{max} and D_{min} with σ_0 for 3C-2F-5DM treated soil for different curing period.

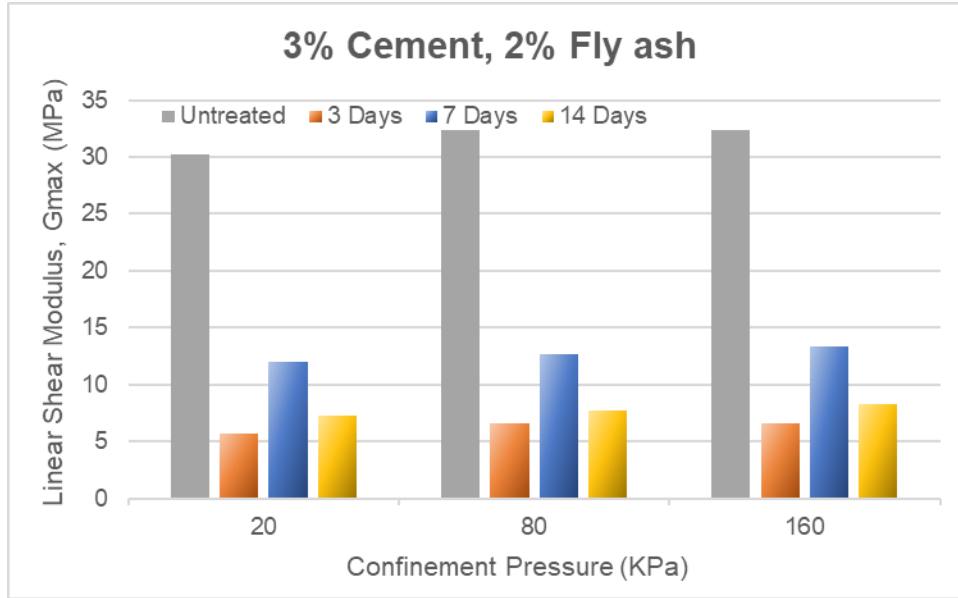


Figure Error! No text of specified style in document.-44: Variation of G_{max} with curing time for control and 3% cement+2% fly ash treated soil for different pressures

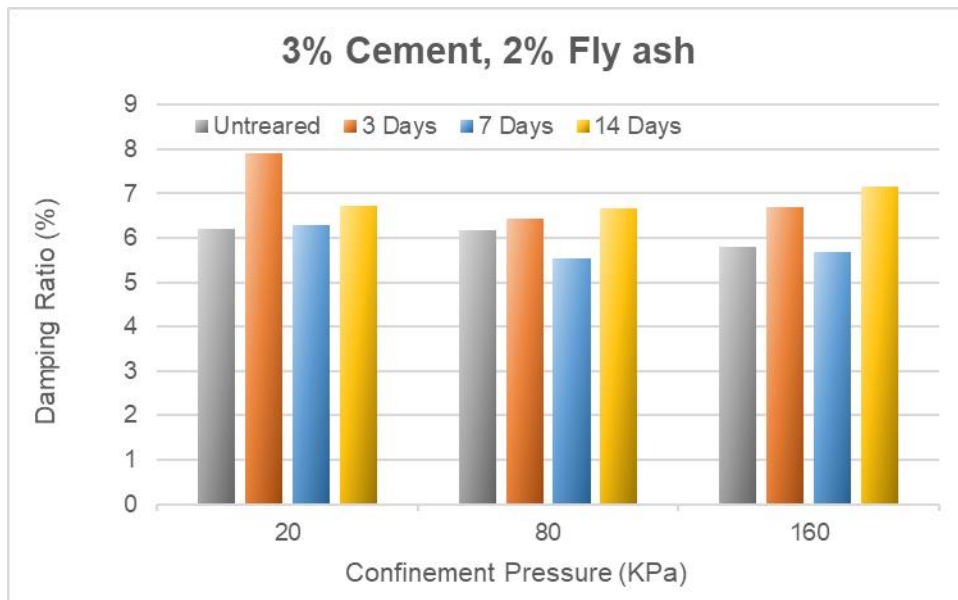


Figure Error! No text of specified style in document.-45: Variation of D_{min} with curing time for control and 3% cement+2% fly ash treated soil for different pressures

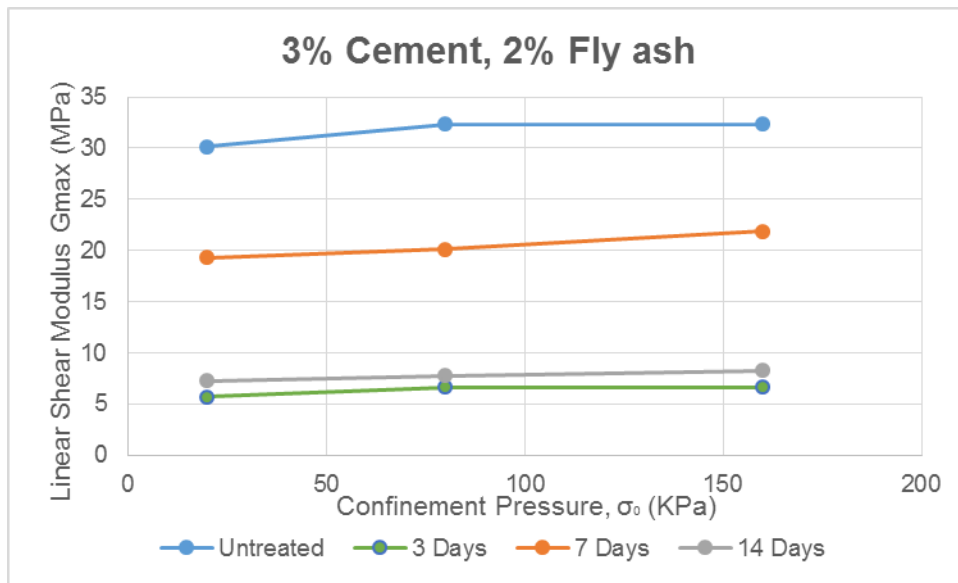


Figure Error! No text of specified style in document.-46: Variation of G_{max} with σ_0 for 3C-2F-5DM treated soil for different curing period

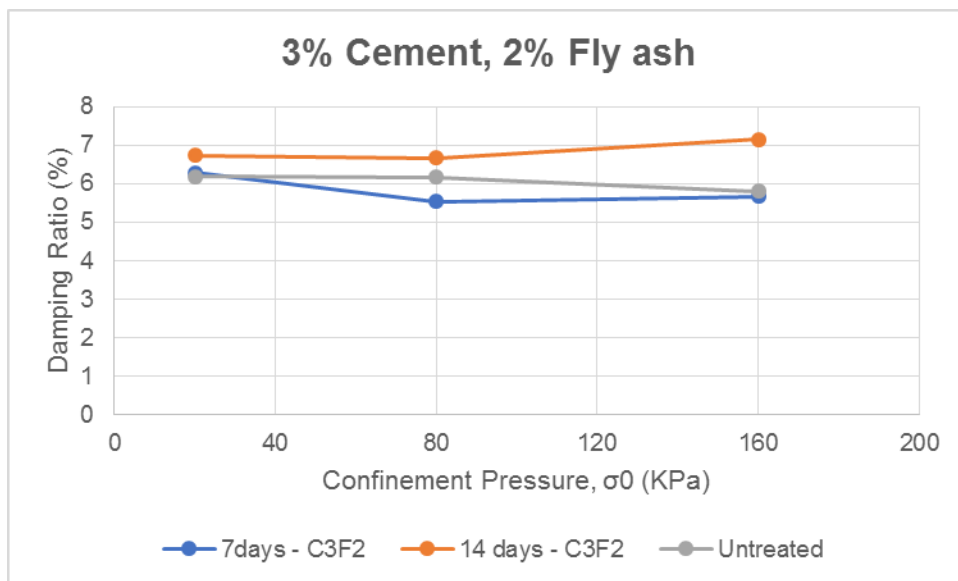


Figure Error! No text of specified style in document.-47: Variation of D_{min} with σ_0 for 3C-2F-5DM treated soil for different curing times

Curing duration

The effect of curing duration was another parameter which was studied in this project. The specimens were cured for 3, 7 and 14 days in curing room and the test results for damping ratios and shear modulus are compared in Figures 5-26 to 5-31. The results show that for 3 days curing 8% lime+2% fly ash shows the most G_{max} . Also, the untreated sample has more G_{max} than two other soils.

Comparing the shear modulus of the soils with 7 days curing and the untreated soil depict that, the untreated soil has the most G_{max} , and following that 6% lime+4% fly ash has the highest G_{max} among the other soils.

Also, comparing the treated soils with 14 days curing and the untreated, it can be inferred that the untreated soil has the highest G_{max} except for 6% lime+4% fly ash under 160 KPa confinement pressure, which has the most G_{max} .

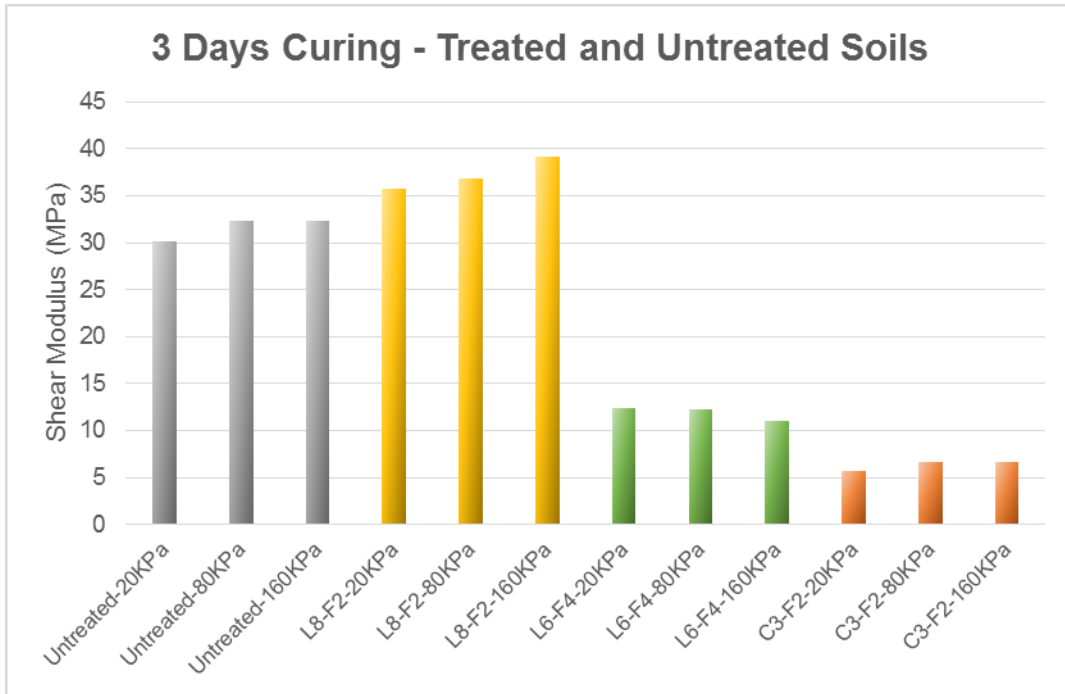


Figure Error! No text of specified style in document.-48: Variation of G_{max} with pressure for 3day curing time for control and treated specimen

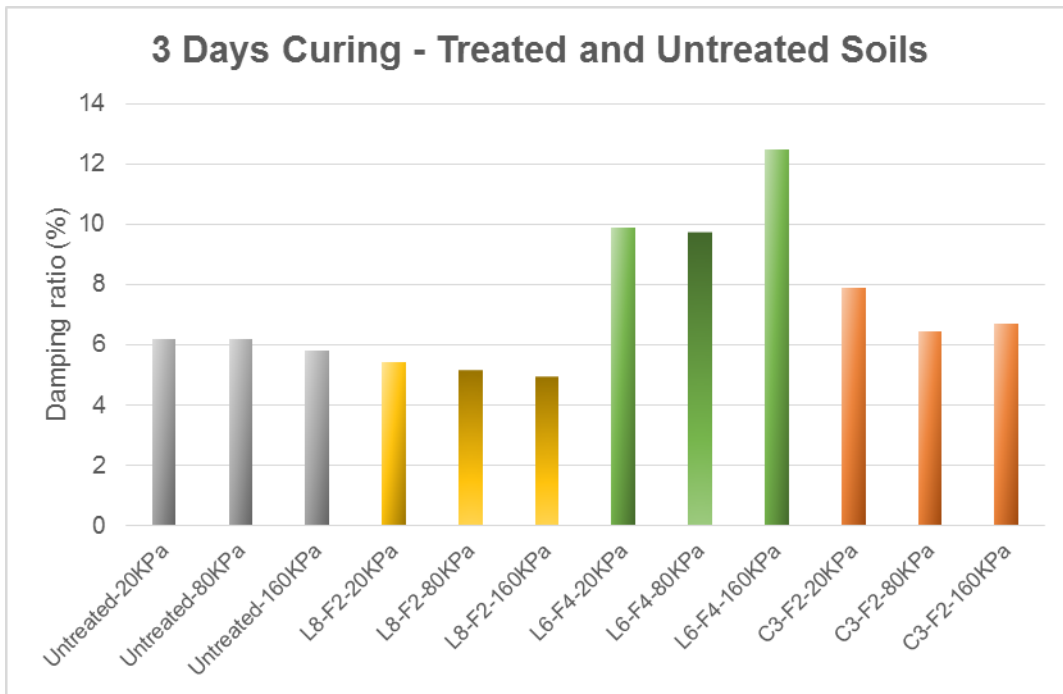


Figure Error! No text of specified style in document.-49: Variation of D_{min} with pressure for 3day curing time for control and treated specimen

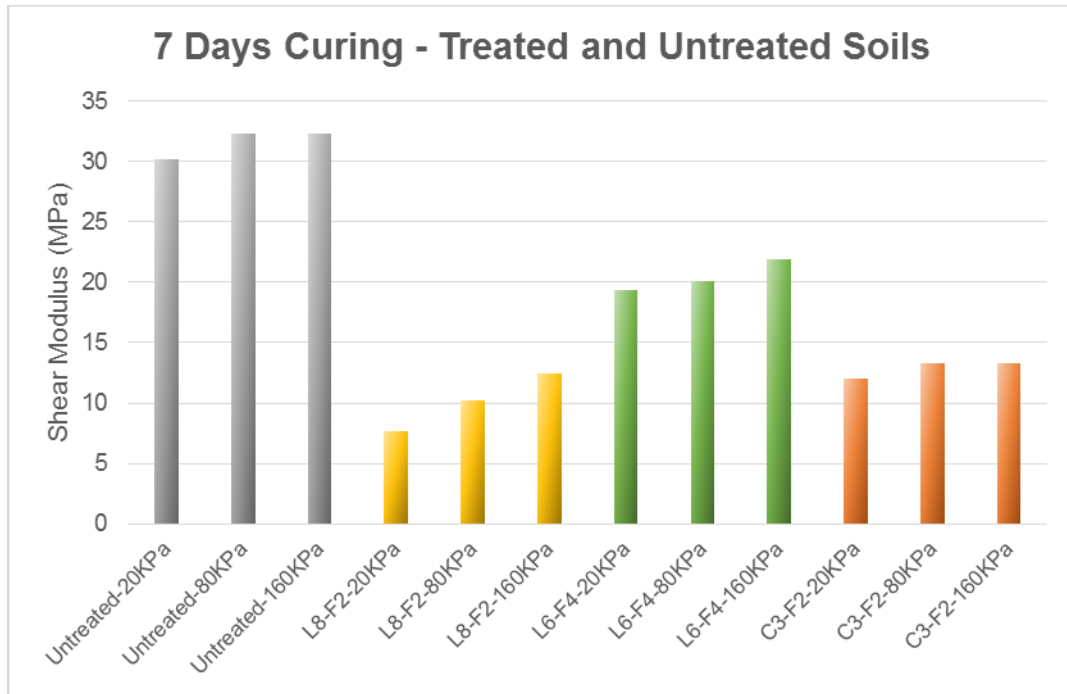


Figure Error! No text of specified style in document.-50: Variation of G_{max} with pressure for 7day curing time for control and treated specimen

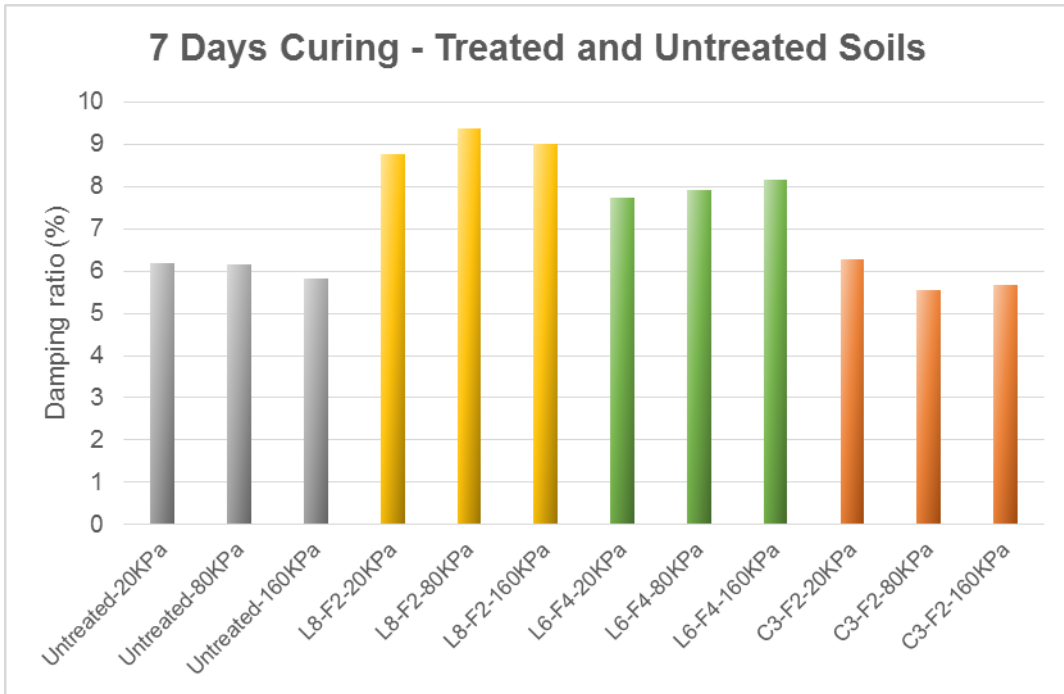


Figure Error! No text of specified style in document.-51: Variation of D_{min} with pressure for 7day curing time for control and treated specimen

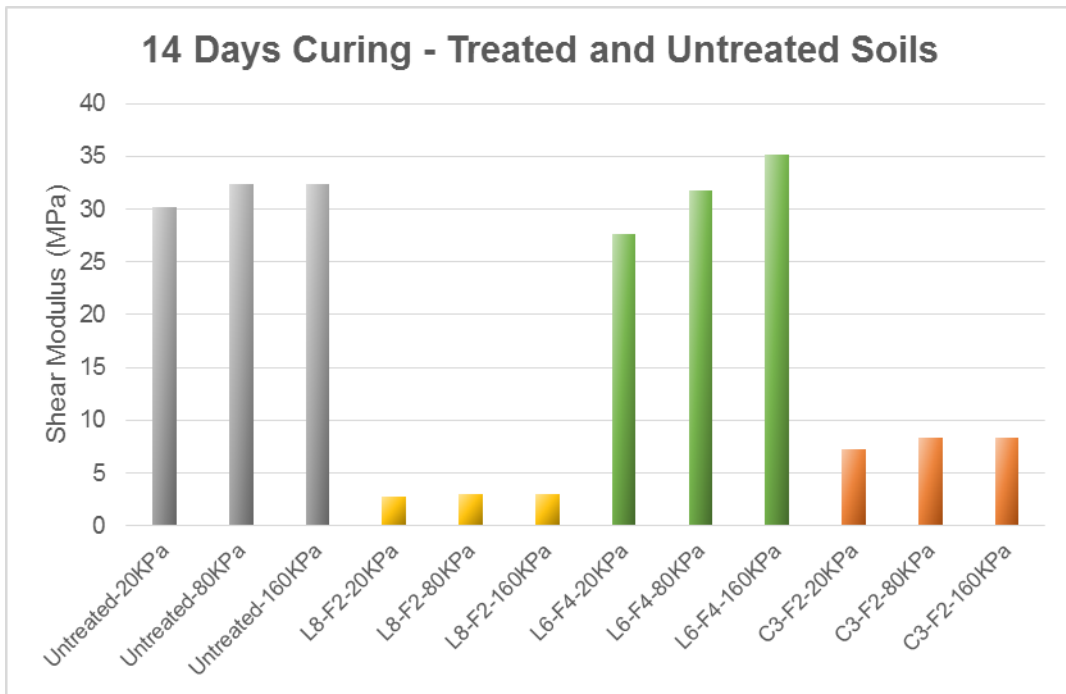


Figure Error! No text of specified style in document.-52: Variation of G_{max} with pressure for 14day curing time for control and treated specimen

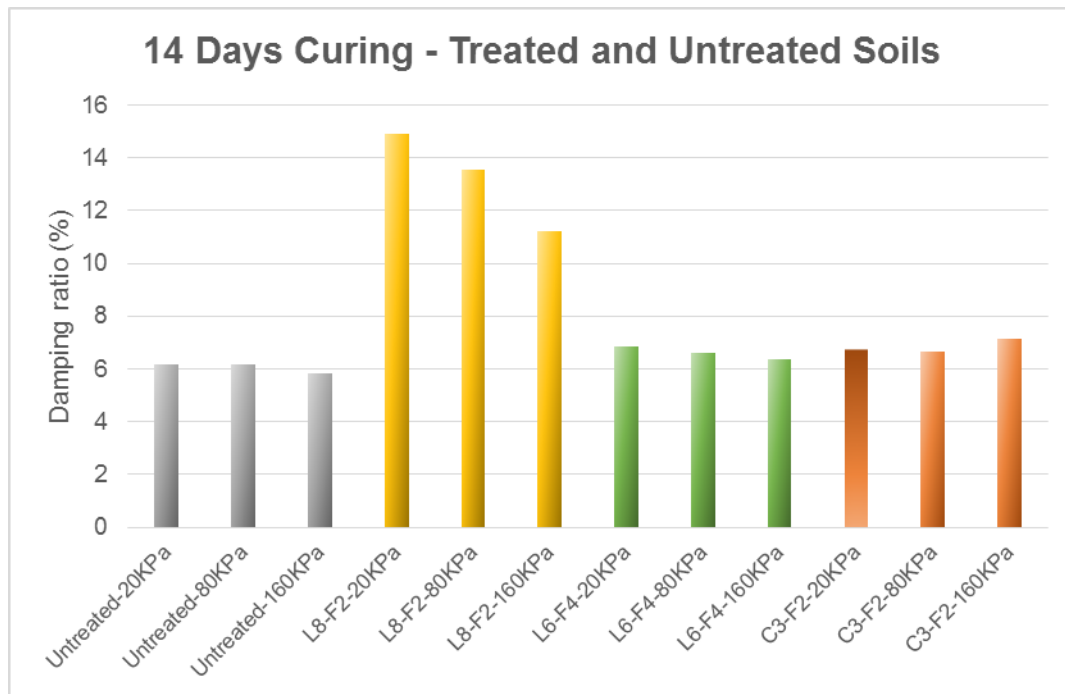


Figure Error! No text of specified style in document.-53: Variation of D_{min} with pressure for 14day curing time for control and treated specimen

Confinement Pressure

The tests were performed in three different confinement pressures. The pressures were 20, 80 and 160 KPa and the damping ratios and shear moduli results are shown in Figures 5-32 to 5-37. The results demonstrate that under 20 KPa confinement pressure, 8% lime+2% fly ash with 3 days curing has the most G_{max} . And following that the untreated soil has the most G_{max} .

Comparing the soils under 80 KPa, again the soil with 3days curing and 8%lime+2% fly ash has the most G_{max} . On the other hand, the untreated soil and 6% lime +4% fly ash have almost the same and highest G_{max} between the remaining soils.

The shear modulus of the 8% lime+2% fly ash is highest among the soils under 160 KPa. And following that the soil with 6% lime+4% fly ash has the highest value.

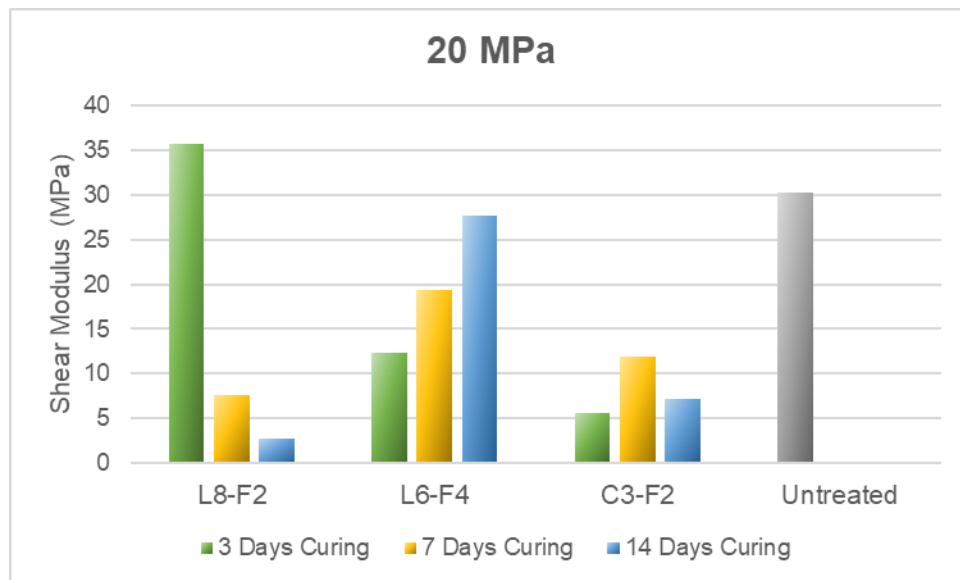


Figure **Error! No text of specified style in document.**-54: Variation of G_{max} with curing time for 20 KPa for control and treated specimen

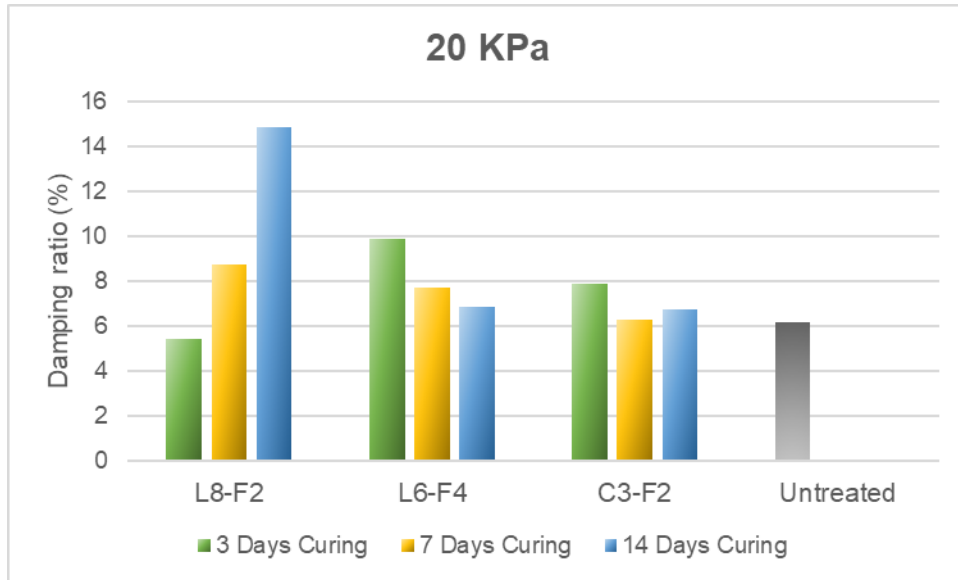


Figure Error! No text of specified style in document.-55: Variation of D_{min} with curing time for 20 KPa for control and treated specimen

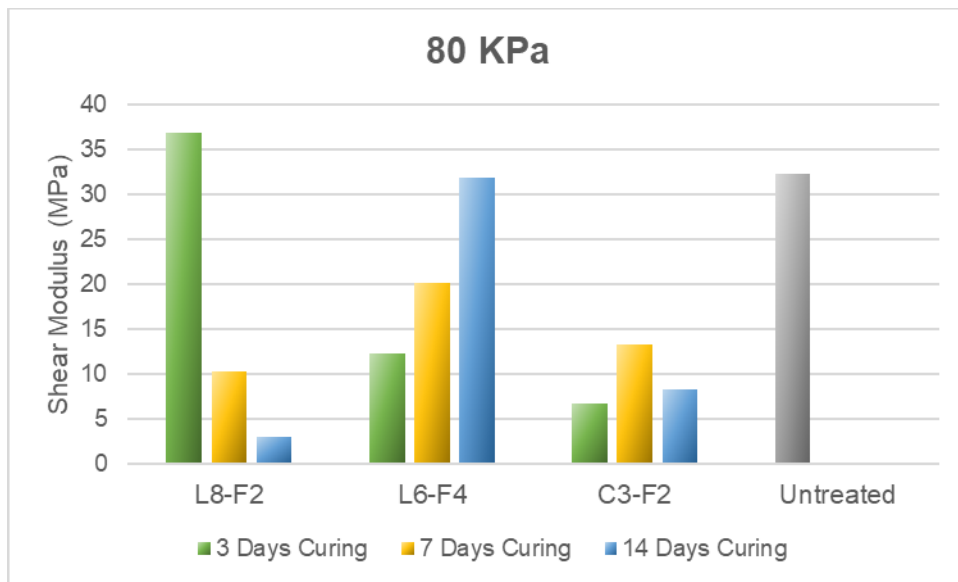


Figure Error! No text of specified style in document.-56: Variation of G_{max} with curing time for 80 KPa for control and treated specimen

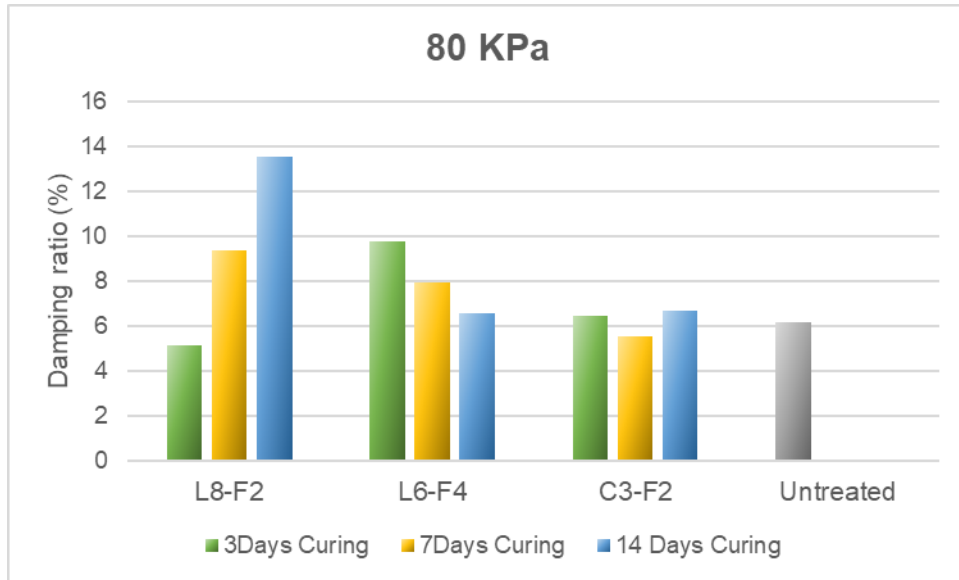


Figure Error! No text of specified style in document.-57: Variation of D_{min} with curing time for 80 KPa for control and treated specimen

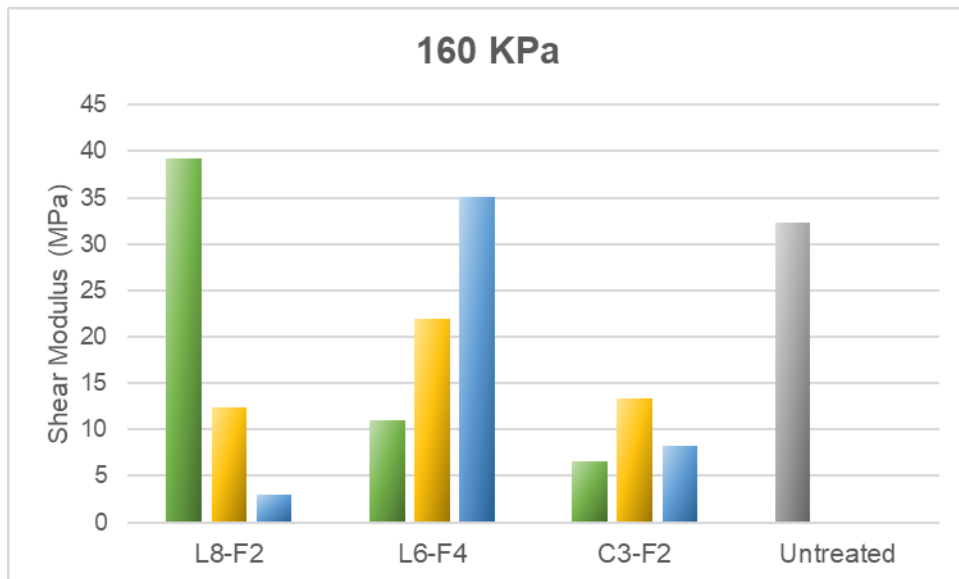


Figure Error! No text of specified style in document.-58: Variation of G_{max} with curing time for 160 KPa for control and treated specimen

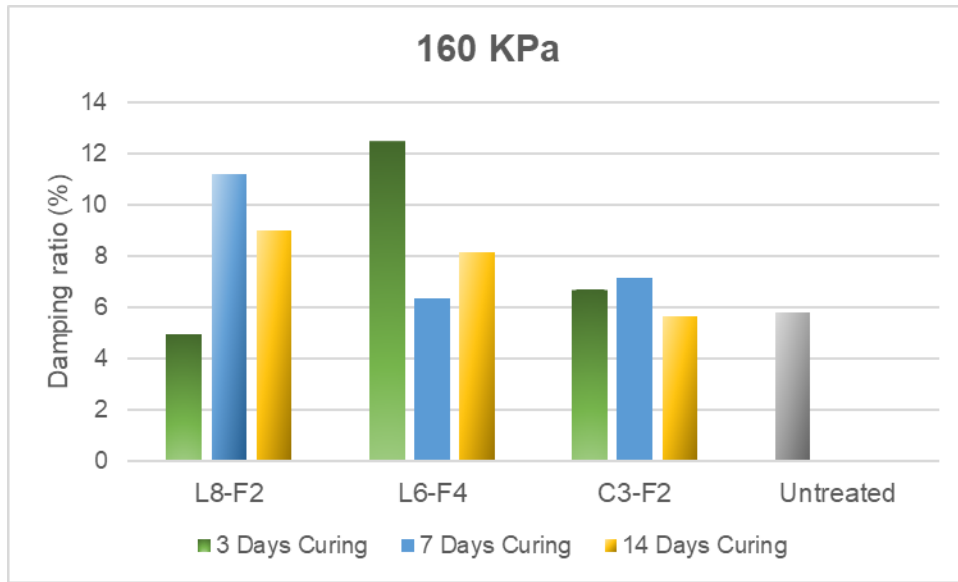


Figure **Error! No text of specified style in document.**-59: Variation of D_{min} with curing time for 160 KPa for control and treated specimen

Normalized shear modulus G/G_{max}

Figures 5-38 to 5-41 show the variations of G/G_{max} with shear strain (γ), for different treatment method for untreated and three days curing. From these figures, it can be observed that the untreated soil shows lesser values of induced strain, followed by 6% lime +4% flay ash treated soil, and then 3% cement+2% fly ash and finally 8% lime+2% fly ash. Therefore, it can be concluded that the untreated specimen is stiffer than the other three specimens at higher shear strain and between the treated ones at,6% lime+4% fly ash is the stiffest at high shear strain.

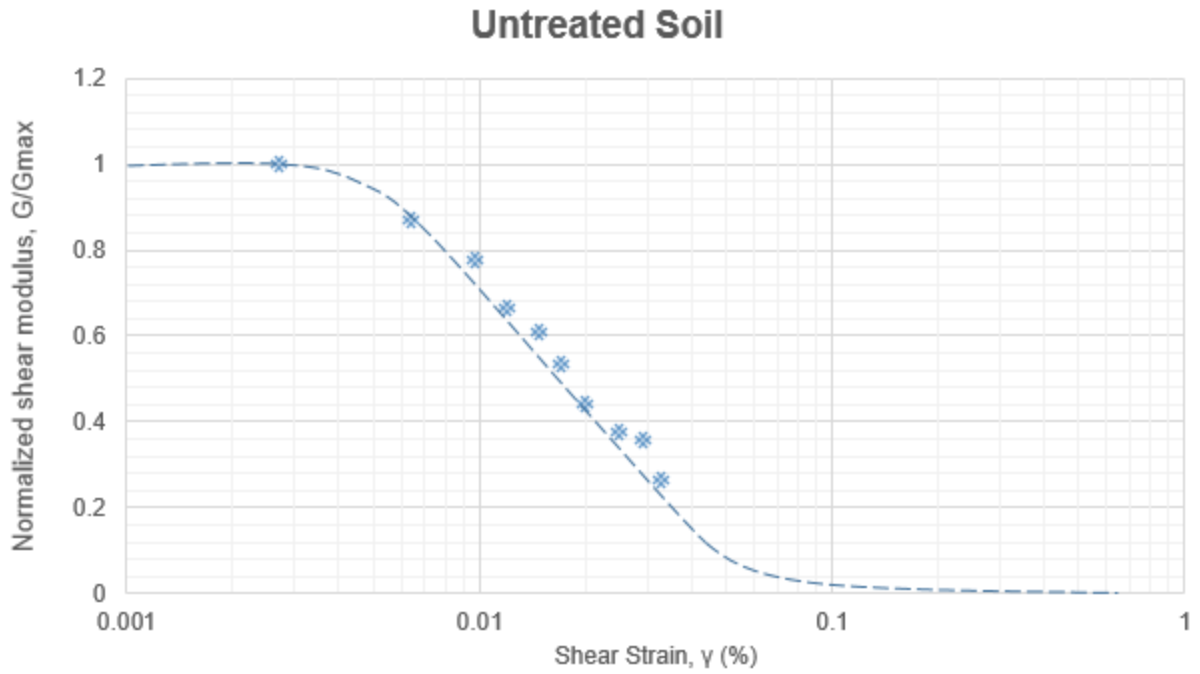


Figure Error! No text of specified style in document.-60: variation normalized shear modulus over shear strain for untreated soil

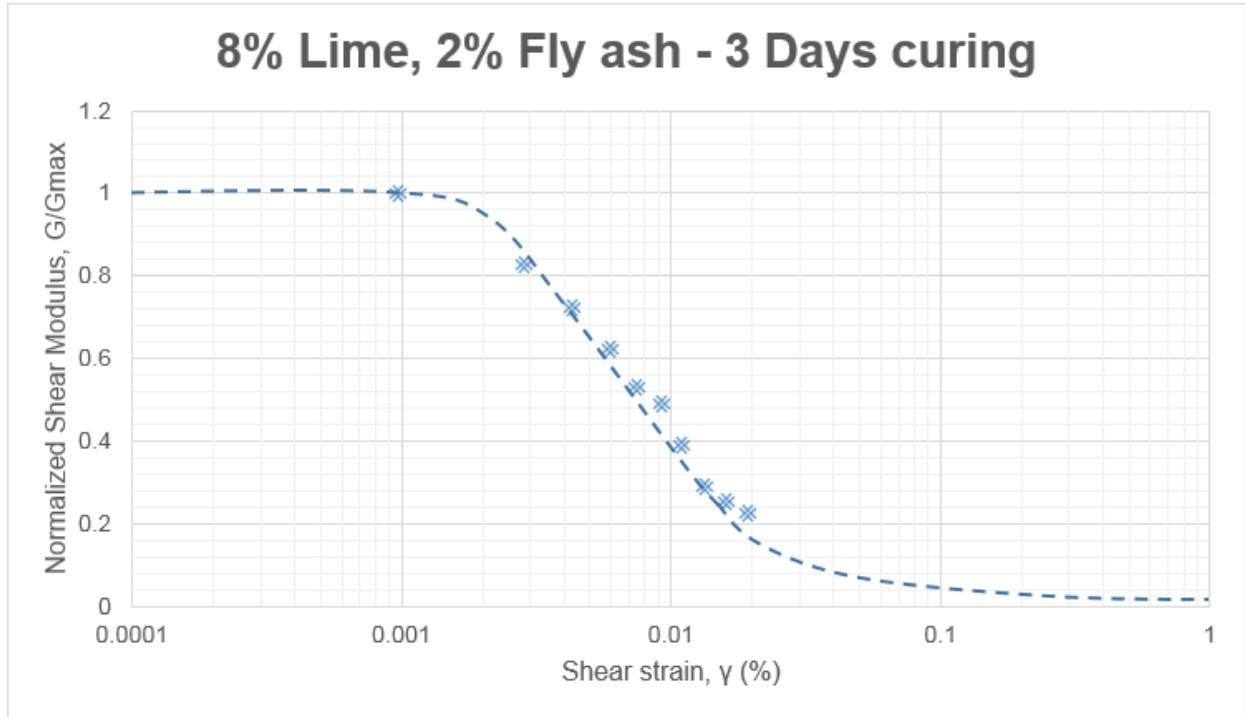


Figure Error! No text of specified style in document.-61: Variation normalized shear modulus over shear strain for 8L-2FA-5DM-3DC treated soil

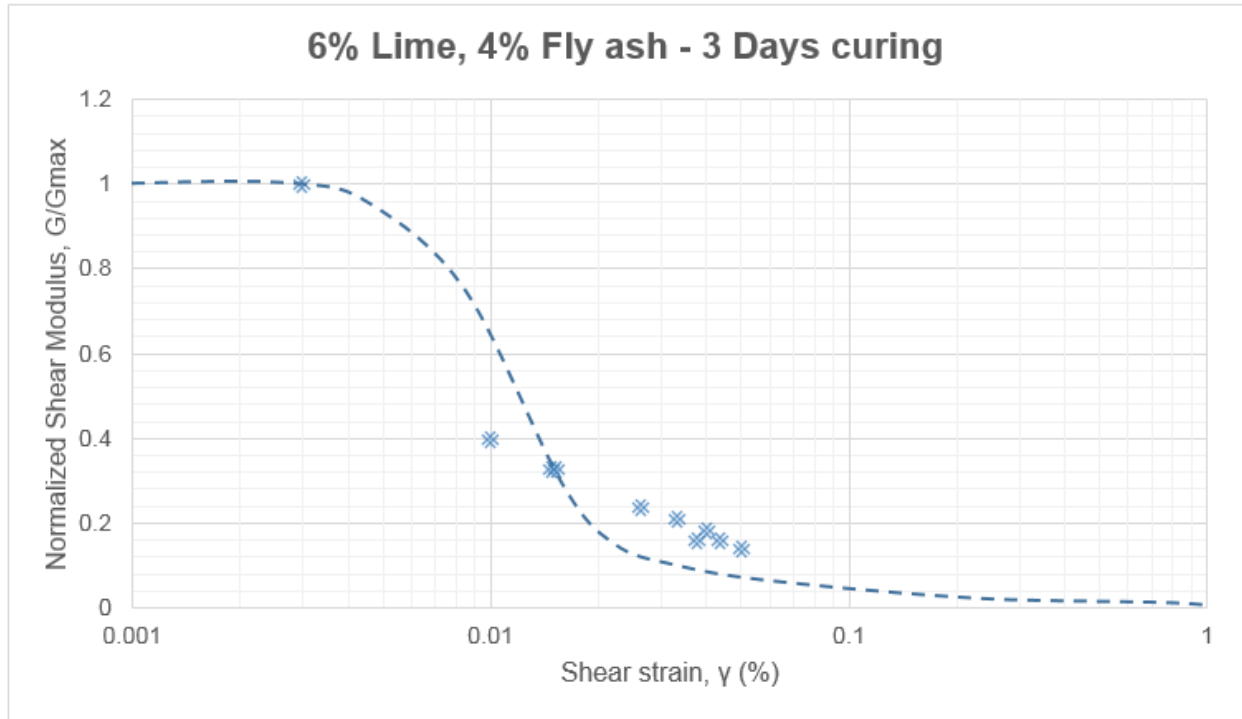


Figure Error! No text of specified style in document.-62: Variation normalized shear modulus over shear strain for 6L-4FA-5DM-3DC treated soil

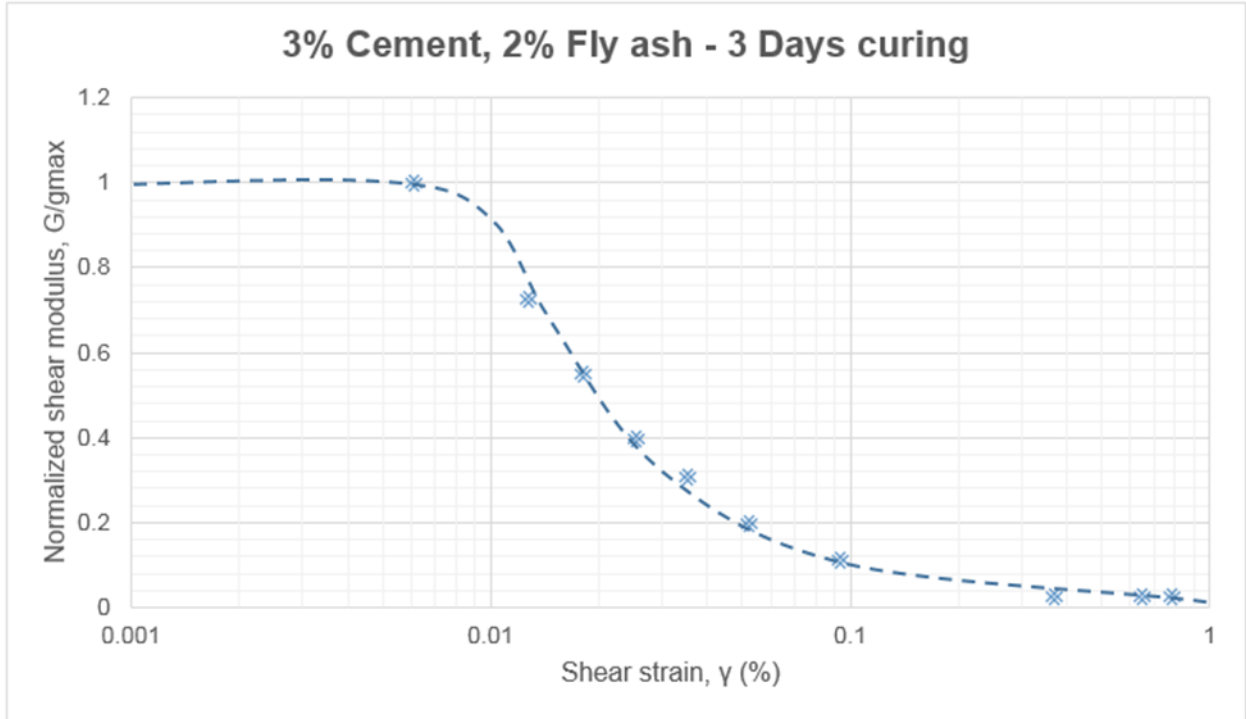


Figure Error! No text of specified style in document.-63: Variation normalized shear modulus over shear strain for 8L-2FA-5DM-3DC treated soil

Figures 5-42 to 5-44 show the variations of G/G_{max} with shear strain (γ), for different treatment methods for 7 days curing. From these figures, it can be observed that the 6% lime +4% fly ash treated soil shows lesser values of induced strain, followed by then 8% lime+2% fly ash, and then the untreated soil and finally 3% cement+2% fly ash. Therefore, it can be concluded that the 6% lime +4% fly ash is stiffer than the other three specimens when subjected to higher shear strain.

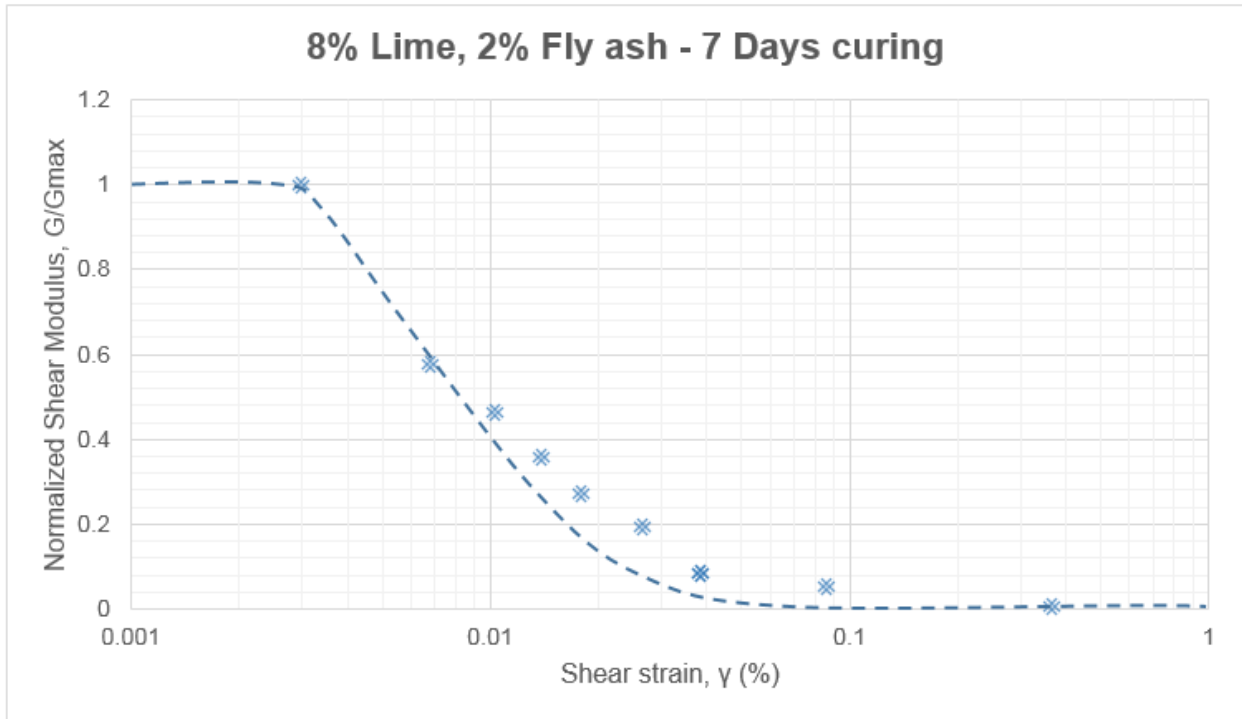


Figure Error! No text of specified style in document.-64: Variation normalized shear modulus over shear strain for 8L-2FA-5DM-7DC treated soil

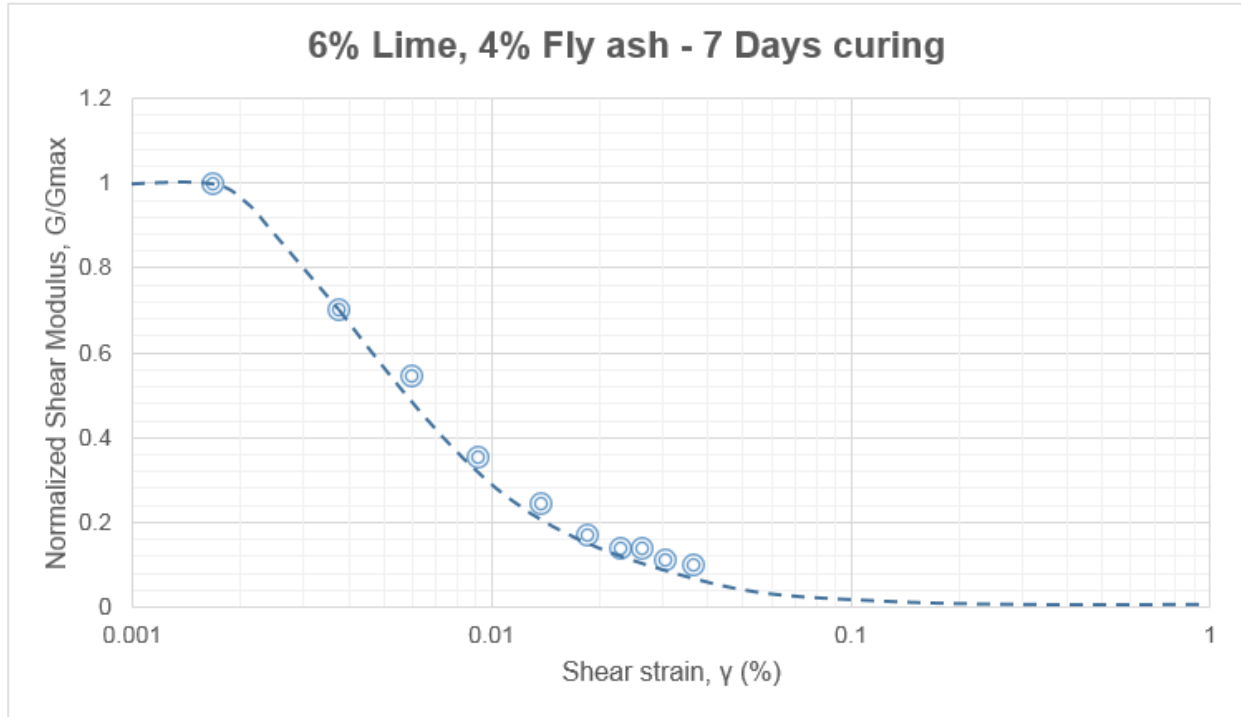


Figure Error! No text of specified style in document.-65: Variation normalized shear modulus over shear strain for 6L-4FA-5DM-7DC treated soil

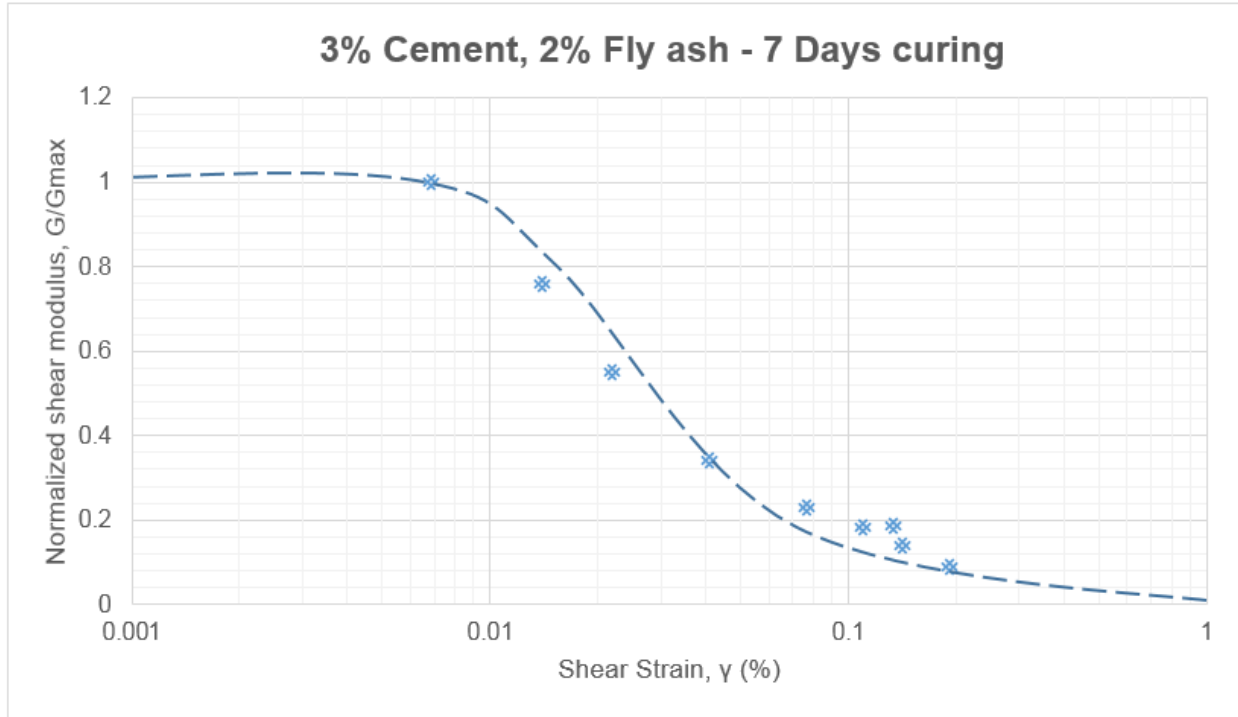


Figure Error! No text of specified style in document.-66: variation normalized shear modulus over shear strain for 3C-2FA-5DM-7DC treated soil

Figures 5-45 to 5-47 show the variations of G/G_{max} with shear strain (γ), for different treatment methods for 14 days curing. From these figures, it can be observed that the 6% lime +4% fly ash treated soil shows lesser values of induced strain, followed by then 8% lime+2% fly ash, and then the untreated soil and finally 3% cement+2% fly ash. Therefore, it can be concluded that the 6% lime +4% fly is stiffer than the other three specimens when subjected to higher shear strain.

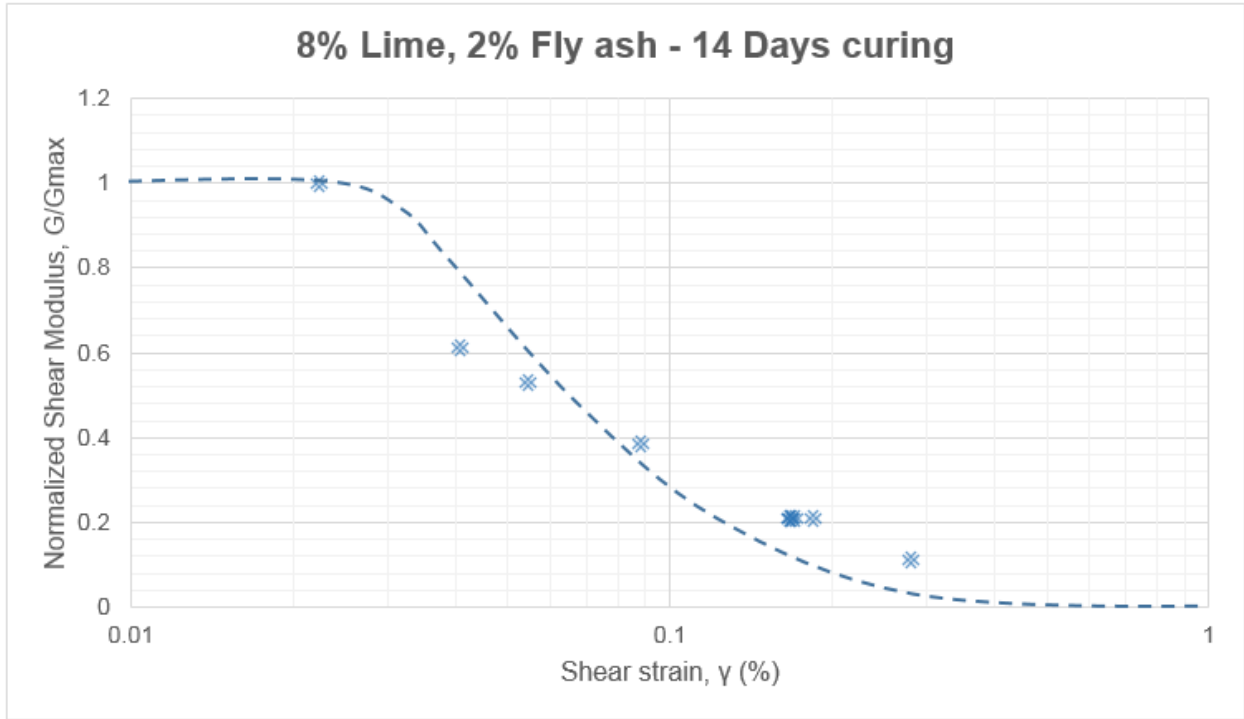


Figure Error! No text of specified style in document.-67: Variation normalized shear modulus over shear strain for 8L-2FA-5DM-14DC treated soil

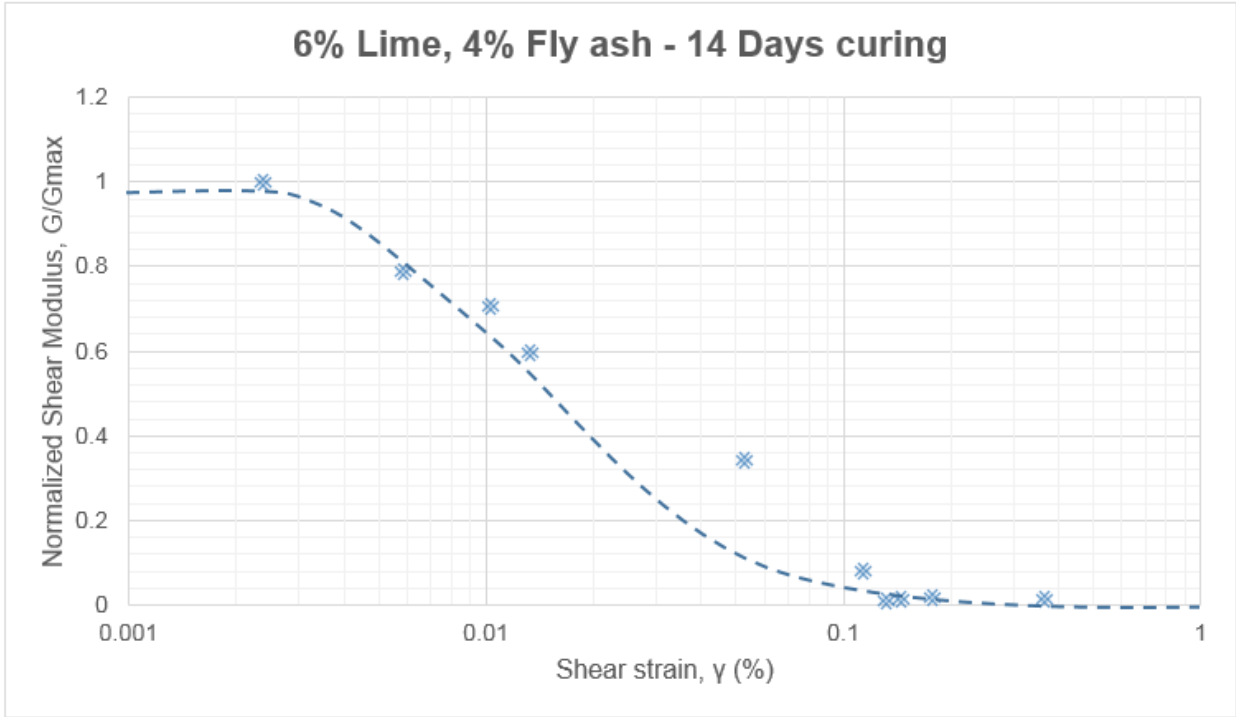


Figure Error! No text of specified style in document.-68: Variation normalized shear modulus over shear strain for 6L-4FA-5DM-14DC treated soil

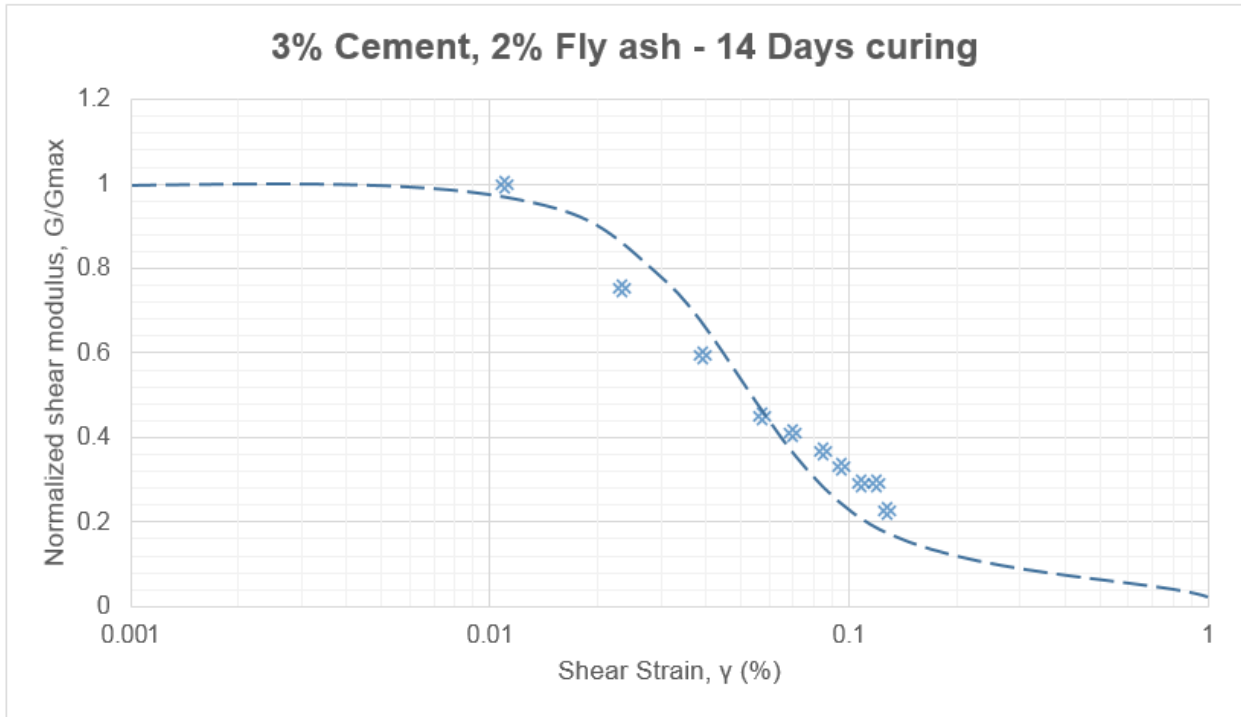


Figure Error! No text of specified style in document.-69: Variation normalized shear modulus over shear strain for 8L-2FA-5DM-3DC treated soil

Chapter 6 - Summary, Conclusions, and Recommendations

6.1 Summary

A comprehensive series of resonant column (RC) tests were conducted on several chemically stabilized specimens of high-plasticity, sulfate-rich expansive clay from Sherman, Texas. Test results were analyzed to assess the influence of lime- and cement-based stabilizer dosage, curing time, and confining pressure on the shear modulus and damping of the treated soil, including 8%lime + 2% fly ash, 6% lime + 4% fly ash, and 3% cement + 2% fly ash. RC tests were also conducted at mid- to high-strain levels to study stiffness degradation effects of torsional shearing.

6.2 Main Conclusions

The main conclusions from the analysis of all RC experimental data can be summarized as follows:

1. In general, results show a detrimental effect of all treatment methods on soil stiffness, namely shear modulus and damping, which can be possibly attributed to Ettringite formation during curing since the sulfate content of the test soil was far more than 2,000 ppm. (Further SEM based analyses of Ettringite formation were beyond the scope of the present work.)
2. The 6% lime + 4% fly ash treated soil, after 14 days curing, yields potentially the best-performing response in terms of stiffness and damping.
3. "Class F" fly ash contains just 1.1% Calcium oxide (CaO), which helps explain the apparently better performance of 6% lime + 4% fly ash treatment after 14 days, compared to others.
4. Some pavements with chemically treated subgrades have been reported to crack due to a lack of enough mellowing prior to compaction, which is further substantiated by some of the present results: more than 5 days of mellowing may be needed.
5. In all cases, the normalized shear modulus G/G_{\max} tend to decrease with increasing shear strain (γ), an indication of the modulus degradation beyond a certain threshold. In general, stiffer samples showed lower threshold strain.

6.3 Recommendations for Future work

Continuing research efforts are recommended to further advance the understanding of the effects of the present test variables on stiffness properties of chemically-stabilized soil, including:

1. Investigating the effects of longer mellowing and curing periods, so that the cementation effects on the strength and stiffness properties can be used to assess the long-term behavior of the treated soils.

2. Further RC testing for thorough regression-based analysis of all experimental data, including analytical relationships between soil stiffness properties, mellowing period, and confining pressure.

3. Additional RC testing using sulfate-resistant Type V cement based treatment, which may be more appropriate for high-sulfate soils.

4. Detailed SEM/XRD based analyses and images to investigate the extent of Ettringite formation during curing and its effects on stiffness of sulfate-rich soil.

References

- Bravo, A. (2013). "Effect of suction on dynamic properties of unsaturated soil at small to mid-shear strain values.
- Hausmann, M. R. (1990). "Engineering Principles of Ground Modification," McGraw Hill, New York.
- Hunter, D. (1988). "Lime-Induced Heave in Sulfate-Bearing Clay Soils," Journal of Geotechnical Engineering, ASCE, Vol. 114, pp. 150-167
- Inthrasombat, N. (2003). "Ettringite formation in lime treated sulfate soils: Verification by mineralogical and swell testing." M.S. Thesis, The Univ. of Texas at Arlington, Arlington, Texas.
- Kota, P. B. V. S., Hazlett, D., and Perrin, L. (1996) "Sulfate-Bearing Soils: Problems with Calcium Based Stabilizers". Transportation Research Record 1546, TRB, National Research Council, Washington, D.C., 1996, pp. 62-69.
- Little, D. N., Nair, S., and Herbert, B. (2010). "Addressing Sulfate-Induced Heave in Lime Treated Soils". Journal of Geotechnical and Geoenvironmental Engineering, ASCE, January 2010, pp. 110-118.
- Mallat A. (2006). "LMSSMat", Retrieved from <http://www.mssmat.ecp.fr/Axe-derecherche>, 1529, accessed on 11/04/2010.
- Mitchell, J. K. (1986). "Practical Problems from Surprising Soil Behavior." Journal of Geotechnical Engineering Division, ASCE, Vol. 112, No. 3, pp. 259-289
- Perrin, L. (1992). "Expansion of Lime-Treated Clays Containing Sulfates". Proceedings of 7th International Conference on Expansive Soils, Vol. 1, ASCE Expansive Soil Research Council, New York, 1992, pp. 409-414
- Puppala, A.J., Naga S. Talluri., Bhaskar S. Chittoori and Ahmed Gaily. (2012). Lessons Learned from Sulfate Induced Heaving Studies in Chemically Treated Soils. Proceedings of the International Conference on Ground Improvement and Ground Control. Research Publishing, Vol. 1, November 2012, pp.85-98.
- Puppala, A. J., Saride, S., Dermatas, D., Al-shamrani, M., and Chikyala, V. (2010). "Forensic Investigations to Evaluate Sulfate-Induced Heave Attack on a Tunnel Shotcrete Liner".
- Richart, F. E., Hall, J. R. Jr., and Woods, R. D. (1970). "Vibration of Soils and Foundations," Prentice-Hall, Inc., Englewood Cliffs, NJ.

Rollings Jr., R. S., Burkes, J. P., and Rollings, M. P. (1999). "Sulfate Attack on Cement Stabilized Sand." *Journal of Geotechnical and Geoenvironmental Engineering*, vol. 125 No.5, pp. 364-372.

Semane, M. (2014). "Stiffness Response of Chemically Stabilized Sulfate Rich Soil via Resonant Column Testing", University of Texas at Arlington.

Talluri, N. (2013). "Stabilization of High Sulfate Soils," PhD Thesis, the University of Texas, Arlington, Texas.

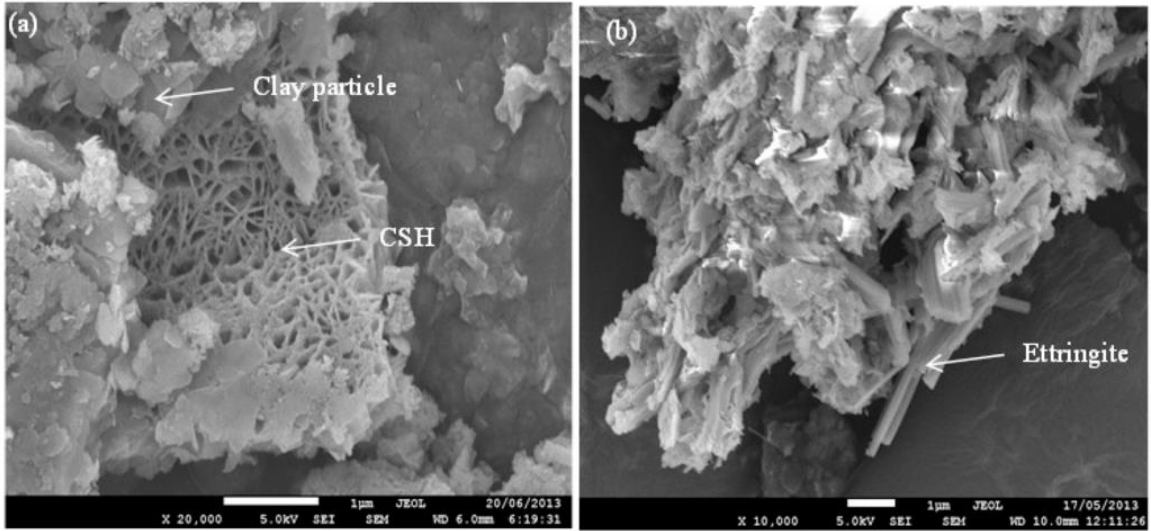
APPENDIX I: "ETTRINGITE" Formation Figures



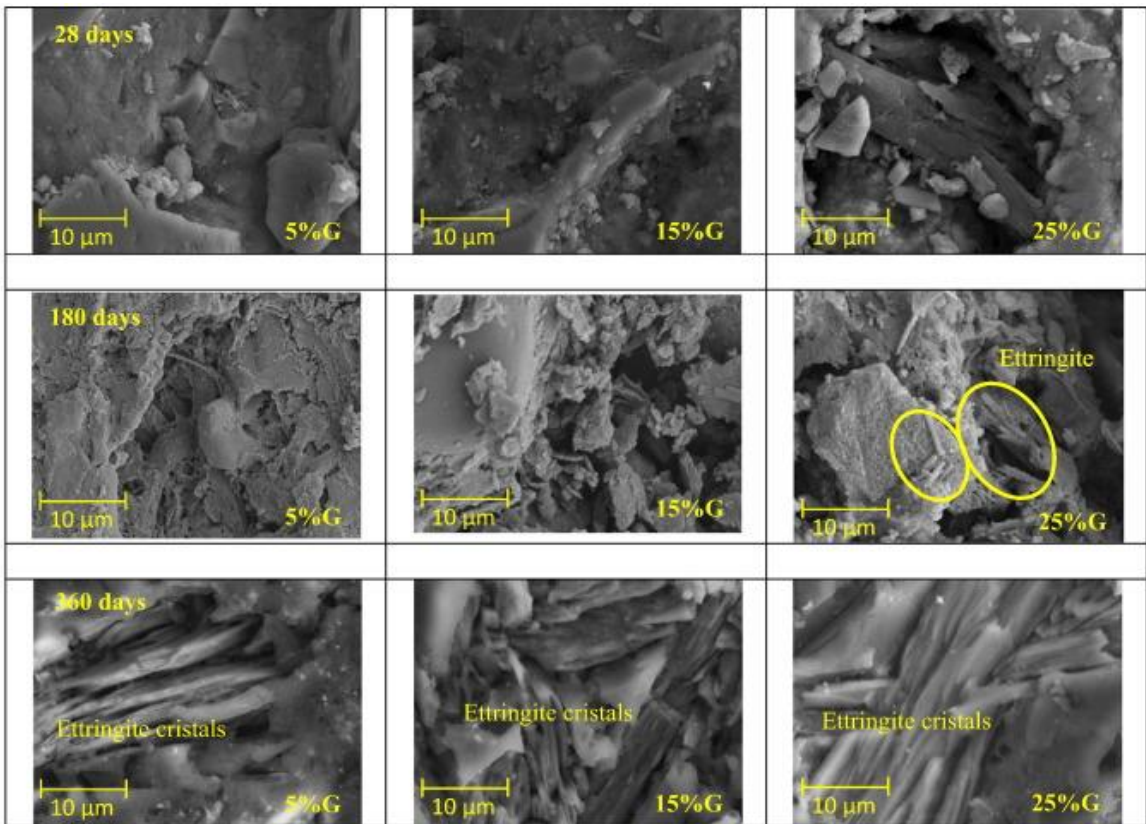
Sample break with the formation of Ettringite because of lime treated soil in the left picture

Source:

Stabilizing soils with sulfates to improve their constructional properties March 8, 2017, PHYS.ORG



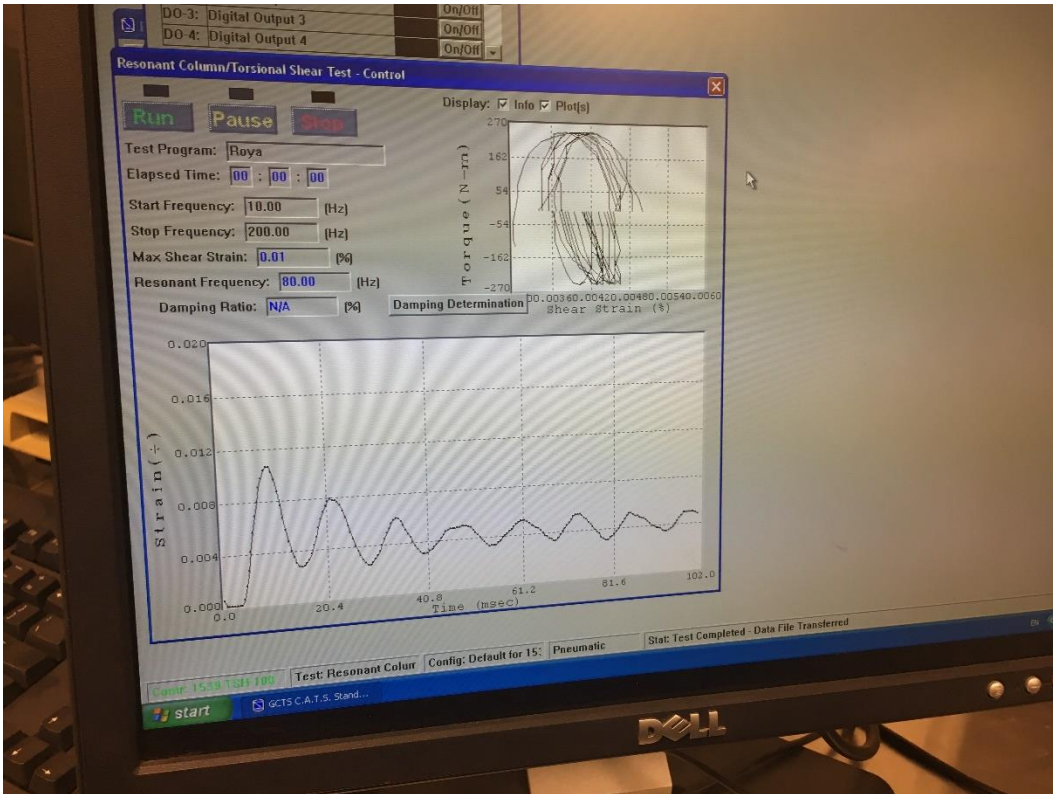
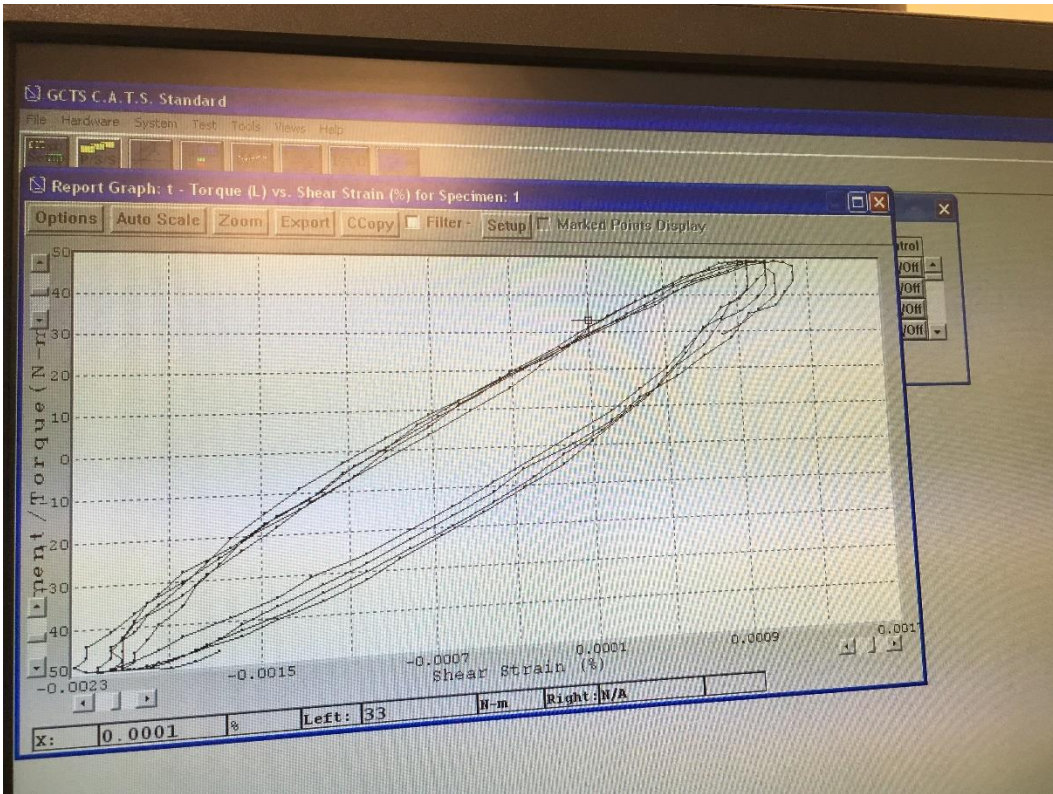
SEM Images of Ettringite - Source: S. Islam et al. 2016

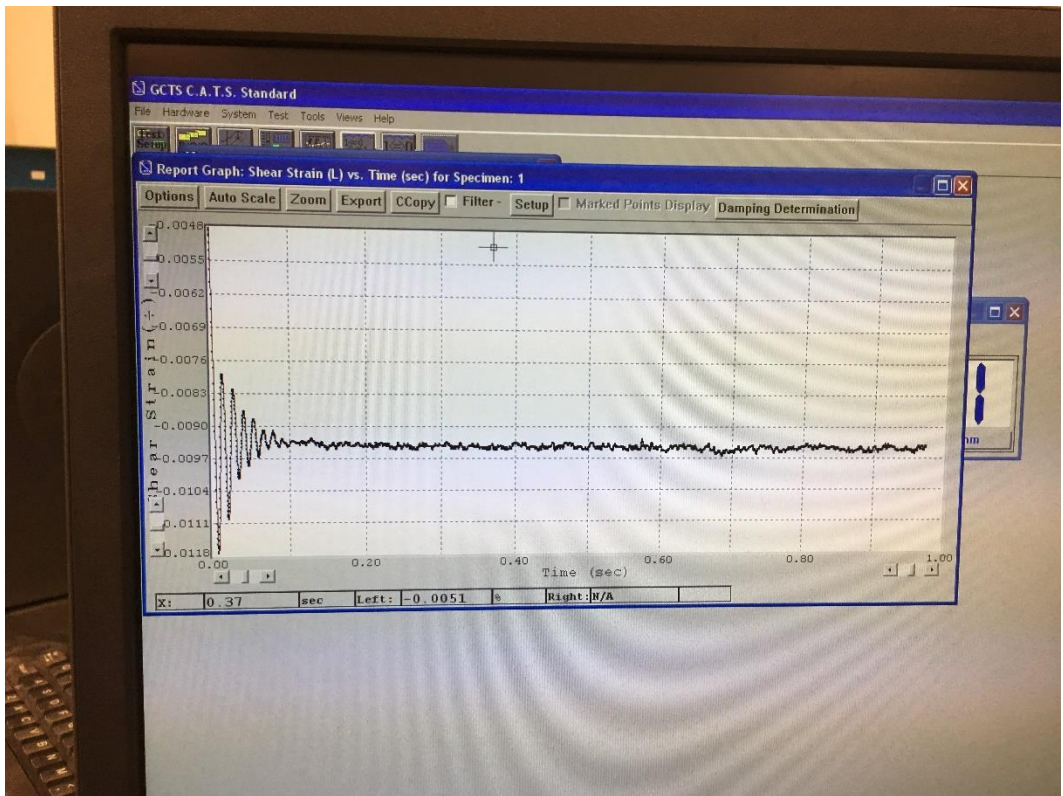
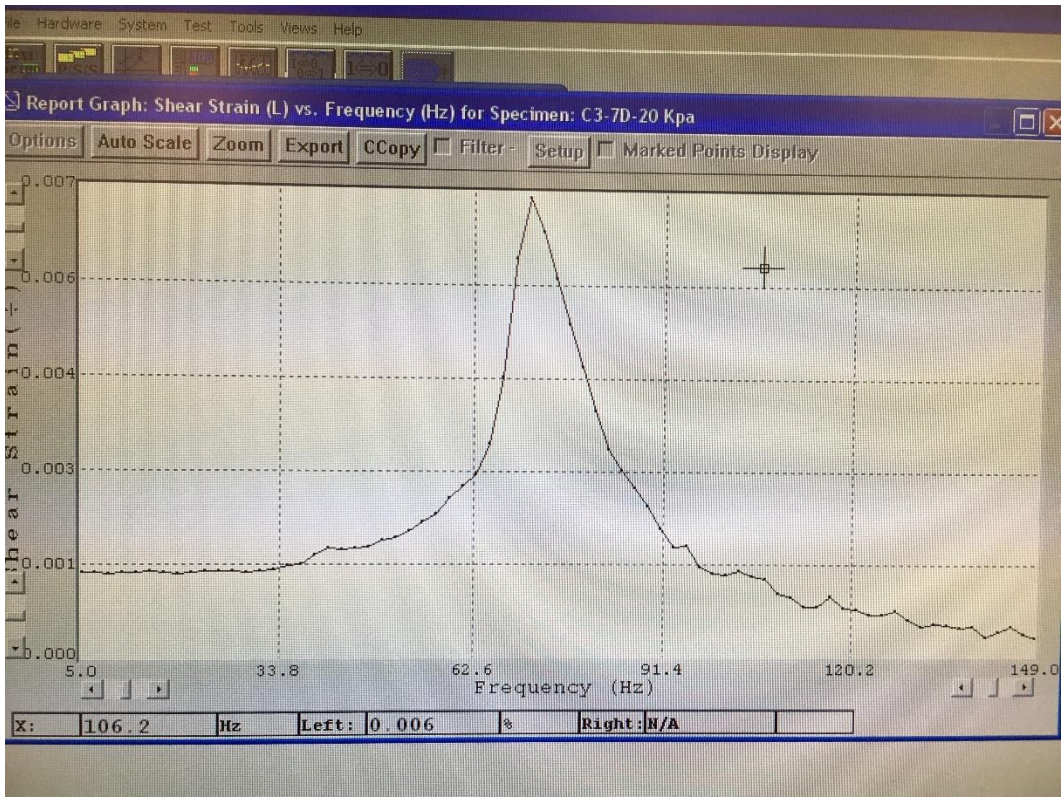


SEM images show cementitious materials and Ettringite development for soil samples cured at 20 °C.

Source: A. Aldaood et al. 2014

APPENDIX II: C.A.T.S Software Outputs





Appendix III- Typical Test Results

Software: ,GCTS C.A.T.S. Standard,Version: ,1.85
Project: ,Azadeh
Sample: ,11
Test: ,Resonant Column/Torsional Shear
Specimen: ,un-20Kpa
Number: ,2
Description: ,_
Container ID: ,_
Type: ,Solid
Height: ,14.70,(cm)
Diameter: ,7.20,(cm)
Equivalent Radius Factor: ,0.707
Equivalent Radius: ,2.55,(cm)
Mass: ,1064.40,(gr)
Initial Water Content: ,0,(%)
Degree of Saturation: ,0,(%)
Specific Gravity: ,0
Initial Void Ratio: ,0
Mass Moment of Inertia: ,689.731,kg-mm²
Area Moment of Inertia: ,1.31917e-006,m⁴
Controller ID: ,1539 TSH-100
Resonant Column/Torsional Shear Inputs
,1,Proximitor 10 mm,Max: ,5,(mm),Min: , -5,(mm)
,Gain: ,20.6164
,Offset: ,0.531265,(Volts)
,DC Excitation: ,Full (\pm 5 VDC)
,GCTS Board #: ,769
,Digital Filter: ,500,(Hz)
,Software Offset: ,1.547,(mm)
,Sensor ID: ,prox_10
,,Sensor Type: ,DC
,,Model #: ,_
,,Serial #: ,_

```

,,DC Sensor Output: ,Absolute
,,Parameter: ,Displacement/Length
,,Range,(mm): ,Max: ,5,Min: ,-5
,,Calibration: ,Date: ,03/20/17
,,Type: ,Non-Linear
,,Non-LinearOutput (mm) = a0 + a1*X + a2*X2 + a3*X3
,,where X is in (volts)
,,a0: ,-8.34169
,,a1: ,32.916
,,a2: ,-35.4167
,,a3: ,15.1503
,2,Not Defined
,3,Gauge Deformation,Max: ,6.35,(mm),Min: ,-6.35,(mm)
,Gain: ,2.61576
,Offset: ,0.0569485,(Volts)
,GCTS Board #: ,981
,Digital Filter: ,50,(Hz)
,Software Offset: ,0.62,(mm)
,Sensor ID: ,Gauge Deformation
,,Sensor Type: ,AC
,,Model #: ,MC CD 375-250
,,Serial #: ,_
,,Parameter: ,Displacement/Length
,,Range,(mm): ,Max: ,6.35,Min: ,-6.35
,,Calibration: ,Date: ,03/20/17
,,Type: ,Non-Linear
,,Non-LinearOutput (mm) = a0 + a1*X + a2*X2 + a3*X3
,,where X is in (volts/Volt)
,,a0: ,-0.0853838
,,a1: ,11.3116
,,a2: ,-0.163608
,,a3: ,0.127634
,4,Not Defined
,5,Controller Tempertr,Max: ,150,(deg C),Min: ,-50,(deg C)
,DC External Excitation:
,,Max: ,1,(VDC)
,,Min: ,0,(VDC)

```

,Digital Filter: ,0.1,(Hz)
,Software Offset: ,0.0,(deg C)
,Sensor ID: ,Controller Tempertr
,,Sensor Type: ,DC
,,Model #: ,AD22100
,,Serial #: ,_
,,DC Sensor Output: ,Absolute
,,Parameter: ,Temperature
,,Range,(°C): ,Max: ,150,Min: ,-50
,,Calibration: ,Date: ,11/21/08
,,Type: ,Linear - Two point
,,Point,Engineering Value (°C),Output (Volts)
,,First,-50,0.25
,,Second,150,4.75
,,Equation: Output (°C) = ,44.4444,*(Volts),+,-61.1111
,6,Not Defined
,7,Not Defined
,8,Not Defined
,9,Not Defined
,10,Not Defined

Test Configuration

,Combined - Mass Polar Moment Of Inertia of Resonant Column drive System: ,793.8,kg-mm²
,Damping of Resonant Column drive system: ,0,(%)
,Distance from Center to Proximito(r): ,8.07,(cm)
,Torque Output Conversion Factor: ,100.00,(N-m)
,Torque Control Output: ,1
,Motor Inhibit Digital Control: ,1
,Inputs
,,Proximito(r): ,AI-1: Proximito(r) 10 mm
,,Acceleration: ,(none)
,,Torque: ,(none)
,,Axial Load: ,(none)
,,Axial Deformation: ,AI-3: Gauge Deformation
,,Cell Pressure: ,(none)
,,Pore Pressure: ,(none)
,,Volume Change: ,(none)

,,Main Angular Displacement Input: ,Proximito(r)s)

Test Setup:

,Number of Cycles to Obtain Steady State: ,10

,Torque Output Amplitude to drive System: ,1,(pfs),=>,100.00,(N-m)

Starting Date: ,07/15/17

Starting Time: ,06:42:09

Test Results: ,Completed

Axial Deformation:,-0.54,mm

Resonant Frequency: ,115.00,(Hz)

Max Shear Strain: ,0.00273340,(%)

Shear Velocity: ,130.09,(m/sec)

Shear Modulus: ,30.10,(MPa)

Damping Ratio:

Free Vibration Decay: ,N/A

Half Power Bandwidth: ,6.69,(%)

Average Frequency from Free Vibration Data FFT Analysis: ,5.01,(Hz)

Natural Frequency:

from Resonant Frequency and Phase Shift: ,11.00,(Hz)

from Resonant Frequency and Free Vibration Decay,N/A

from FFT Frequency and Free Vibration Decay,N/A

Tested Frequencies: ,73

Frequency,Shear Strain,Proximito(r)s) Amplitude,Phase Shift
(Hz),(%),mm,rad,deg

5.00	0.00059787	0.003	3.03	173.6
7.00	0.00057167	0.003	3.04	174.3
9.00	0.00056805	0.003	3.11	178.1
11.00	0.00055851	0.003	0.01	0.5
13.00	0.00055965	0.003	0.10	5.7
15.00	0.00055114	0.003	0.33	18.8
17.00	0.00056457	0.003	0.55	31.5
19.00	0.00054223	0.003	0.68	38.9
21.00	0.00055412	0.003	0.89	51.0
23.00	0.00054346	0.003	1.25	71.4
25.00	0.00055793	0.003	1.75	100.2
27.00	0.00055704	0.003	1.93	110.7
29.00	0.00055403	0.003	2.22	127.1
31.00	0.00053947	0.003	2.68	153.4

33.00,0.00053872,0.003,0.04,2.2
35.00,0.00056888,0.003,0.66,37.9
37.00,0.00056529,0.003,0.96,55.0
39.00,0.00057883,0.003,1.44,82.7
41.00,0.00055626,0.003,2.30,132.0
43.00,0.00055394,0.003,2.98,170.9
45.00,0.00054858,0.003,0.65,37.2
47.00,0.00056687,0.003,1.51,86.4
49.00,0.00056247,0.003,1.97,112.7
51.00,0.00056084,0.003,2.56,146.8
53.00,0.00057777,0.003,0.15,8.8
55.00,0.00059118,0.003,0.72,41.3
57.00,0.00059499,0.003,0.98,56.4
59.00,0.00064460,0.003,1.39,79.4
61.00,0.00065696,0.003,2.24,128.4
63.00,0.00063776,0.003,0.39,22.1
65.00,0.00062305,0.003,1.68,96.0
67.00,0.00068695,0.003,2.96,169.8
69.00,0.00067579,0.003,0.78,44.7
71.00,0.00069018,0.003,1.33,76.2
73.00,0.00070081,0.003,2.33,133.2
75.00,0.00071281,0.003,3.12,178.7
77.00,0.00075403,0.004,1.06,60.6
79.00,0.00075077,0.003,1.59,91.3
81.00,0.00075487,0.004,2.05,117.7
83.00,0.00079622,0.004,3.05,174.5
85.00,0.00082232,0.004,1.22,69.8
87.00,0.00083106,0.004,2.80,160.2
89.00,0.00089430,0.004,1.47,84.0
91.00,0.00089082,0.004,0.28,16.2
93.00,0.00102262,0.005,2.11,121.2
95.00,0.00106578,0.005,0.80,45.8
97.00,0.00106067,0.005,2.44,140.0
99.00,0.00115093,0.005,0.76,43.7
101.00,0.00130238,0.006,1.69,96.9
103.00,0.00139062,0.006,2.18,125.0
105.00,0.00148023,0.007,2.02,115.5

107.00,0.00180615,0.008,0.59,33.7
109.00,0.00194626,0.009,1.67,95.4
111.00,0.00209133,0.010,1.95,112.0
113.00,0.00248432,0.012,3.02,173.1
115.00,0.00273340,0.013,0.69,39.7
117.00,0.00265868,0.012,2.34,134.3
119.00,0.00248701,0.012,0.81,46.2
121.00,0.00226952,0.011,1.32,75.6
123.00,0.00207337,0.010,2.50,143.5
125.00,0.00183467,0.009,0.26,14.9
127.00,0.00178520,0.008,1.71,98.1
129.00,0.00149454,0.007,2.75,157.5
131.00,0.00132641,0.006,1.22,69.9
133.00,0.00122744,0.006,2.14,122.3
135.00,0.00114144,0.005,0.47,26.8
137.00,0.00109025,0.005,1.18,67.7
139.00,0.00108678,0.005,2.21,126.9
141.00,0.00096988,0.005,1.48,84.6
143.00,0.00089351,0.004,3.14,179.7
145.00,0.00088158,0.004,1.83,105.0
147.00,0.00076603,0.004,2.83,162.1
149.00,0.00065711,0.003,0.85,48.6

Untreated Final - Excel

Asghariastaneh, Azadeh

1	Shear Str	Frequency	fn	Zmax	0.707 Zma	fn-Row
2	(%)	(Hz)	115	0.002814	0.00199	58
3	0.000604	5	Z"1	0.001686	F"1	107
4	0.000575	7	Z"1	0.001995	F"1	109
5	0.000571	9		f1		108.9629
6	0.000579	11				
7	0.000565	13	Z"2	0.002019	F"2	123
8	0.00057	15	Z"2	0.001738	F"2	125
9	0.000572	17		f2		123.2072
10	0.000553	19				
11	0.000563	21	D	6.193205		
12	0.000577	23				
13	0.000539	25				
14	0.000549	27				
15	0.000559	29				
16	0.000567	31				
17	0.000556	33				
18	0.000552	35				
19	0.000579	37				
20	0.000565	39				
21	0.000536	41				
22	0.000533	43				
23	0.000553	45				

20 KPa

3D-Lime8-flyash2-3days - Excel

Asghariastaneh, Azadeh

1	Frequency	Shear Strain
2	(Hz)	(%)
3	5	0.000308
4	7	0.000298
5	9	0.000293
6	11	0.000268
7	13	0.000286
8	15	0.000283
9	17	0.000289
10	19	0.000267
11	21	0.00028
12	23	0.000274
13	25	0.000264
14	27	0.000288
15	29	0.000278
16	31	0.000272
17	33	0.000283
18	35	0.000272
19	37	0.000264
20	39	0.000262
21	41	0.000284
22	43	0.000267
23	45	0.00027

20 kpa

3D-Lime6-Flyash2 - Excel

Asghariastaneh, Azadeh

File Home Insert Page Layout Formulas Data Review View Tell me what you want to do

Clipboard Font Alignment Number Styles Cells Editing

SECURITY WARNING External Data Connections have been disabled Enable Content

M11

1	Frequency (Hz)	Shear (%)	Strax (mm)	Proximito (rad)	Phase Shift (deg)
2	20	0.000887	0.004	3	172.1
3	22	0.000908	0.004	0.17	9.8
4	24	0.000916	0.004	0.24	13.7
5	26	0.000937	0.004	0.36	20.9
6	28	0.00095	0.004	0.66	37.7
7	30	0.000969	0.004	0.84	48.3
8	32	0.001064	0.005	1.3	74.5
9	34	0.001023	0.005	1.67	95.7
10	36	0.001005	0.005	1.81	103.7
11	38	0.001045	0.005	1.84	105.7
12	40	0.001099	0.005	2.05	117.5
13	42	0.001078	0.005	2.42	138.9
14	44	0.00108	0.005	2.97	170
15	46	0.001007	0.005	0.72	41.2
16	48	0.001056	0.005	1.51	86.5
17	50	0.001107	0.005	2.58	147.6
18	52	0.001279	0.006	2.88	165.3
19	54	0.001372	0.006	2.93	167.7
20	56	0.001574	0.007	0.52	29.8

Ready

3D-Cement3-Flyash2 - Excel

Asghariastaneh, Azadeh

File Home Insert Page Layout Formulas Data Review View Tell me what you want to do

Clipboard Font Alignment Number Styles Cells Editing

P8

1	Frequency (Hz)	Shear (%)	Strax (mm)	Proximito (rad)	Phase Shift (deg)
2	10	0.001062	0.005	3.03	173.8
3	12	0.001092	0.005	3.13	179.3
4	14	0.001097	0.005	0	0.2
5	16	0.001108	0.005	0.16	8.9
6	18	0.001101	0.005	0.26	15
7	20	0.001131	0.005	0.56	32.3
8	22	0.001154	0.005	0.89	50.8
9	24	0.001181	0.006	1	57.2
10	26	0.001194	0.006	1.12	64.3
11	28	0.001252	0.006	1.38	79.1
12	30	0.001343	0.006	1.61	92
13	32	0.001353	0.006	2.05	117.6
14	34	0.001435	0.007	2.44	139.9
15	36	0.001515	0.007	2.57	147.1
16	38	0.001633	0.008	2.61	149.3
17	40	0.001751	0.008	2.89	165.6
18	42	0.001982	0.009	0.09	4.9
19	44	0.002264	0.011	0.69	39.7
20	46	0.002773	0.013	1.46	83.6
21	48	0.004032	0.019	1.97	112.8
22	50	0.006477	0.03	2.23	128

Ready

7day-lime 8 - Excel

File Home Insert Page Layout Formulas Data Review View Tell me what you want to do

Clipboard Font Alignment Number Styles Cells Editing

	A	B	C	D	E	F	G	H	I	J	K	L	M	N	O	P	Q	R	S	T
1	Shear Strain	Frequency																		
2	(%)	(Hz)																		
3	0.00101352	5																		
4	0.00097812	6																		
5	0.00099095	7																		
6	0.00095897	8																		
7	0.00096507	9																		
8	0.0009445	10																		
9	0.00095793	11																		
10	0.00094649	12																		
11	0.0009659	13																		
12	0.00094876	14																		
13	0.00094864	15																		
14	0.00091801	16																		
15	0.00092355	17																		
16	0.00095186	18																		
17	0.00095529	19																		
18	0.00091713	20																		
19	0.00093174	21																		
20	0.00095071	22																		
21	0.00092843	23																		
22	0.00096494	24																		
23	0.00097539	25																		

20 Kpa 80 Kpa 160 Kpa T=2 T=3 T=4 T=5 T=6 T=7 T=8 T=9 T=10

7D-lime6 - Excel

File Home Insert Page Layout Formulas Data Review View Tell me what you want to do

Clipboard Font Alignment Number Styles Cells Editing

	A	B	C	D	E	F	G	H	I	J	K	L	M	N	O	P	Q	R	S	T	U
1	Shear Stra	Frequency																			
2	(%)	(Hz)																			
3	0.000468	5																			
4	0.000474	7																			
5	0.000458	9																			
6	0.000454	11																			
7	0.00045	13																			
8	0.000459	15																			
9	0.000446	17																			
10	0.000439	19																			
11	0.000451	21																			
12	0.000433	23																			
13	0.000445	25																			
14	0.00046	27																			
15	0.000435	29																			
16	0.000436	31																			
17	0.00045	33																			
18	0.000455	35																			
19	0.000456	37																			
20	0.000463	39																			
21	0.000468	41																			
22	0.000434	43																			
23	0.000429	45																			

20 Kpa 80 Kpa 160 kpa T=2 T=3 T=4 T=5 T=6 T=7 T=8 T=9 T=10

Ready Average: 47.28254282 Count: 30 Sum: 709.2381424 100%

7day-Cement 3-Flyash2 - Excel

Asghaniastaneh, Azadeh

File Home Insert Page Layout Formulas Data Review View Tell me what you want to do

Clipboard Font Alignment Number Styles Cells Editing

R71

Shear Strain (%)	Frequency (Hz)
0.00135343	5
0.00135219	7
0.00132751	9
0.00133527	11
0.00135196	13
0.00135734	15
0.00134439	17
0.00134791	19
0.00134993	21
0.00135794	23
0.00137075	25
0.00136744	27
0.00137142	29
0.00135204	31
0.00141479	33
0.00141822	35
0.00150732	37
0.00162701	39
0.00168874	41
0.00168041	43
0.00168928	45

20 Kpa 80 Kpa 160 Kpa T=2 T=3 T=4 T=5 T=6 T=7 T=9 T=10 GGmax ...

Average: 36.58575827 Count: 30 Sum: 548.786374

L8,F2-14 Days - Excel

Asghaniastaneh, Azadeh

File Home Insert Page Layout Formulas Data Review View Tell me what you want to do

Clipboard Font Alignment Number Styles Cells Editing

Q97

Shear Strain (%)	Frequency (Hz)
0.00553404	5
0.00552413	7
0.00552908	9
0.00564763	11
0.00572787	13
0.005811	15
0.00601968	17
0.0062821	19
0.00663914	21
0.00707651	23
0.00766484	25
0.00846369	27
0.0095608	29
0.01140178	31
0.01529244	33
0.02193529	35
0.02011124	37
0.01796613	39
0.01727023	41
0.01603555	43
0.01389091	45

20 Kpa 80 Kpa 160 Kpa T2 T3 T4 T5 T6 T7 T8 T9 T10 GGmax Pi ...

Average: 19.05401761 Count: 30 Sum: 285.8102641

L6,F4-14Days - Excel

Asghariastaneh, Azadeh

File Home Insert Page Layout Formulas Data Review View Tell me what you want to do

Clipboard Font Alignment Number Styles Cells Editing

S97

	A	B	C	D	E	F	G	H	I	J	K	L	M	N	O	P	Q	R	S	T	U
1	Shear Stra	Frequency																			
2	(%)	(Hz)																			
3	0.000723	5																			
4	0.000674	7																			
5	0.000659	9																			
6	0.000667	11																			
7	0.000655	13																			
8	0.00066	15																			
9	0.000635	17																			
10	0.000623	19																			
11	0.000622	21																			
12	0.000632	23																			
13	0.000639	25																			
14	0.000644	27																			
15	0.000632	29																			
16	0.000643	31																			
17	0.000641	33																			
18	0.000641	35																			
19	0.000625	37																			
20	0.000677	39																			
21	0.000646	41																			
22	0.000624	43																			
23	0.000611	45																			

20 KPa 80 KPa 160 KPa T2 T3 T4 T5 T6 T7 T8 T9 T10 GGmax Pr ...

Average: 57.16158011 Count: 30 Sum: 857.4237016

C3-F2-14Days - Excel

Asghariastaneh, Azadeh

File Home Insert Page Layout Formulas Data Review View Tell me what you want to do

Clipboard Font Alignment Number Styles Cells Editing

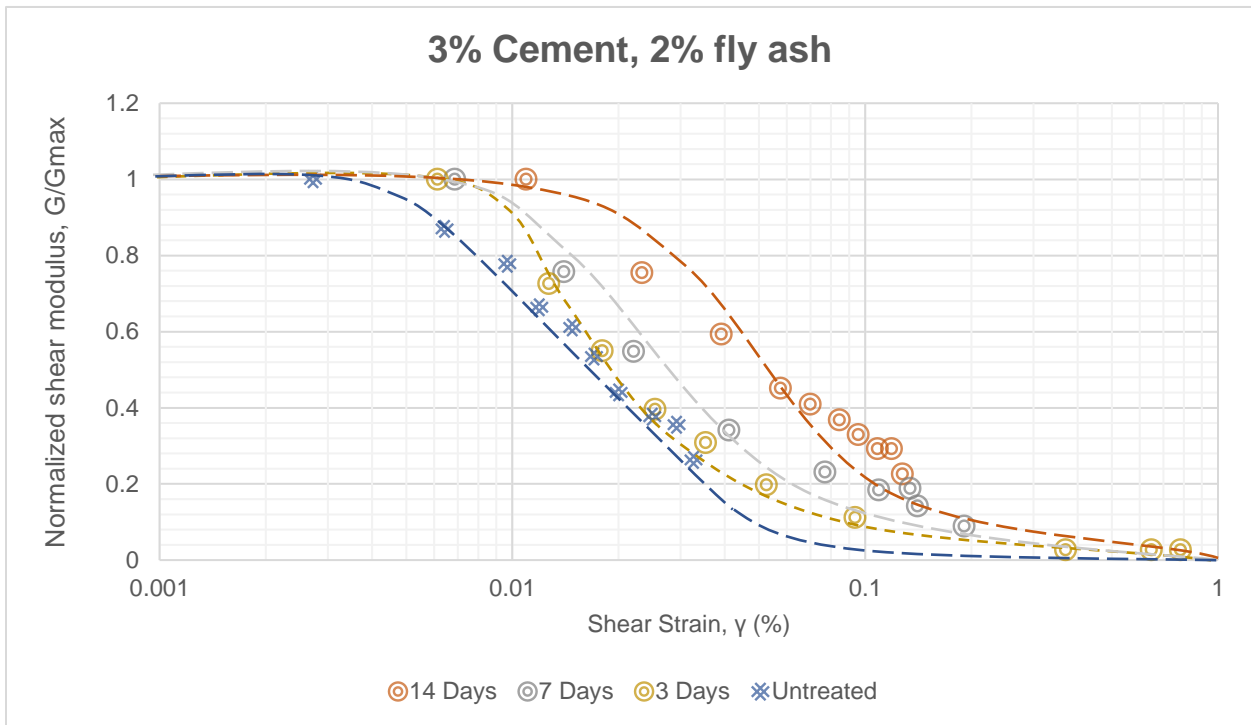
R66

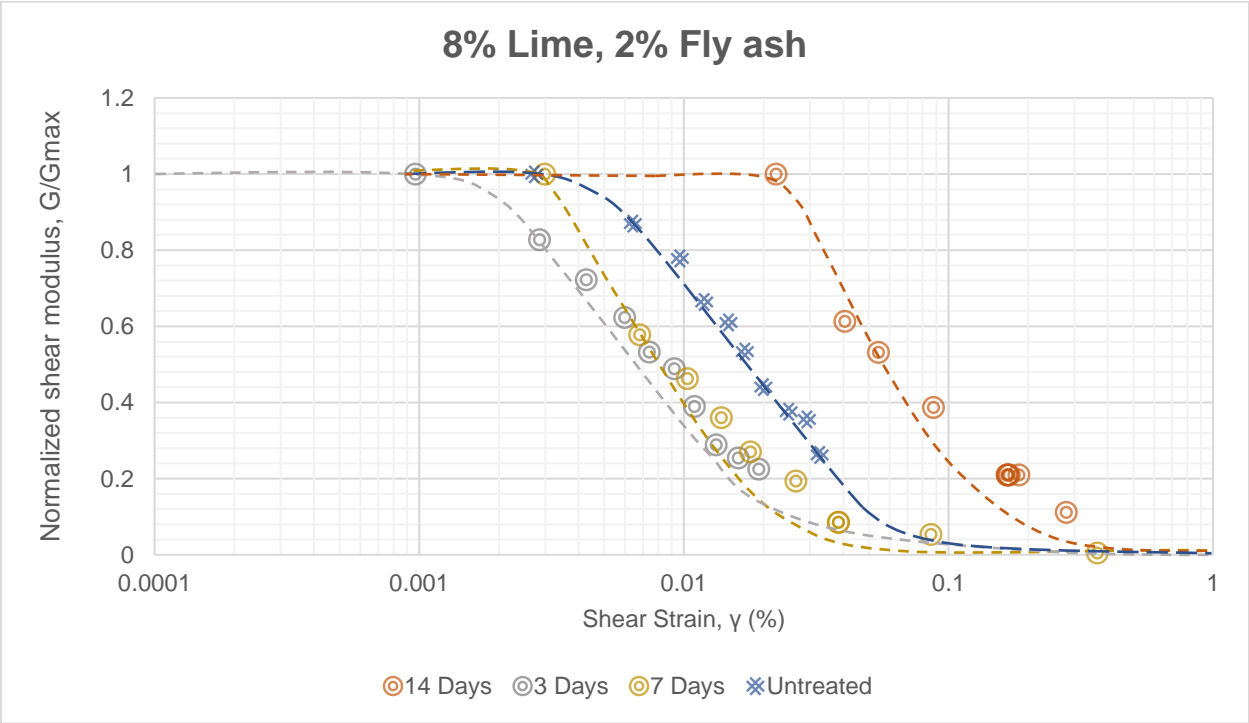
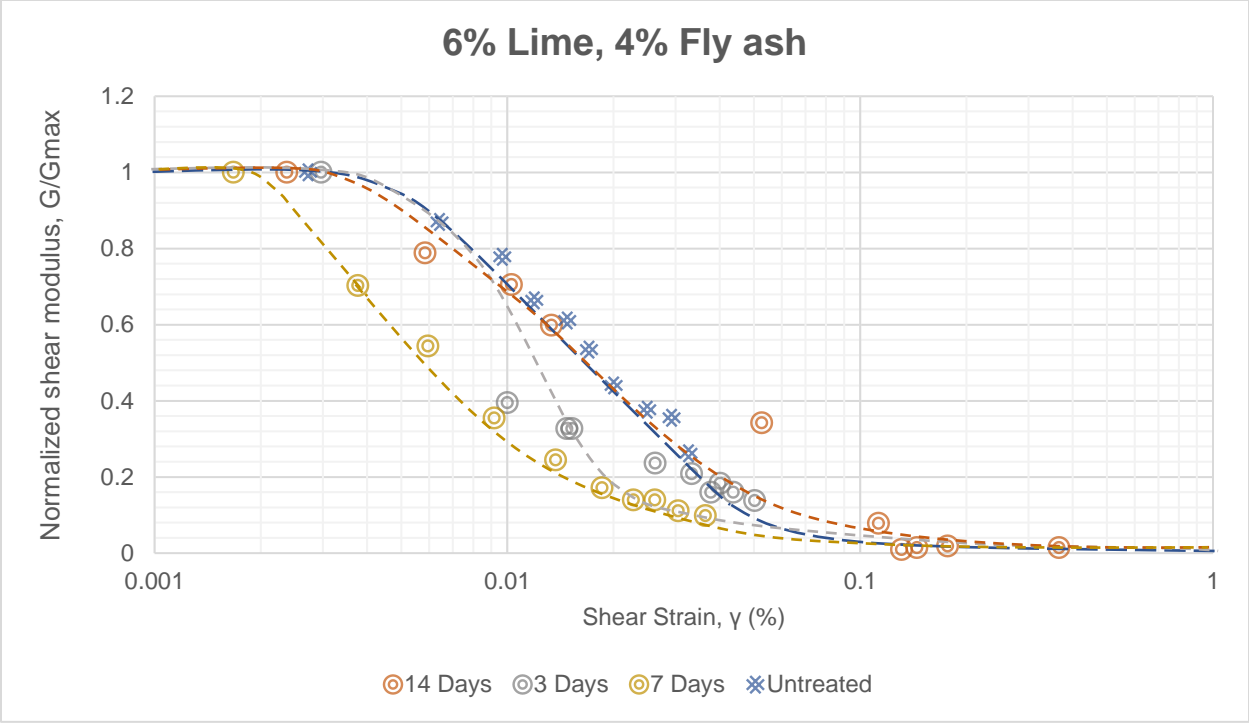
	A	B	C	D	E	F	G	H	I	J	K	L	M	N	O	P	Q	R	S	T
1	Shear Strain	Frequency																		
2	(%)	(Hz)																		
3	0.00199434	5																		
4	0.00201229	7																		
5	0.00199538	9																		
6	0.00201996	11																		
7	0.00201934	13																		
8	0.00201559	15																		
9	0.00205601	17																		
10	0.00207071	19																		
11	0.00207862	21																		
12	0.00211987	23																		
13	0.00213585	25																		
14	0.00218455	27																		
15	0.00226912	29																		
16	0.00240751	31																		
17	0.00257064	33																		
18	0.00259693	35																		
19	0.00267496	37																		
20	0.00279682	39																		
21	0.00297031	41																		
22	0.00308428	43																		
23	0.00311137	45																		

20 KPa 80 KPa 160 KPa T2 T3 T4 T5 T6 T7 T8 T9 T10 GGmax Pr ...

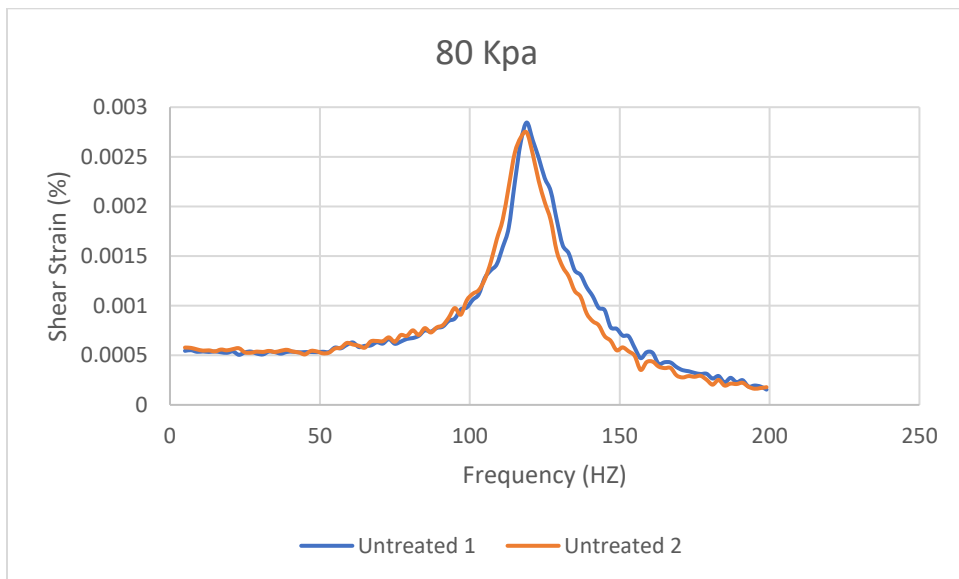
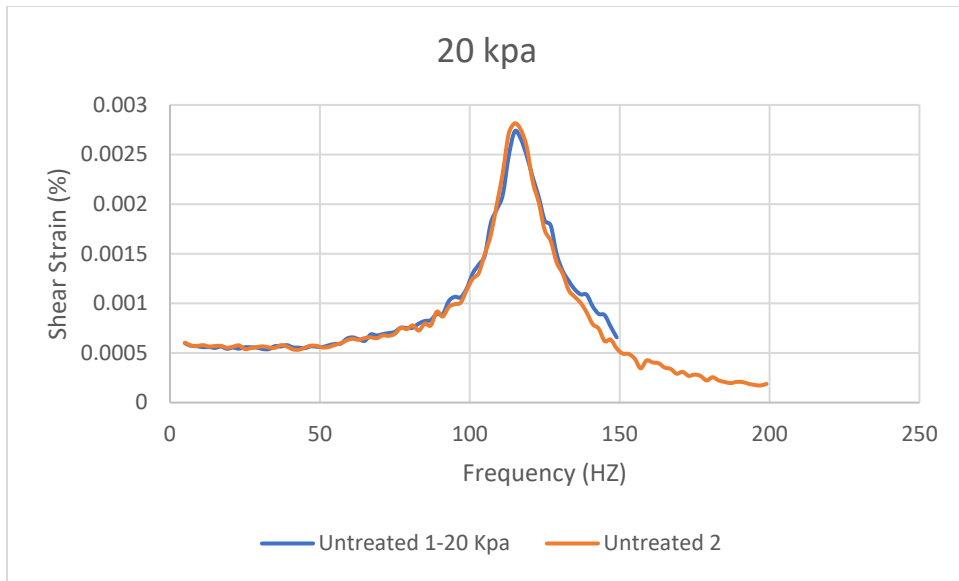
Average: 29.63837654 Count: 30 Sum: 444.5756481

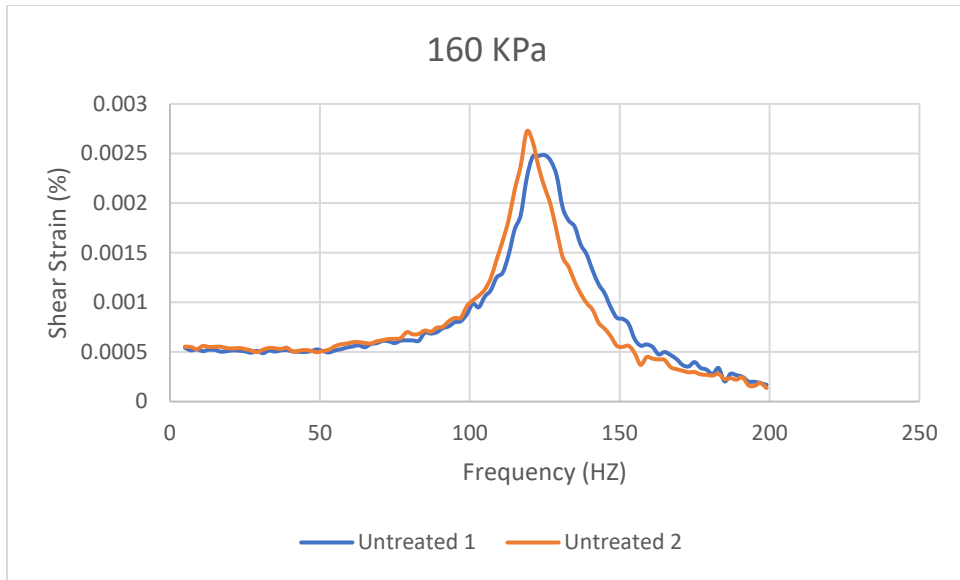
Appendix IV – Variation normalized shear modulus over shear strain for treated and untreated soils for different curing durations





Appendix V Test Repeatability





Appendix VI: Class F Fly ash

Property	Result
(1)	(2)
Strength activity index with cement at 7 days (%)	85.2
Strength activity index with cement at 28 days (%)	96.2
Required water (%)	97.5
Moisture content (%)	0.2
Loss on ignition (%)	2.2
Retained on No. 325 (%)	29.8
Specific gravity (-)	2.28
Calcium oxide, CaO (%)	1.1

Component	Result
(1)	(2)
Silicon dioxide, SiO ₂ (%)	56.7
Aluminum oxide, Al ₂ O ₃ (%)	29.5
Iron oxide, Fe ₂ O ₃ (%)	4.9
Calcium oxide, CaO (%)	1.1
Magnesium oxide, MgO (%)	0.8
Sulfur trioxide, SO ₃ (%)	0.1
Alkalis or equivalent, Na ₂ O (%)	0.3